

https://dspace.org/

Combating the effects of rockbursts caused by seismically-induced shock waves

Mudau, Avhasei

2017

https://hdl.handle.net/10539/24116

Mudau, Avhasei (2017) Combating the effects of rockbursts caused by seismically-induced shock waves, University of the Witwatersrand, <https://hdl.handle.net/10539/24116>

Downloaded from a DSpace repository. https://dspace.org/

Combating the effects of rockbursts caused by seismically-induced shock waves

Avhasei Mudau

A thesis submitted to the Faculty of Engineering and the Built Environment, University of the Witwatersrand, Johannesburg, in fulfillment of the requirements for the degree of Doctor of Philosophy.

Johannesburg, September 2017

Declaration

I declare that this thesis is my own unaided work. Where use has been made of the work of others, it has been duly acknowledged. It is being submitted for the Degree of Doctor of Philosophy in the University of the Witwatersrand, Johannesburg. It has not been submitted before in any form for any degree or examination in any other University.

.....

(Signature of candidate)

.....29TH..... day of .....SEPTEMBER..... 2017

Abstract

Rockburst occurrences and their consequent damage remain a problem in modern mining, particularly at great depth. The problem of rockbursts has also escalated in deep civil engineering tunnels due to high levels of in-situ stress at such depths. Key advancements have been made to date to help mitigate the drastic impacts caused by rockburst damage, with rock support remaining a line of defense to provide stability in rockbursting situations. There is, however, an ongoing inability of support to contain severe rockburst damage, especially conventional support systems.

More than two decades ago, a support concept termed "sacrificial support" was proposed as a potential additional method to help inhibit rockburst damage. The philosophy behind a sacrificial support system is that, under dynamic loading conditions, support, in the form of a liner must fail (*i.e.* be ejected from rock surface), leaving behind, undamaged, what was once supported rock mass. It is because of this reason that this support is referred to as a sacrificial support due to its ability to protect the rock from damage whilst the support itself fails. Since the inception of this support idea, it was only recently that the behaviour of support in real rockburst events manifested the sacrificial behaviour in rockbursting, which warranted the need for further research. The sacrificial support concept stated here is applicable in situations where the source (*i.e.* seismic event) of the rockburst is located remote from where rockburst damage is likely to occur.

To investigate the behaviour of sacrificial support, controlled laboratory experiments based on the split Hopkinson pressure bar (SHPB) technique were conducted to study some aspects of dynamic rock fracturing in tension at high strain rates, and also the role a sacrificial layer plays in combating dynamic rock failure (*i.e.* rockburst damage). To achieve this, a single Hopkinson pressure bar configured for spalling tests, comprised of a relatively long cylindrical intact rock specimen attached at the bar free end, was impacted by a striker on the opposite free end of the bar in order to generate a dynamic stress pulse responsible for spall failure upon reflection from the specimen free end. Different liners and/or liner combinations were then introduced at the specimen free end as sacrificial support. This experimental arrangement allowed the role of, and failure mechanisms associated with, sacrificial support under dynamic loading to be demonstrated, and comparisons were made with "sacrificial support" behaviour observed in real rockburst events in a mine. Analysis of experimental results revealed that varying liner thickness and mechanical impedance between rock and support liner plays a significant role in helping to limit rockburst damage.

Apart from experimental investigations, numerical simulations were undertaken to further probe the behaviour of sacrificial support under dynamic loading. Elastic models subjected to p-wave propagation indicated failure of the sacrificial layer, manifested by ejection of the liner due to reflection of compressive wave at the free surface. This failure mechanism was noticed for all the liners, independent of variation in liner thickness, and wavelength characteristic of the applied wave to the model. The sacrificial support method presented in this thesis presents an opportunity to further enhance safety in seismically active mines.

Acknowledgements

Success in the work of this nature depends on the involvement of number of individuals and organizations. The following individuals and organizations are thanked for their contributions in one way or another.

- Firstly, I would like to express my sincere gratitude to my supervisor Professor Dick Stacey for his guidance throughout the study. I am highly grateful for financial assistance and moral support you have always provided when I needed it the most. Your aptitude in simplifying complex engineering problems is amazing.

- Many thanks go to the National Research Foundation (NRF) of South Africa, Wits University Postgraduate Merit Award (PMA) and Wits School of Mining Engineering bursary through the Centennial Chair of Rock Engineering for their provision of funding to make this study a success.

- The former and current Heads of School of Mining Engineering, Professor(s) Fred Cawood and Cuthbert Musingwini, are thanked for their encouragement and creating best environment possible to allow us carry out research with less difficulties, respectively.

- Staff and supporting staff members within our school are also thanked. A special thanks to Andrew Carpede, Paulos Sibeko and Musa Ncebekhulu for their assistance with laboratory specimen preparation and

rock testing.

- Ken Harman of Wits School of Civil and Environmental Engineering is acknowledged for his assistance in setting up early experimental work conducted in this study.

- I am indebted to Blast Impact and Survivability Research Unit (BISRU) within the Department of Mechanical Engineering at the University of Cape Town for allowing me to make use of their testing facilities for free. The reception by BISRU staff members and postgraduate students within the research unit has always been warm during my periodic visits to their laboratory. Dr. Reuben Govender is highly thanked for mentorship and introducing me to split Hopkinson pressure bar technique.

- SRK consulting South Africa is thanked for opening doors to make use of their UDEC software for numerical modelling. Senior geotechnical mining engineer at SRK Joseph "Papi" Muaka is thanked for guidance and always keeping humorous environment all the time. Dr. Ping Zhang of Lulea University of Technology from Sweden is thanked for providing script file for UDEC dynamic modelling.

- My family members are specially thanked for always being there for me during hard and trying times.

- My fellow postgraduates students and friends are thanked for their stimulating discussions and concern about my wellbeing. Matthews, Mpeo, Farisani, Cassius, Khethani, Desmond, Jacques, Tawanda, Akua, Martha, Monica and Ntakadzeni are thanked for all the memories we have shared.

- Mikovhe Gadisi and Arinao Anneline Murivhami are thanked for always listening to me even though I did not make sense in most of the times.

Dedication

As Vaillant puts it, there are two pillars of happiness. "One is love," he writes. "The other is finding a way of coping with life that does not push love away."

I would like to dedicate this work from my heart to selected individuals who shined the light of hope and love both in good and hard times.

To my family:

To my mother and sister – the pillars of family – I cannot thank you enough for all the sacrifices you have made in my life. I love you.

In remembrance of my late two brothers who never lived long enough to see this day. I thank you for your love and always sustaining our needs as family.

To my supervisor: Professor Emeritus Dick Stacey

I have no words worthy to express my gratitude. I would like to thank you for being the best supervisor in the world. Your love, kindness and patience is amazing.

In memory of Professor Emeritus Geoffrey Eustace Blight

I am forever grateful to have had an opportunity to do a masters degree under your supervision and for your early involvement in this study. I will forever cherish all the great memories we have had.

"If the only prayer you can ever say in your life is 'Thank you,' it will be enough." – Meister Eckhart

Contents

1 Introduction 1

1.1 Background . . . 1

1.2 Problem statement and the need for further research . . . 5

1.3 Methodology and approach of this study . . . 6

1.4 Philosophy and organization of this thesis . . . 6

1.5 Chapter summary . . . 7

2 Literature review 8

2.1 Definition of a rockburst . . . 9

2.2 Rockburst mechanisms . . . 14

2.2.1 Rockburst source mechanisms . . . 14

2.2.2 Types of rockbursts . . . 18

2.2.2.1 Strainbursts . . . 18

2.2.2.2 Rupture type rockbursts . . . 36

2.3 Design considerations to help reduce rockburst damage in underground excavations . . . 52

2.3.1 Design of the geometries of excavations, mine layout geometry and mining sequence . . . 54

2.3.2 Design of ameliorating measures to reduce seismic hazard by "changing" rock mass conditions . . . 56

2.3.3 Design of suitable support systems to cater for dynamic loading conditions . . . 58

2.3.3.1 Defining of seismic events and their potential corresponding damage . . . 59
2.3.3.2 Support specification for dynamic loading conditions . . . 63
2.4 The sacrificial support concept – an alternative method to enhance safety in rockbursting environments . . . 69
2.4.1 Method of and means for inhibiting rockbursts . . . 70
2.4.2 Behaviour of sacrificial support in rockbursting environment – a case study . . . 72
2.4.2.1 Tensile wave trap mechanism – a possible explanation of sacrificial support behaviour . . . 75
2.5 Objectives and aims of the study . . . 78
2.5.1 Specific objectives . . . 79
2.6 Chapter summary . . . 79

3 Experimental programme for testing the performance of sacrificial support under dynamic loading **81**
3.1 Review of previous studies on physical testing of ground support elements and systems under "simulated" rockburst conditions . 82
3.1.1 Drop weight tests . . . 82
3.1.2 Large-scale blasting experiments . . . 87
3.2 Experimental programme for testing the performance of sacrificial support under dynamic loading . . . 94
3.2.1 Plate impact tests . . . 95
3.2.2 Split Hopkinson Pressure Bar tests . . . 98
3.2.3 A test methodology to demonstrate the mechanism of sacrificial support . . . 99
3.2.3.1 Theoretical and mechanical details of SHPB test configured for spalling . . . 100

3.2.3.2 Spall test specimen preparation 104
3.2.3.3 Liner material preparation 106
3.2.3.4 Quasi-static material characterization 108
3.2.4 Dynamic compression testing with SHPB 109
3.3 Chapter summary 117

4 Dynamic rock failure containment using a sacrificial layer 118

4.1 General observations from spall tests conducted without support liners 119
4.2 Evaluating the performance of support liners consisting of materials with differing mechanical properties 121
4.2.1 Tests with minimum liner thickness per liner material type 121
4.2.1.1 Tests with 45 mm thick concrete liner (concrete liner series) 121
4.2.1.2 Tests with 10 mm thick clay liner (clay liner series) 123
4.2.1.3 Tests with 30 mm thick concrete/clay liner combination (concrete clay combination) 125
4.2.1.4 Tests with a 140 mm thick steel liner (steel liner series) 127
4.2.2 Effect of varying liner thickness on dynamic rock failure . 129
4.2.2.1 Concrete liner series 129
4.2.2.2 Concrete/clay liner combination 130
4.2.2.3 Clay series 133
4.2.3 Effect of mechanical impedance on rock damage in layered systems 134
4.2.3.1 Impedance mismatch between rock materials and concrete liner 136

4.2.3.2 Impedance mismatch between rock materials and clay liner 136
4.2.3.3 Impedance mismatch between rock materials and steel liner 137
4.3 Comments on experimental findings 137
4.4 Chapter summary 138

5 Numerical modelling of the behaviour of sacrificial support using Universal Distinct Element Code (UDEC) 139

5.1 An overview of UDEC in computing rock mass response 140
5.2 Steps necessary for generation of models in UDEC 141
5.2.1 Conceptual model for dynamic analysis in this study . . 142
5.2.2 Model geometry and meshing 142
5.2.3 Material properties and constitutive model 143
5.2.4 Model boundary conditions 144
5.2.5 Dynamic input in the model 144
5.3 Behaviour of a sacrificial layer under dynamic loading – a numerical study 146
5.3.1 Effect of elastic wave propagation on the behaviour of a sacrificial layer characterized by welded and unwelded interfaces 147
5.3.2 Effect of seismic wavelength on the behaviour of a sacrificial layer 153
5.3.3 Effect of varying liner thickness 158
5.4 Discussion of numerical modelling findings 162
5.5 Chapter summary 163

6 Synthesis of experimental and numerical modelling results 164

7 Conclusions 167

7.1 Concluding remarks 167
7.2 Practical application of sacrificial support 169

8 Recommendations for future work 170

List of Figures

Figure 1.1 Rockburst damage and fragmentation (Stacey and Rojas, 2013) 3

Figure 1.2 Protruded rock support elements after dynamic (rockburst) rock failure (Stacey and Rojas, 2013) 4

Figure 1.3 Floor heave of nearly 2 m experienced in rockburst damage (Stacey and Rojas, 2013) 4

Figure 2.1 Schematic representation of acoustic emission tests for (a) compression test (Scholz, 1968) and (b) true-triaxial test (He *et al.*, 2010) 10

Figure 2.2 A sequence of crack growth and nucleation from acoustic emission signals (a) and complete stress-strain curve for granite specimen under triaxial compression (b) (Lockner *et al.*, 1991) 12

Figure 2.3 Stages of shear rupture development in intact rock specimen under high stress confinement (Tarasov and Potvin, 2013) 13

Figure 2.4 Examples of basic mechanisms of mining induced seismic events in tabular mining environment (Hasegawa *et al.*, 1989) 15

Figure 2.5 Typical local rock mass failure mechanisms that potentially cause seismic events: (a) fault movement, (b) stress change causing rock mass fracturing near excavations, (c) stope overbreak, (d) contrast in rock mass material properties causing strainbursting, (e) crushing of mine pillars, and (f) stress increase causing rock mass deformation (Hudyma, 2008) 16

Figure 2.6 (a) Stress-strain curves of rocks, energy storage capacity of the rock and illustrations of Class I and Class II behaviours from ISRM (1999), modified by Stacey (2013), and (b) Class II characteristic behaviour (after Vogler and Stacey, 2016) 19

Figure 2.7 Universal scale of brittleness for rock materials (Tarasov and Potvin, 2013) 21

Figure 2.8 An example of the influence of rock strength and stiffness in strainbursting occurrence (Broch and Sorheim, 1984) . 23

Figure 2.9 Empirical stability classification of square tunnels (Hoek and Brown, 1980) 26

Figure 2.10 Tunnel instability and brittle failure (shaded gray squares) as a function of Rock Mass Rating (RMR) and the ratio of the maximum far-field stress ($_1$) to the laboratory unconfined compressive strength (σ_c) (Martin *et al.*, 1999) 28

Figure 2.11 An example of violent dynamic rock failure in competent rock at very low stress levels (Stacey et al., 2007) 30

Figure 2.12 An example of violent fracture development in a quarry (Stacey et al., 2007) 30

Figure 2.13 Examples of fragments size variation caused by strainbursts and buckling (Illustrations and photographs by Ortlepp, 1997) 32
Figure 2.14 Illustration of buckling process nearby an excavation (Qui *et al.*, 2014) 33
Figure 2.15 Illustration of buckling process in excavation surface when only maximum compressive stress is considered (Dyskin and Germanovich, 1993) 34
Figure 2.16 Reconciliation of rockburst damage mechanisms identified by (a) Kaiser et al. (1996) and (b) Ortlepp (1992) (modified by Morissette, 2015) 35
Figure 2.17 Total closure of a section in a tunnel caused by rockburst damage following $M_L = 3.6$ mine tremor occurrence (photograph W.D. Ortlepp, Durrheim 2010) 36
Figure 2.18 Six- storey building collapse in Welkom caused by $M_L =$ 5.2 mine tremor (Durrheim, 2010) 37
Figure 2.19 Plot of cluster groups (left) at RENO sector compared to location of faults (right) (Potvin *et al.*, 2010a) 39
Figure 2.20 Superimposition of faults G, F, C and N1 with large seismic events (Potvin *et al.*, 2010a) 40
Figure 2.21 Cumulative seismic moment in selected faults at RENO sector (Potvin *et al.*, 2010a) 42
Figure 2.22 Cumulative seismic moment obtained using numerical modelling (Potvin *et al.*, 2010a) 43
Figure 2.23 Illustration of theoretical radiation patterns of P and S waves around the seismic source (Aki and Richards, 1980)) 45

Figure 2.24 Illustration of the effects of a single fracture on the transmitted waveform and corresponding amplitude spectra (Myer *et al.*, 1990) 46
Figure 2.25 Wave propagation patterns expressed by snapshots of peak velocity at earlier time and latter time for different crack models. (i) Elastic (ii) Crack density 0.05, crack size 2 mm (iii) Crack density 0.10, crack size 3 mm (Hildyard *et al.*, 2005) 47
Figure 2.26 Snapshots of seismic wave propagation in (a) base model (b) model with mined out area areas (c) model with stope areas backfilled with cementitious materials (Saleh *et al.*, 2015) 48
Figure 2.27 Photoelastic analysis of stress wave propagation when (a) wave interacting with a long narrow opening, and (b) when interacting with similar opening but bounded by two discontinuity plane above and below the narrow stope (Daehnke, 1997) 49
Figure 2.28 The engineering wheel of design (Stacey, 2009) 53
Figure 2.29 Illustration of the effect of destressing around excavation (Roux *et al.*, 1957) 57
Figure 2.30 Potential areas to reduce strainbursting using destress blasting (Mitri, 2000) 58
Figure 2.31 Gutenberg-Richter frequency-magnitude relationship showing two distinct groups of seismic events (Hudyma, 2008) 60
Figure 2.32 Seismic hazard map generated from clusters of seismic events (Potvin, 2009) 61
Figure 2.33 Performance of surface support systems under dynamic loading (Potvin *et al.*, 2010b) 65

Figure 2.34 Naked rockbolts indicating shear loading in a rockburst ejection (Stacey and Rojas, 2013) 65
Figure 2.35 Mechanical behavioral principles of NPR bolt under dynamic loading (He *et al.*, 2014) 67
Figure 2.36 Correlation of support systems with seismicity (Stacey and Ortlepp, 2007) 68
Figure 2.37 Propagation of compressive wave in jointed rock mass media (Stacey, 1991) 71
Figure 2.38 The mechanism of sacrificial layer behaviour in resisting rockburst damage (Stacey, 1991) 72
Figure 2.39 Rockburst damage in lower sidewalls of tunnel (Stacey and Rojas, 2013) 73
Figure 2.40 Rockburst damage caused by floor heave (Stacey and Rojas, 2013) 74
Figure 2.41 Concrete support panels ejected during rockburst event (Stacey and Rojas, 2013) 75
Figure 2.42 Passage of a compressive wave and reflection at the concrete/air interface creating a tensile wave (Stacey and Rojas, 2013) 76
Figure 2.43 Ejection of the concrete due to the tensile wave (Stacey and Rojas, 2013) 76
Figure 2.44 Propagation of a compressive wave through rock, concrete, and water/mud (Stacey and Rojas, 2013) 77
Figure 2.45 Reflection of a compressive shock wave at the interface between the air and the water/mud (Stacey and Rojas, 2013) 78

Figure 3.1 Illustration of drop weight test facility (After Ortlepp and Stacey, 1997) 86

Figure 3.2 Profile of the tunnel after the blast test (Ortlepp, 1969) . 88
Figure 3.3 Photograph of concrete panels and the test studs grouted in position ready for testing 89
Figure 3.4 Geometry of underground blast experiment (Haile *et al.*, 2001) 90
Figure 3.5 (a) A side and (b) front view of plate impact test set-up . 96
Figure 3.6 Classification of loading techniques and an overview of material's response at high strain rates (Cai *et al.*, 2006) 98
Figure 3.7 A schematic representation of spall failure in a long cylindrical road loaded by impact (Govender *et al.*, 2011) . . . 101
Figure 3.8 Schematic experimental set-up for spalling test (a) without liner and (b) with liner 102
Figure 3.9 Laboratory core drilling of spall test specimens from (a) a block of rock and (b) existing core sample 105
Figure 3.10 (a) Concrete liners with different thicknesses, and (b) liners with varying thickness attached to rock specimens . . 107
Figure 3.11 (a) Preparation of clay liner material, and (b) attached clay liner material contained in plastic tube 108
Figure 3.12 A schematic representation of SHPB set-up for dynamic compression 110
Figure 3.13 Typical strain gauge signals for SHPB test (of cast iron) (Govender, 2011) 111
Figure 3.14 Example of face stresses for Anorthosite rock type under compression test with SHPB 114
Figure 3.15 Example of face stresses showing good equilibration (Govender *et al.*, 2012) 114
Figure 3.16 Strain vs true strain for tested rock material 115

Figure 3.17 Strain rate for a typical SHPB test using a conical striker (modified after Govender *et al.*, 2012) 116
Figure 3.18 Photograph of profiled strikers 117

Figure 4.1 Frames of different rocks tested, before and after spalling 120
Figure 4.2 Different rock test specimens supported with 45 mm concrete liner 122
Figure 4.3 Different rock test specimens supported with 10 mm clay liner 124
Figure 4.4 Different rock test specimens supported with 30 mm concrete/clay liner 126
Figure 4.5 Different rock test specimens supported with 140 mm steel liner 128
Figure 4.6 Dynamic behaviour of different rock types with various thicknesses of concrete liner 130
Figure 4.7 Dynamic behaviour of different rock types with various thicknesses of concrete/clay liner combination 132
Figure 4.8 Dynamic behaviour of different rock types with various thicknesses of clay liner 134

Figure 5.1 Configuration of UDEC model to study the behaviour of a sacrificial layer 142
Figure 5.2 1D p-wave signal expressed as peak particle velocity . . . 146
Figure 5.3 Displacement velocity for welded joint model 148
Figure 5.4 Stable sacrificial liner in welded interface model 149
Figure 5.5 Peak particle velocities recorded in welded model 150
Figure 5.6 Displacement of sacrificial liner due to reflection of seismic wave from free surface 151

Figure 5.7 Ejection of the sacrificial liner resulting from the tensile wave trap mechanism 152
Figure 5.8 Ejection velocity of the sacrificial liner 153
Figure 5.9 (a) Displacement and (b) velocity vectors of sacrificial support caused by low frequency P-wave propagation . . 155
Figure 5.10 Ejected sacrificial support caused by low frequency P-wave propagation 156
Figure 5.11 (a) Displacement and (b) velocity vectors of sacrificial support caused by high frequency P-wave propagation . . 157
Figure 5.12 Ejected sacrificial support caused by high frequency P-wave propagation 158
Figure 5.13 Displacement vectors for 0.05 m thick concrete support liner in ejection 159
Figure 5.14 Displacement vectors for 0.2 m thick concrete support liner in ejection 160
Figure 5.15 Ejection velocity for 0.05 m thick concrete liner 161
Figure 5.16 Ejection velocity for 0.2 m thick concrete liner 162

List of Tables

Table 2.1 Classification of seismic source mechanisms (Ortlepp, 1992a) 17

Table 2.2 Examples of dynamic rock fracturing at low to intermediate stress conditions (Stacey and Yathavan, 2003) 29

Table 2.3 Ejection velocities obtained through back analysis and experimentally 62

Table 3.1 Comparison of the dynamic loading simulation methods for each trial (reproduced from Hadjigeorgiou and Potvin, 2011) 83

Table 3.2 Ground support systems tested using blasting experiemnts in Western Australian mines (reproduced from Heal, 2010) 90

Table 3.3 Selected properties of silver steel 104

Table 3.4 Mechanical properties of rocks tested 109

Table 5.1 Mechanical properties of rock and liner materials 144

1 Introduction

1.1 Background

The problem of rockburst is not a new subject, but its existence now spans over a century and, unfortunately, the problem is still with us even today. Rockbursting involves violent "explosion" of highly stressed rock from the excavation boundary, particularly at great depth. According to Ortlepp (2005), the earliest record of catastrophic rockburst event occurred at Altenberg tin mine in Germany around 1640. The dire consequences of this event caused the entire mine operation to shut down from 1640 to 1860, and the shocks generated by the event were felt 45 km away from the mine. In his review of contributions made through Rockburst and Seismicity in Mines (RaSiM) series of conferences from 1982 to 2001, Ortlepp (2005) shared his global perspective about the problem of rockbursts and arrived to the conclusion that *"..... the problem of rockbursts is not confined by geographic boundaries and that the problem affects mining communities of different language groups and cultures, in different ways."* Among many countries which suffer from the problem of rockbursting, Ortlepp mentioned that *"in no other mining country has the rockbursting problem been anywhere near as severe as in the South African gold mines"* due to their unique depth of operation. In South Africa, the "symptoms" of rockburst damage were noticed as early as during the commencement of *20th* century in the Witwatersrand basin gold mines, and the problem es-

calated as the mining operations deepened. It is worthwhile mentioning that much of what is known about rockbursts around the world is the result of the work conducted in the deep gold mines of South Africa. These successes have been recognized both locally and internationally, and the research to help address the problem of rockbursts is still ongoing in most parts of the world (*e.g.* South Africa, Australia, Canada, Sweden, China, Chile *etc.*).

Numerous cases of rockbursting in tunnels developed at great depth have become prevalent around the world due to the increase in in-situ stress fields at depth. For example, recent experience gained at the Jinping II Hydropower Station in China during the construction of several parallel deep tunnels revealed the occurrence of severe rockburst incidences that caused loss of life, many injuries and equipment damage (Zhang *et al.*, 2012; Shan and Yan, 2010). Depending on the scale of damage, the structural integrity of underground excavations could be compromised because of the violent nature of ejected rock from the surface of excavations, causing destruction to equipment, and in some cases, claiming scores of lives. Rockbursts are cataclysmic to an extent that the resultant collapse or damage might dictate that the entire mining operation is shut down (Ortlepp, 2005; Potvin and Wesseloo, 2013a). Severe rockburst damage can result in large financial losses in seismically active mines. Seismically active mines are those that are prone to dynamic rock failure (Heal, 2010).

From the above, it is apparent that rockbursting is inevitable whenever deep mining is being practised and in tunnels driven at great depth due to increase in seismicity in the high stress fields. However, as opposed to the common knowledge that rockburst propensity increases with depth, some cases of dynamic rock failure at low stress conditions experienced in shallow mine operations are reported in the literature (example, Stacey and Yathavan, 2003; Stacey *et al.*, 2007; Nyungu and Stacey, 2014).

Rockbursts are more likely to be associated with hard rock conditions, geological structures such as faults or dykes, high mining extraction ratios, and mining method/s employed to extract a deposit (Kaiser and Cai, 2012). While it is acknowledged that seismic risk in the mines cannot be totally eliminated, Potvin (2009) highlighted the need to have in place sound strategic planning and design to help control such risks in the mines. Improvements have been made thus far in terms of control measures to help combat rockburst damage, and monitoring of seismic events using sophisticated seismic monitoring techniques is possible today. However, with the existing knowledge about rockbursts, it cannot be claimed that the problem is well understood, nor that its solution has been attained. Many cases are still being reported worldwide despite the current know-how on the subject of rockbursts. Figures 1.1 and 1.2 below are examples of rockburst damage and support failure under dynamic (rockburst) loading conditions. Floor heave is also common in rockbursting situations, and the damage can be enormous since floors in most cases are not furnished with support to resist such dynamic events (see figure 1.3)



Figure 1.1: Rockburst damage and fragmentation (Stacey and Rojas, 2013)

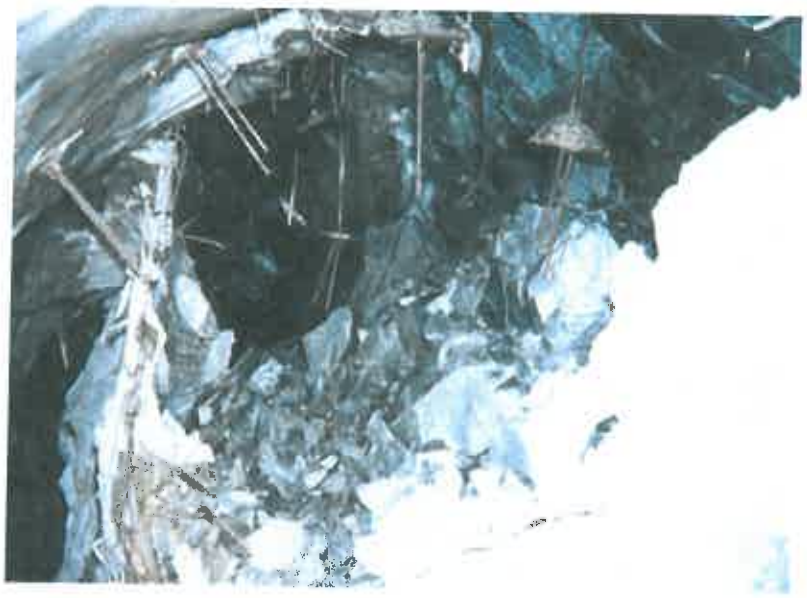

Figure 1.2: Protruded rock support elements after dynamic (rockburst) rock failure (Stacey and Rojas, 2013)



Figure 1.3: Floor heave of nearly 2 m experienced in rockburst damage (Stacey and Rojas, 2013)

1.2 Problem statement and the need for further research

Despite significant research regarding rockbursts, it cannot be claimed that the problem is now well understood, nor that a solution has been attained as stated previously. Many have regarded rockbursts as one of the least understood subjects. For example, designing a rockburst-resistant support system appears to be far-fetched, considering the complexities associated with quantifying the capacities of support elements (collectively known as the support system) and the demand imposed by accelerated rock strata under dynamic loading conditions. Stacey (2011; 2012) attributed the continuing support system failure in burst prone conditions to be a result of design indeterminacy resulting from a lack of understanding of the support system capacity, and the demand imposed by ejected rock strata in a dynamic loading environment. The problem seems to be pervasive and the solution elusive (Stacey, 2012). There is still an urgent need, therefore, to seek alternative mitigation measures to help contain rockburst damage.

Records show that, on many occasions, conventional support elements such as rock bolts, wire mesh, shotcrete and lacing fail to withstand severe rockburst damage. For this reason, this thesis presents an additional alternative potential method to help contain rockburst damage using a sacrificial layer, based on observations made after rockburst events in a mine (Stacey and Rojas, 2013). The philosophy behind a sacrificial support/liner is that, under dynamic loading conditions, support in the form of a liner will fail; leaving behind, undamaged, what was previously supported rock mass. The sacrificial support concept introduced here is applicable in situations where the source (*i.e.* seismic event) of the rockburst is located remote from where rockburst damage is likely to occur. This support concept is based on a wave trap mech-

anism previously suggested by Stacey (1991), and the concept is described in detail in Chapter 2. The proposed support method can be used to complement the existing rock support used in rockbursting environment.

1.3 Methodology and approach of this study

Two approaches, namely experimental and numerical analysis, are adopted in this study to evaluate the performance of sacrificial support under dynamic loading. The split Hopkinson pressure bar (SHPB) technique was chosen to investigate the potential benefits and failure mechanisms associated with sacrificial support due to its capability of studying dynamic rock fracturing at high strain rates in a controlled laboratory environment. Numerical simulations are conducted to verify the behaviour mechanisms associated with sacrificial layers under simulated dynamic loading conditions.

1.4 Philosophy and organization of this thesis

Each chapter presented in this thesis is first introduced to provide an overview of the main topics to be covered. A summary of individual chapters is presented at the end of each chapter together with an overview to inform the reader what the following chapter entails.

The thesis is structured as follows:

Chapter 2 focuses on the review of literature pertinent to the topic of investigation. A detailed review of rockburst mechanisms and design measures to ameliorate rockburst damage is provided. The sacrificial support concept is comprehensively covered towards the end of this chapter followed by research questions and study objectives.

Chapter 3 begins by providing a review of past studies on physical testing of rock support elements and systems under "simulated" rockburst conditions. Most importantly, the chapter details the experimental programme designed to investigate the performance and behaviour of sacrificial support using the split Hopkinson pressure bar (SHPB) technique.

Chapter 4 discusses the experimental results obtained from SHPB tests and the interpretation of these results.

Chapter 5 presents numerical simulations to demonstrate the behaviour of sacrificial support under dynamic loading conditions.

Chapter 6 compares the experimental and numerical analysis results.

Chapter 7 summarizes the findings of this thesis.

Chapter 8 outlines recommendations for future work.

1.5 Chapter summary

In this chapter, the problem of rockburst damage and the need for further research, and the research methodology, are highlighted. An alternative potential support method to help combat rockburst damage is also introduced.

The following chapter provides a detailed account of rockburst damage mechanisms and design measures to help combat the impact of rockbursts based on previous research. The sacrificial support concept is described in detail followed by research questions and study objectives.

2 Literature review

Chapter 1 discussed some of unresolved challenges associated with rockbursts which are common around the world. The need for further research and a summary of current research methodology to help achieve the task at hand were presented. An additional alternative potential support method to help limit detrimental impacts of rockburst damage caused by seismically-induced shock waves was introduced.

It is fundamental to have some insights into how this elusive phenomenon (*i.e.* rockburst) comes about, as well as its ensuing damage. If that is achieved, such information could aid in the development of the methods for the design of a rockburst-resistant support system. In this chapter, a definition of a rockburst is thoroughly examined. Following this is a comprehensive review of rockburst mechanisms common in burst-prone mining environments. Design considerations and mitigation measures to help control rockbursts damage are reviewed in detail. Towards the end of the chapter, the concept of sacrificial support, together with a case study to provide better understanding of the behaviour of sacrificial layers under rockbursting conditions is presented. Lastly, research questions and objectives of the present study are framed, based on the identified potential method.

2.1 Definition of a rockburst

Ortlepp (1997) defined a rockburst as a seismic event which causes violent and significant damage to a tunnel or excavation in a mine. A seismic event has been defined by Mendecki *et al.* (1999) as a sudden inelastic deformation which occurs within a given volume of rock from a seismic source that radiates detectable seismic/shock waves. In order to understand the evolution of the seismic event process, small-scale laboratory tests (*i.e.* acoustic emission (AE) tests) could be used to study some aspects of micro-fracturing and inelastic deformation of rock (Mogi, 1962; Scholz, 1968; Lockner *et al.*, 1991; He *et al.*, 2010). Figure 2.1 shows small cylindrical and cubic-shape rock test specimens, equipped with acoustic emission sensors, loaded in both axial and true-triaxial stresses, respectively. During the loading of these test specimens, elastic energy stored within test specimen is released in the form of elastic waves whenever new cracks develop, or due to further growth of existing cracks (He *et al.*, 2010).

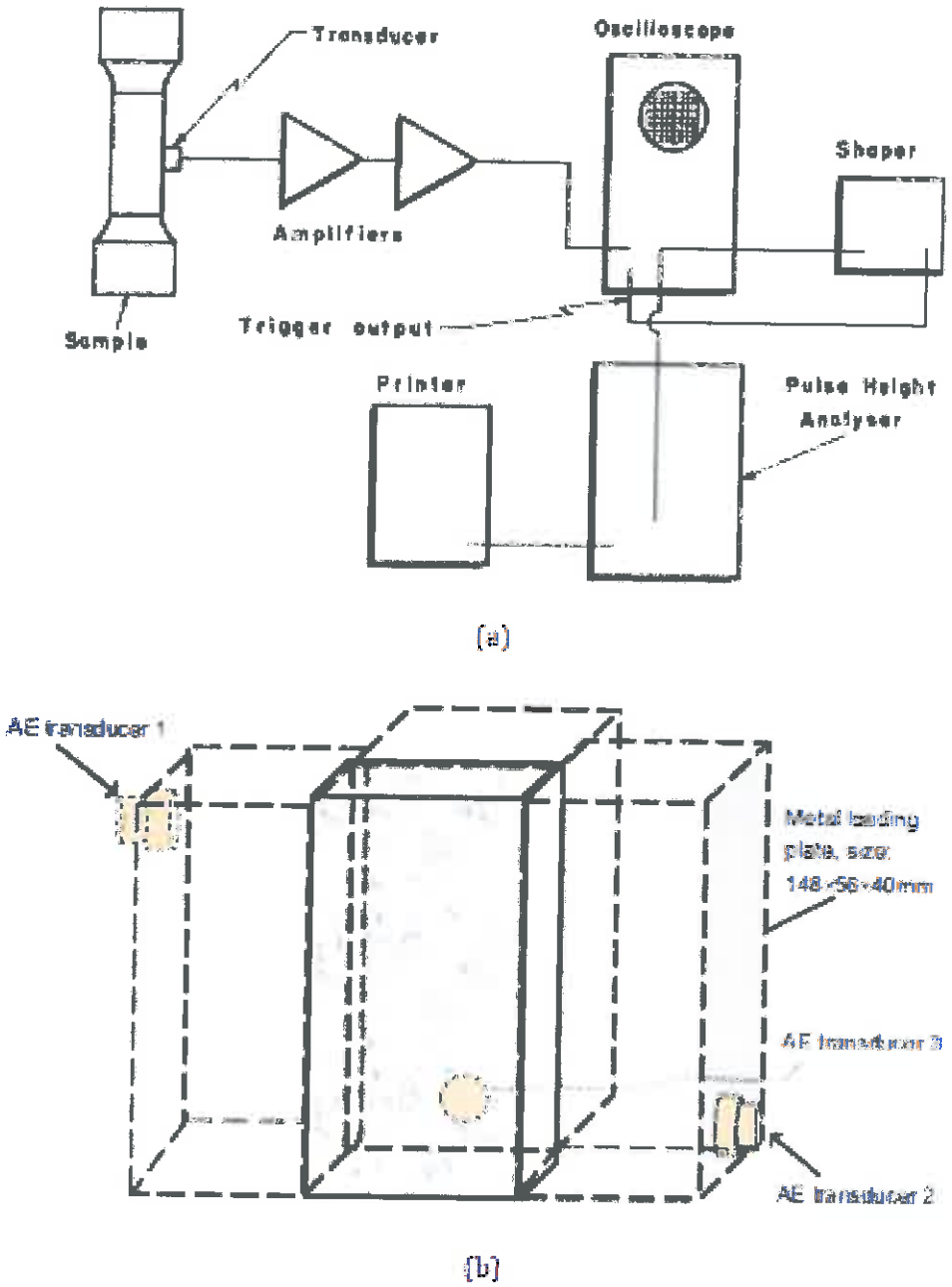

Figure 2.1: Schematic representation of acoustic emission tests for (a) compression test (Scholz, 1968) and (b) true-triaxial test (He *et al.*, 2010)

Figure 2.2 shows the locations of microseismic events, presumably indicating spontaneous micro-fracturing events within the rock test specimens, gathered from the recorded acoustic emission signals. Results reported by Lockner *et*

al. (1991) provide useful information concerning fracture growth and nucleation in brittle rock material loaded beyond its peak strength under triaxial stresses. Shear plane development is pronounced, as can be seen from figure 2.2 (a) (iii) to (vi). Tarasov and Potvin (2013) presented possible stages (figure 2.3) involved in shear rupture development, using a fan structure mechanism for brittle rock specimens under high triaxial stress confinement. Shear rupture (seismic source) development in an intact rock mass is one of the source mechanisms responsible for the occurrence of rupture type rockbursts, as discussed later. Microcracking and inelastic deformation in brittle rock material precede cataclastic failure of rock, which can be referred to as a rockburst in this context.

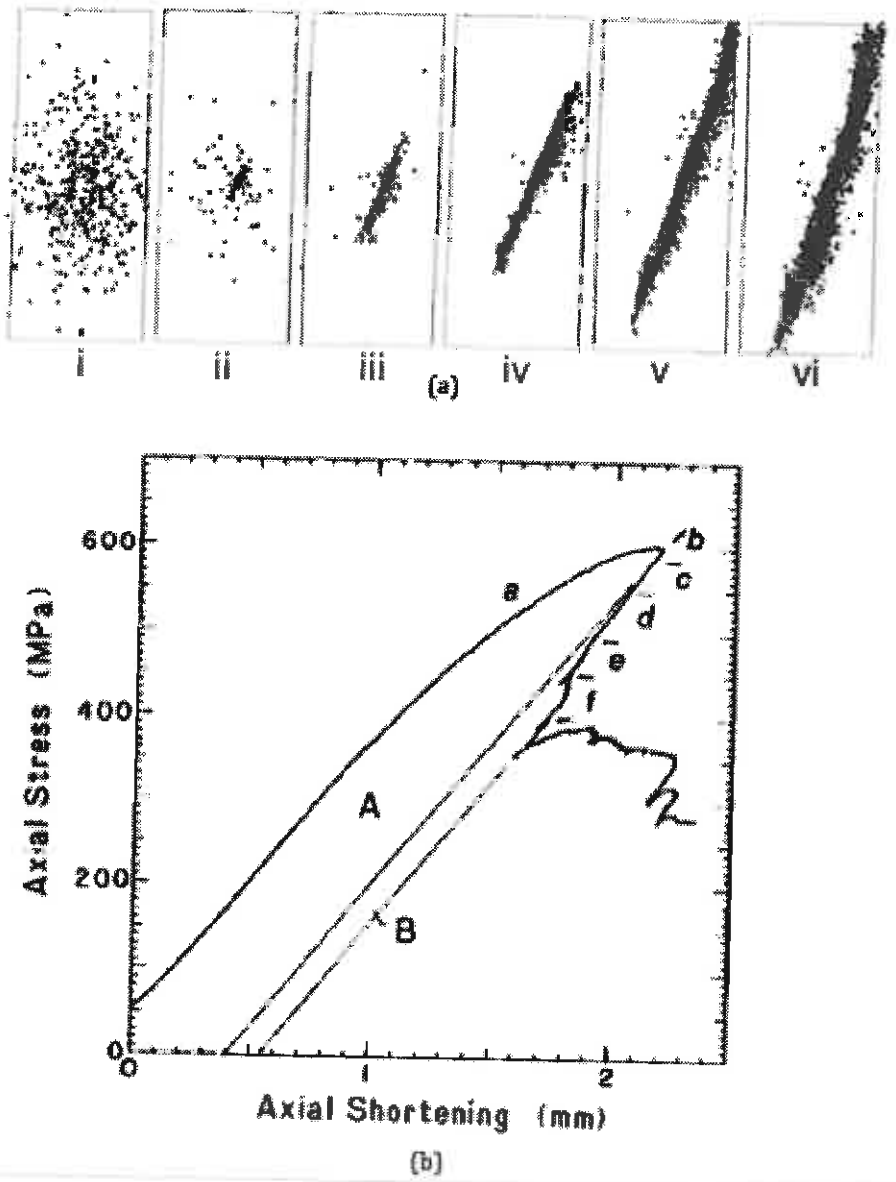

Figure 2.2: A sequence of crack growth and nucleation from acoustic emission signals (a) and complete stress-strain curve for granite specimen under triaxial compression (b) (Lockner *et al.*, 1991)

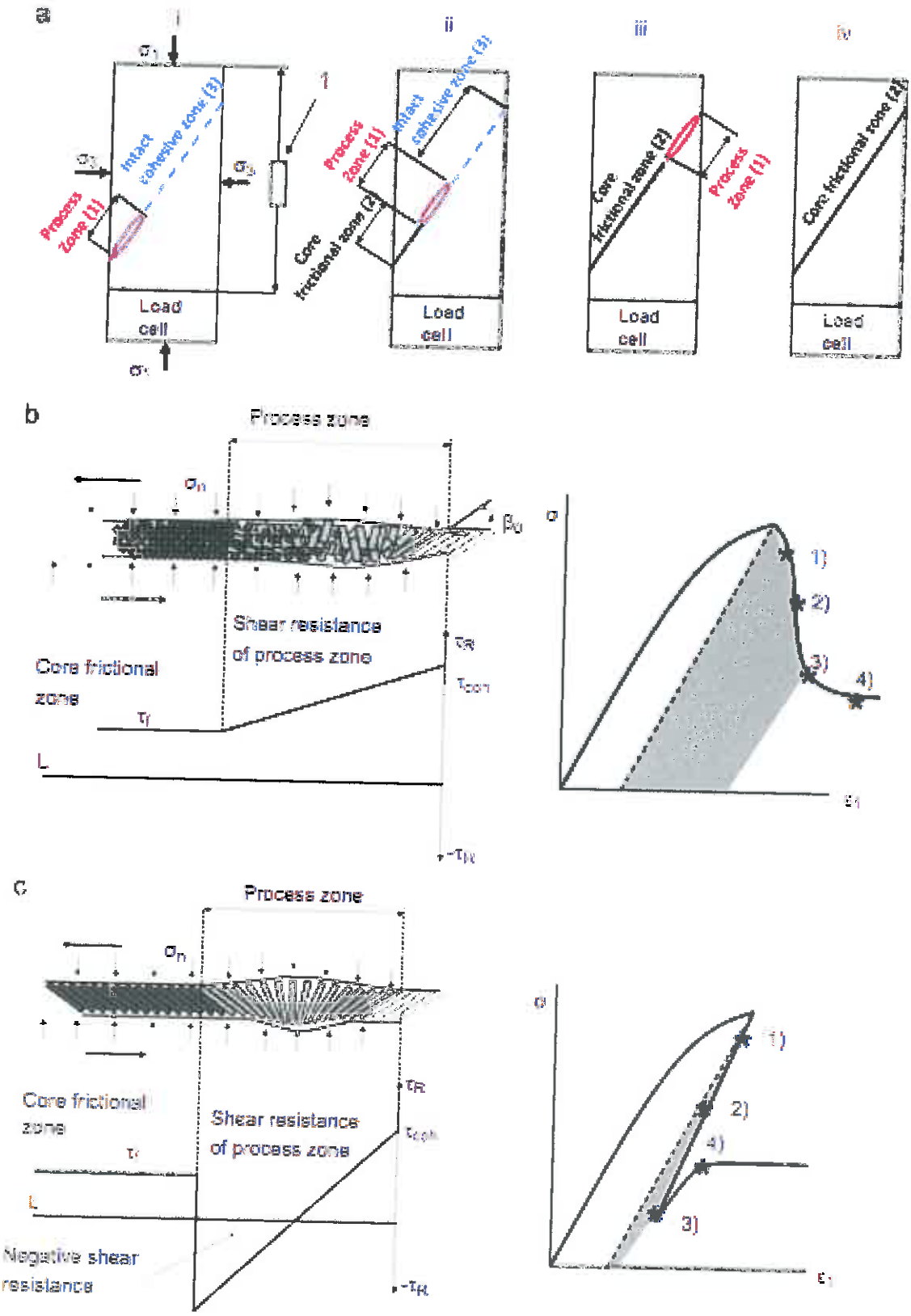

Figure 2.3: Stages of shear rupture development in intact rock specimen under high stress confinement (Tarasov and Potvin, 2013)

Most of the early research geared towards the understanding of micro-fracturing and inelastic deformation of brittle rock through analysis of acoustic emission signals was conducted to gain some insights into the formation of earthquakes (for example, Mogi, 1960; Scholz, 1968; Lockner *et al.*, 1991).

In an underground mining context, radiated detectable waves (*i.e.* P and S waves) generated from a large seismic event can cause significant damage to both rock and ground support upon their interaction with underground openings. The main purpose in this section has been to draw distinction between rockburst (*i.e.* damage) and seismic event (*i.e.* cause). A seismic event and the resulting damage can coincide with each other or be separated by significant distance from each other. The following section discusses various rockburst mechanisms.

2.2 Rockburst mechanisms

Rockburst classification is regarded as one of the topics of investigation which has sparked the interest of many researchers (Li *et al.*, 2007), and there has been considerable advancement in this area of study to date. This section is divided into two main sub-sections, namely rockburst source mechanisms and rockburst types.

2.2.1 Rockburst source mechanisms

Source mechanism may be regarded as a 'mirror' that one can use to gain better understanding on how a rockburst comes about. This encompasses those phenomena associated with the failure of a rock mass, more often at the pre-existing weak zones such as faults or dykes, which emit seismic energy (Hagan *et al.*, 2001).

There are several modes of failure of rock masses which may result in a

seismic event. It is commonly accepted that not all seismic events will result in a rockburst. Several studies have been conducted to help establish a classification system to differentiate between seismic events related to mining activities and those events that are not. In the following examples, figure 2.4 shows basic mechanisms of mining-induced seismic events common in tabular mining which might not necessarily result into rockburst, while figure 2.5 is an indication of local rock mass failure mechanisms which potentially cause seismic events in large open stoping mechanized mining operations.

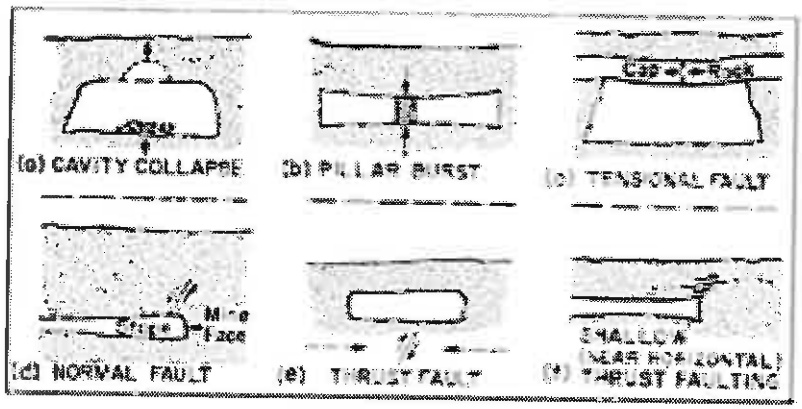

Figure 2.4: Examples of basic mechanisms of mining induced seismic events in tabular mining environment (Hasegawa *et al.*, 1989)

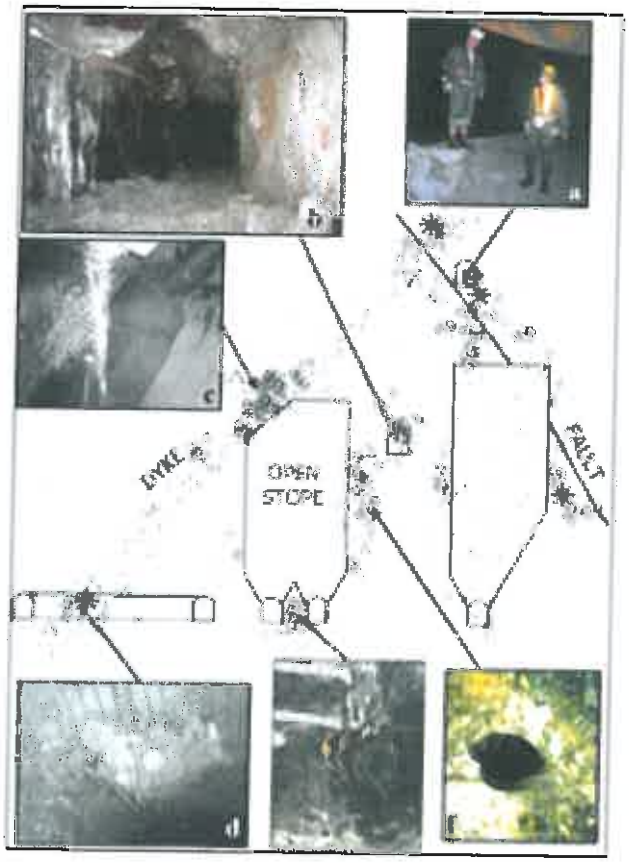

Figure 2.5: Typical local rock mass failure mechanisms that potentially cause seismic events: (a) fault movement, (b) stress change causing rock mass fracturing near excavations, (c) stope overbreak, (d) contrast in rock mass material properties causing strainbursting, (e) crushing of mine pillars, and (f) stress increase causing rock mass deformation (Hudyma, 2008)

Ortlepp (1992a) developed a simplified classification scheme of seismic event types, which has received attention and is widely adopted around the world by those involved in rockburst research. This valuable work was further refined by Ortlepp and Stacey (1994) and Ortlepp (1997). Their work played a significant role in bringing about the understanding that rockburst and seismic event are not necessarily one and the same thing, as had often been mistakenly assumed. In table 2.1, the classification system is structured to show firstly the different types of seismic event, with their respective postulated source mechanisms. The remaining columns in the table show the seismic motion received from

seismic sensors, and the approximate magnitude range of each seismic event category, respectively.

Table 2.1: Classification of seismic source mechanisms (Ortlepp, 1992a)

Seismic Event	Postulated Source Mechanism	Seismic Motion From Seismic Records	Richter Magnitude M_L
Strainbursting	Superficial spalling with violent ejection	Usually undetected; could be implosive	–0.2 to 0
Buckling	Outward expulsion of pre-existing large slabs parallel to opening	Implosive	0 to 1.5
Face crush	Violent expulsion of rock from opening	Implosive	1.0 to 2.5
Shear rupture	Violent propagation of shear through intact rock mass	Double-couple shear	2.0 to 3.5
Fault-slip	Violent renewed movement on existing fault	Double-couple shear	2.5 to 5.0

Based on the observations made after studying rockburst incidences for many years, it has been noticed that in the first three categories of source mechanisms, the source and damage locations coincide or are indistinguishable, i.e. the rock involved in the source is probably the same rock involved in the damage (Stacey, 2013). In the last two categories, the source and damage locations are distinguishable; the source can be near to or remote from the location of the damage (Ortlepp and Stacey, 1994). Stacey (2013) adopted a simple approach, categorizing rockbursts into two types, namely strainbursts and rupture type rockbursts. Strainbursts relate to those rockbursts where

the source and damage locations are coincident, while rupture type rockbursts refer to those rockbursts where the source and damage locations are separated by some distance.

2.2.2 Types of rockbursts

2.2.2.1 Strainbursts

The conditions which are necessary for the occurrence of strainbursts are well presented by Stacey (2013), who stated that, for strainbursts to occur, the following "properties" must be present simultaneously:

"a. The rock material in which the excavation is created must have the capacity to store strain energy, and to release it violently on failure of the rock.

b. The rock mass surrounding the excavation must have the capability of storing sufficient strain energy to result in a rockburst. This capability involves the rock mass characteristics (competence, massiveness or degree of jointing), as well as the excavation geometry, including the extent of exposed surface area. The rock mass competence in the immediate vicinity (walls) of the opening will be influenced by excavation method.

c. The conditions must be conducive to the occurrence of dynamic failure. In situ and induced stresses must be sufficiently high for dynamic failure to occur. This does not imply that high stress levels are a necessary condition, since rockbursts have been experienced in low stress environments."

The following sections will attempt to unpack the above "properties" under the topics: capacity, capability and conditions.

a. Capacity

Stacey (2013) stated that both the capacity of rock and rock mass to store strain energy depends on its strength, its stiffness and its brittleness. The influence of these properties on strainbursting potential is subtly presented in

figure 2.6 below.

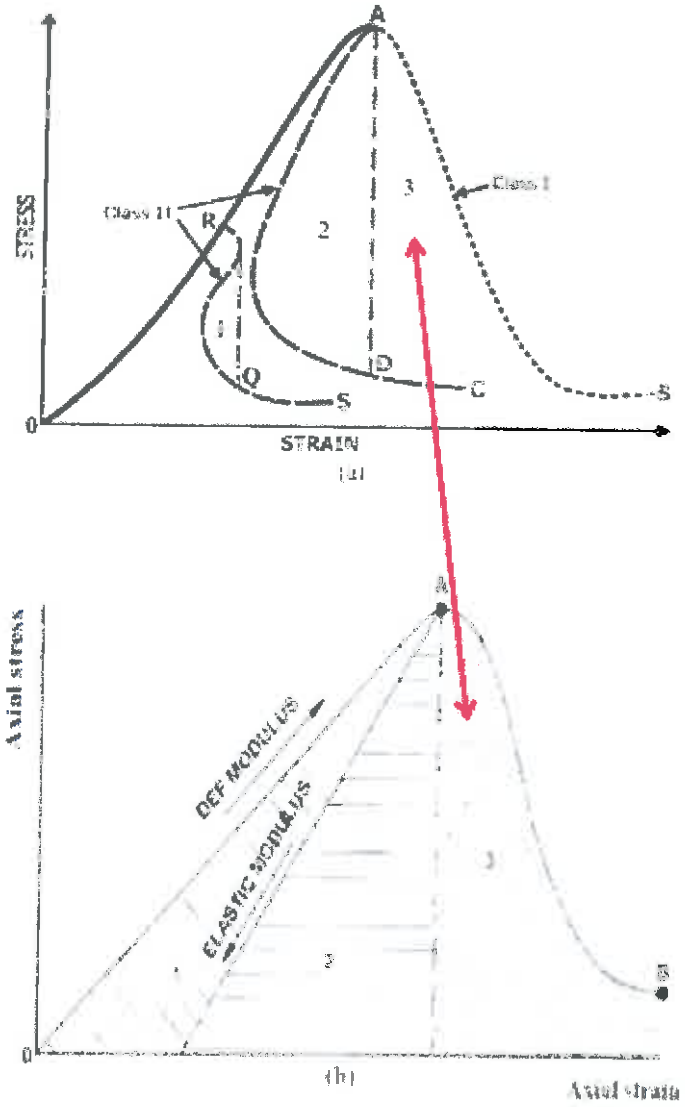

Figure 2.6: (a) Stress-strain curves of rocks, energy storage capacity of the rock and illustrations of Class I and Class II behaviours from ISRM (1999), modified by Stacey (2013), and (b) Class II characteristic behaviour (after Vogler and Stacey, 2016)

The description of the figure above is as follows:

Line OAB: Typical Class I behaviour of rock.

Area AB: (shaded 3 in fig. 2.6b) "Additional energy to be supplied by the machine to continue the test from point A to B." (Vogler and Stacey, 2016)

Line OAC: Typical Class II behaviour of rock (Test specimen no. 1)

Area 2: "Excess elastic energy stored in the test specimen, which is the energy available in the specimen but not required for further deformation. In order to achieve controlled testing from A to C, and to avoid uncontrolled, violent failure, this surplus elastic energy must be rapidly removed by the testing machine. If the rate at which the energy can be extracted is sufficiently rapid, failure of the specimen will be controlled; if not, violent failure will take place." Vogler and Stacey (2016)

Line ORS: Typical Class II behaviour of rock (Test specimen no. 2)

Area 1: Similar description as that of Area 2

The fundamental difference between rocks exhibiting Class I and Class II behaviours is based on the quantities of elastic energy that these rocks can store, and Class II rocks are generally considered to be more brittle than Class II rock types. For Class I rocks as highlighted above, sufficient energy needs to be supplied by the testing machine to bring the specimen to complete failure from point A to C in the post-peak region. In case of Class II behaviour, as noted by Wawersik and Fairhurst (1970), *"the elastic strain energy stored in the sample when the applied stress equals the compressive strength is sufficient to maintain fracture propagation until the specimen has lost virtually all strength."* The excess stored elastic energy is available for self-sustained failure of the rock. The strain energy stored within a rock under loading is effectively given by the product of stress and the strain, and thus, the lower the strength of the rock the less the energy it can store, and hence the occurrence of a strainburst. For example in figure 2.6 (a), when the peak strength of test specimen no. 1 of Class II is at point A (double the strength of test specimen no. 2), the quantity of stored energy available quadruples that in test specimen no. 1.

On the other hand, the brittleness of rock material dictates its ability to release the elastic strain energy stored with the rock (Tarasov and Potvin,

2013). Rocks exhibiting Class II behaviour are more brittle than Class I rocks, as highlighted, and this is evident in the brittleness index scale below (Tarasov and Potvin, 2013).

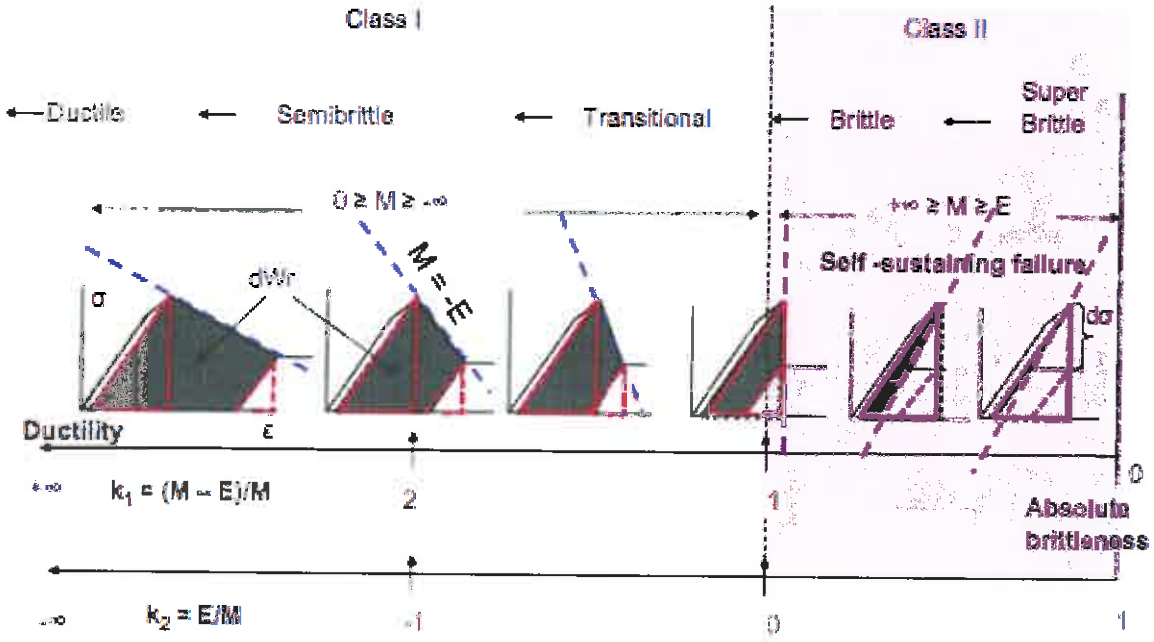

Figure 2.7: Universal scale of brittleness for rock materials (Tarasov and Potvin, 2013)

A stiff, servo-controlled rock testing machine is used to load a rock specimen under triaxial stress conditions in order to obtain the complete stress-stain curve. Two indices (k_1 and k_2) are then used to measure the intrinsic brittleness of rock using the following equations:

$$k_1 = (E - M)/M \tag{2.1}$$

$$k_2 = E/M \tag{2.2}$$

where, E=Pre-peak elastic modulus; M=Post-peak elastic modulus (E and M are the gradients determined by the average method).

Since post-peak behaviour data provides the opportunity to classify rocks as either Class I or Class II, such information has been used in light of the above brittleness criterion to evaluate the potential for rockburst occurrence and rock fragmentation (Morissette, 2015; Akinbinu, 2015; 2016). Recent findings by Vogler and Stacey (2016) suggest that caution must be exercised when one uses the post-peak region data. They commented, *"It is thus possible that the same rock material can exhibit Class I or Class II behaviour, depending on the geometry of the test specimen. A further consequence is that, whether a test specimen fails in a brittle, explosive manner or not, the behaviour is also dependent on the test specimen geometry and thus equally not only a material characteristic."*

Broch and Sorheim (1984) observed a correlation of some sort between the rock strength and the severity of rockburst damage experienced in a tunnel, illustrating the influence of rock strength, stiffness and brittleness. In the figure, it is apparent that, as the rock strength and stiffness increase, the the greater is the severity of strainbursting. This is because rocks exhibiting both high strength and stiffness are able to store more energy than their weak rock counterparts, as already mentioned. Dynamic rock failure (*i.e.* strainburst) will take place if the elastic strain energy stored in the rock around the excavation is released violently.

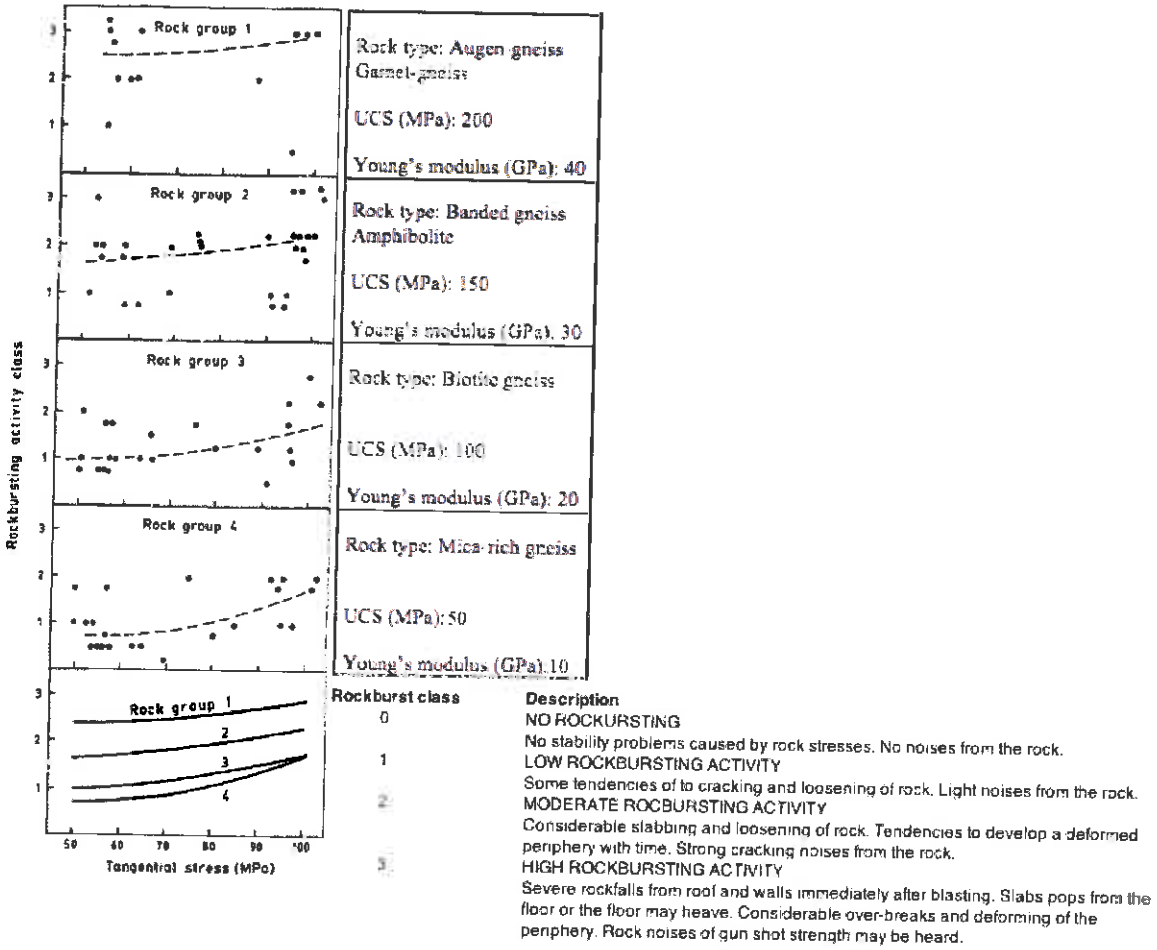

Figure 2.8: An example of the influence of rock strength and stiffness in strainbursting occurrence (Broch and Sorheim, 1984)

Broch and Sorheim (1984) further noticed that dynamic failure of strong rock around the excavation is independent of stress magnitudes around the excavation. This means that rock failure should be expected even at low stress fields for underground excavations driven in strong competent rock masses, and there are several cases to confirm this in literature, as will appear later, in the *conditions* section. While it is agreeable that strainbursting is more prone in rock with high strength, Stacey and Thompson (1991) reported that strainbursting occurrences are not excluded in relatively low strength and non-brittle rock under low stresses.

b. Capability

Capability is an equally important property, likely to increase the chances of strainburst occurrence. For strainbursting to occur, the rock mass must have the capability of storing strain energy, as well as the capacity to store strain energy. According to Stacey (2013), the capability depends on several factors such as rock mass quality, method of rock excavation, and size of the excavation.

Rock mass quality

Rock mass quality is of significant importance especially from stability of underground excavations point of view. If the rock mass is characterized by dense weak zones (joints), the resulting rock mass will be less brittle, with low stiffness, and less energy will be stored within the rock to later result in strainbursting. Conversely, a massive brittle rock mass has the potential to store an enormous amount of strain energy and this increases the likelihood of strainburst damage.

Method of excavation

It has been observed that tunnels developed by Tunnel Boring Machines (TBMs) in highly stressed rock may suffer more from dynamic rock fracturing problems than those tunnels developed using traditional drill and blast methods (Stacey and Thompson, 1991; Diederichs, 2007). Blasting has been adopted as one of the ameliorating measures to help reduce strainbursts because of its potential influence to alter the capacity of rock and rock mass to store strain energy.

Size of excavation

Large open excavations present a significant risk of strainbursting since large exposed surfaces may release greater amounts of energy in the form of rock "explosion". The contrary will be case for small-sized excavations.

c. Conditions

Apart from the properties discussed above, there are certain conditions which need to be further satisfied for strainbursting to be likely to occur. The in-situ stress levels and mine-induced stresses must be sufficient to induce failure. In-situ stresses (*i.e.* vertical and horizontal stresses) can roughly be estimated by the following equations for an excavation planned at a particular depth:

$$\sigma_v = \gamma z \tag{2.3}$$

where, σ_v is the vertical stress, γ is the unit weight of the overlying rock, and z (m) is the depth beneath the surface.

On the other hand, horizontal stress (σ_h) can easily be estimated by the following expression:

$$\sigma_h = k\sigma_v \tag{2.4}$$

where, k is referred to as the k-ratio. Hoek *et al.* (1995), among others, suggested that an equation by Sheorey (1994) can be used to provide better estimation:

$$k = 0.25 + 7E_h\left(0.001 + \frac{1}{z}\right) \tag{2.5}$$

where, z is the depth beneath surface and E_h is the average deformation modulus of the earth's upper crust, measured in the horizontal direction.

However, it advisable that in situ stress measurements be conducted in order to increase the confidence level regarding the field stress magnitudes and their orientations, since such information is crucial in understanding rock behaviour around excavations. Alternatively, a stress measurement database in a region of proposed mining activity, if available, could be used to gain some insights

into pre-mining stresses (Wesseloo and Stacey, 2006).

Once an opening is excavated in the ground, stress re-distribution due to the excavation is inevitable. Failure in the periphery of an excavation should be expected if the induced stresses exceed the strength of the rock, as highlighted previously. In brittle hard rock, however, this is not always the case. Early experience gained in South African gold mines revealed that strainbursts or progressive spalling failure was common when the maximum far-field stress (σ_1) (which can be obtained using equation 2.3) was less than the uniaxial compressive strength of the rock (σ_c) (Hoek and Brown, 1980). Hoek and Brown (1980) used the maximum far-field stress to laboratory uniaxial compressive strength ratio criterion to assess the dynamic instability of tunnels developed in brittle rock. From figure 2.9, minor spalling will occur when $\sigma_1/\sigma_c > 0.1$ – 0.2 and severe rockbursting should be expected when $\sigma_1/\sigma_c = 0.5$.

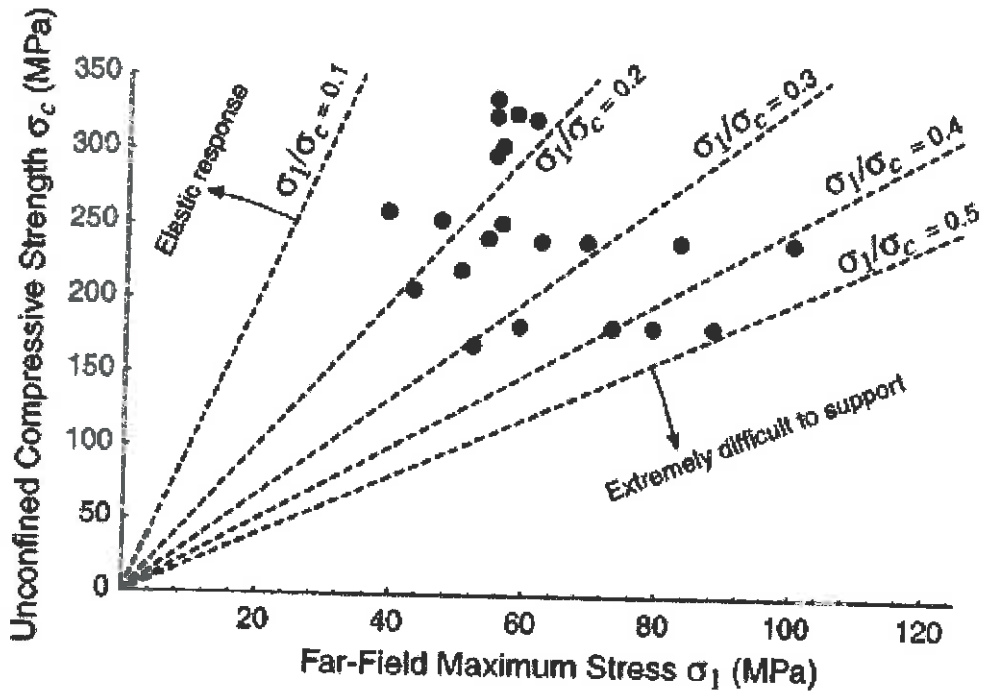

Figure 2.9: Empirical stability classification of square tunnels (Hoek and Brown, 1980)

Martin *et al.* (1999) used the ratio of the tangential maximum stress (σ_{max})

to the laboratory uniaxial compressive strength to assess brittle rock failure around tunnels. Their empirical damage index (D_i) defined by σ_{max}/σ_c suggests that brittle failure initiation will occur when $D_i > \approx 0.4$. Figure 2.10 is an example of tunnel instability and brittle failure (shaded gray squares) as a function of Rock Mass Rating (RMR) (Bieniawski, 1989) and the ratio of the maximum far-field stress (σ_1) to the laboratory unconfined compressive strength (σ_c), as well as the corresponding ranges of mining or excavation stress concentrations defined by σ_{max}/σ_c (Martin *et al.*, 1999).

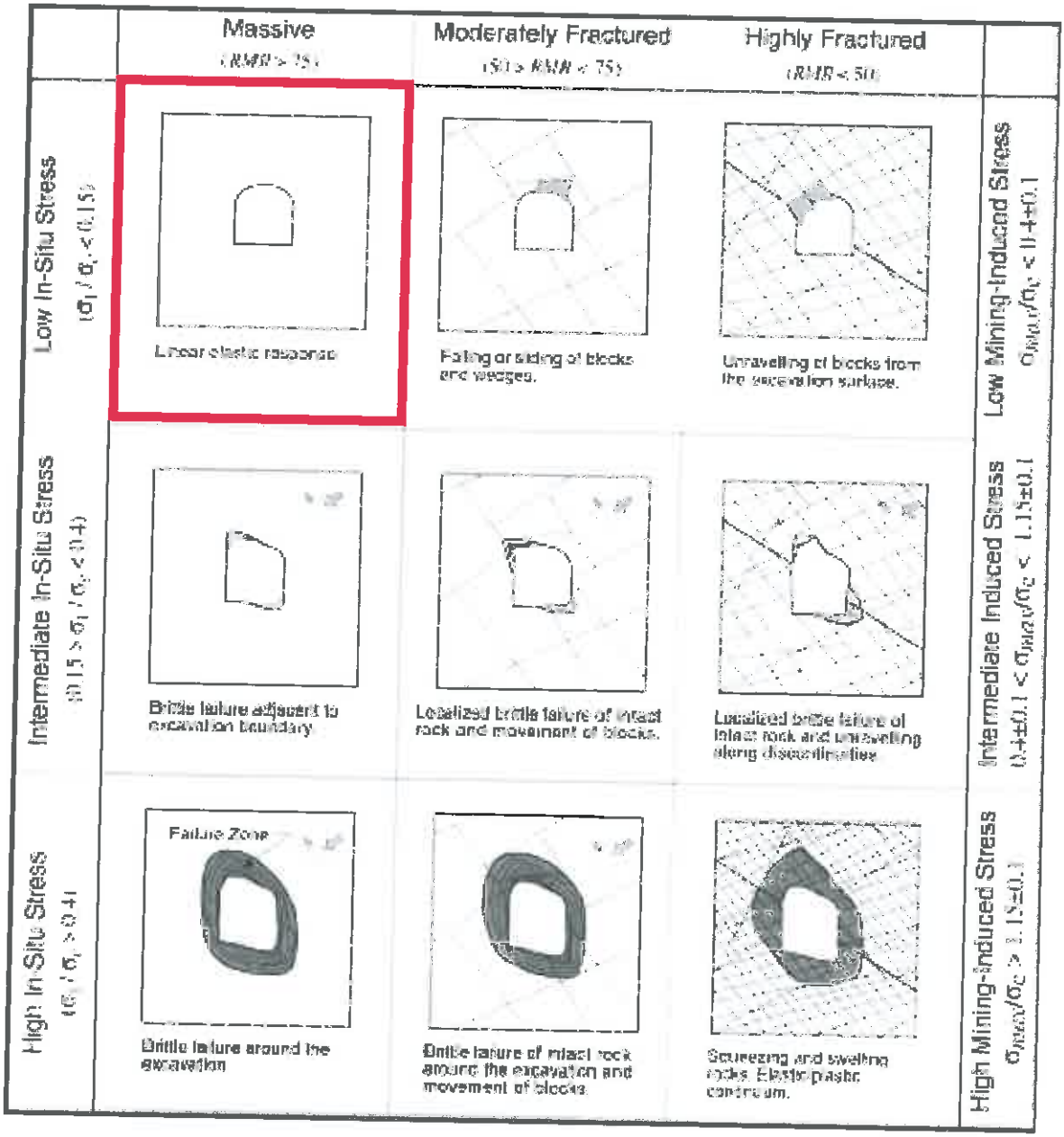

Figure 2.10: Tunnel instability and brittle failure (shaded gray squares) as a function of Rock Mass Rating (RMR) and the ratio of the maximum far-field stress ($_1$) to the laboratory unconfined compressive strength (σ_c) (Martin *et al.*, 1999)

From the figure above, one may gain the impression that brittle failure or dynamic rock failure is only possible in the region between intermediate and high in-situ stresses as portrayed. Stacey and Yathavan (2003) conducted a review of rockburst incidences experienced at very low stress conditions. Table

2.2 below summarizes numerous case studies of rockbursting encountered in Norwegian tunnels, and this corroborates the fact that dynamic rock failure is possible in the low stress region highlighted in red in figure 2.10.

Table 2.2: Examples of dynamic rock fracturing at low to intermediate stress conditions (Stacey and Yathavan, 2003)

Tunnel	σ_1/σ_c	Rock damage
Strynefjellet	0.23	Slabbing
Hoyanger I	0 – 0.33	Spalling
Hoyanger II	0.19 – 0.33	Spalling
Kobbskaret	0.15 – 0.35	Spalling
Heggura	0.10 – 0.20	Spalling
Svartisem II	0.4	Slabbing
Tafjord	0.14 – 0.3	Spalling
Fjarland	0.23	Spalling
Frudalem	0.17 – 0.43	Spalling
Tosem	0.10 – 0.18	Spalling
Fodnes	0.20 – 0.30	Spalling
Amla	0.13 – 0.20	Spalling
Laerdalstunnel	0.26 – 0.40	Spalling

Figures 2.11 and 2.12 are examples of dynamic rock fracturing at low stress conditions experienced in shallow coal mining environment and quarry mining, respectively.



Figure 2.11: An example of violent dynamic rock failure in competent rock at very low stress levels (Stacey et al., 2007)

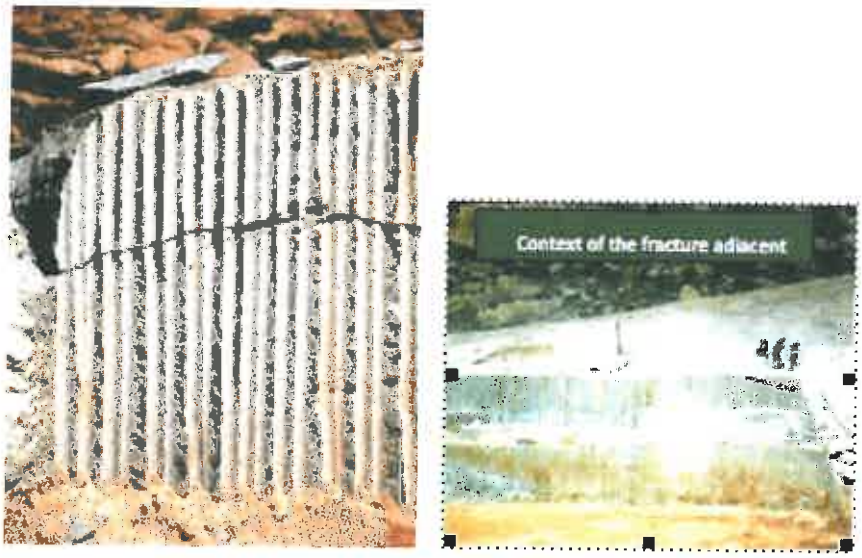

Figure 2.12: An example of violent fracture development in a quarry (Stacey et al., 2007)

Damage mechanisms associated with strainbursts

Diederichs (2007) defined strainbursting as the violent rupture of a volume of wall rock subjected to high stress. The rock involved in damage is often brittle

and massive in nature as discussed in the previous section. The dominant mode of brittle rock failure in deeply buried excavations may manifest in the form of spalling, slabbing or breakouts (Fairhurst and Cook, 1966; Ortlepp *et al.*, 1972, Gay, 1973; Stacey and De Jongh, 1977; Hoek and Brown, 1980; Nemat-Nasser and Horii, 1982; Stacey, 1981; Stacey, 1989; Zheng *et al.*, 1989; Stacey and Thompson, 1989; Ewy and Cook, 1990; Martin, 1993, Diederichs, 2000), and if such failure is extreme or violent, it may be classified as strainbursting (Hoek *et al.*, 1995; Wesseloo and Stacey, 2000; Diederichs, 2007).

Strainburst generated fragments are characterized by sharp thin plates of rock with sharp edges (see figure 2.13 (c)). According to Ortlepp and Stacey (1994), *"the nature of the surfaces of the ejected fragments usually indicates extensional fractures; and the mechanism is probably buckling of the thin diaphragm, slab, or column rock."* In many cases, strainbursting and buckling are treated as two different rockburst damage mechanisms. However, the description of ejected rock fragments given by Ortlepp and Stacey (1994) shares some similarities with the fragments observed in what seems to be slabbing or buckling (figure 2.13 (e)), but at relatively large scale in terms of the size of rock fragments generated.

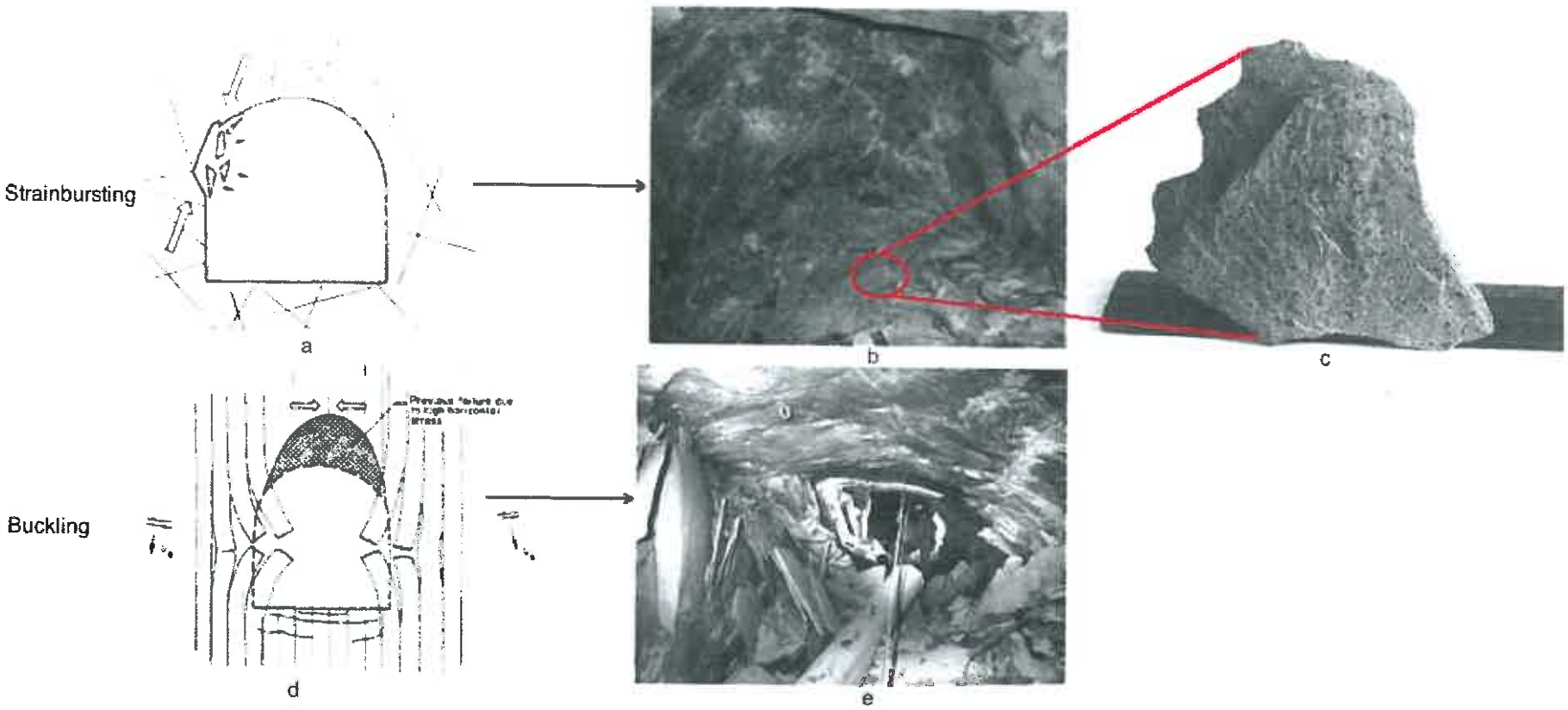

Figure 2.13: Examples of fragments size variation caused by strainbursts and buckling (Illustrations and photographs by Ortlepp, 1997)

From figure 2.13 (a), strainbursting occurs in the form of spontaneous spalling or ejection resulting from stress concentration in the immediate skin of an excavation, where the tangential stress is maximum. This spontaneous, violent failure occurs before the extension cracks penetrate or develop further away from the excavation wall (Ortlepp and Stacey, 1994). Rock fragments following strainbursts can be ejected at high velocities, say 10 m/s or even more, which presents a serious safety hazard.

Figure 2.13 (d) is an example of outward expulsion of laminated rock strata parallel to the sidewalls of a tunnel indicating Euler buckling behaviour. Buckling can be a result of pre-existing or newly formed extension fractures orthogonal to the direction of the minor principal stress. The concept of rock splitting (in the form of buckling) in the direction parallel to the maximum compressive stress in the vicinity of excavations has long been recognized as rockbursting. Below are two examples indicating the evolution of the buckling process (Figures 2.14 and 2.15). The process of buckling generally involves crack initiation which is followed by the formation of extension fractures. The spacing of these fractures from one another may ultimately define the thickness of rock slabs. According to Diederichs (2007), *"It is the instability created (e.g. buckling) by the formation of parallel and thin spall slabs that provides for the sudden energy released..."*

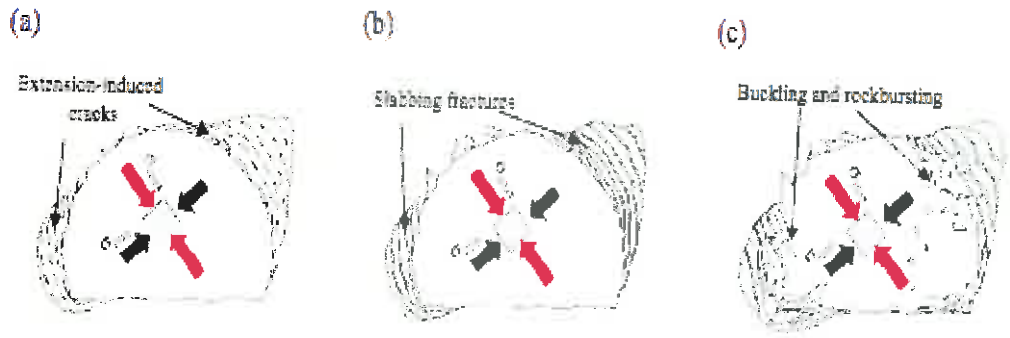

Figure 2.14: Illustration of buckling process nearby an excavation (Qui *et al.*, 2014)

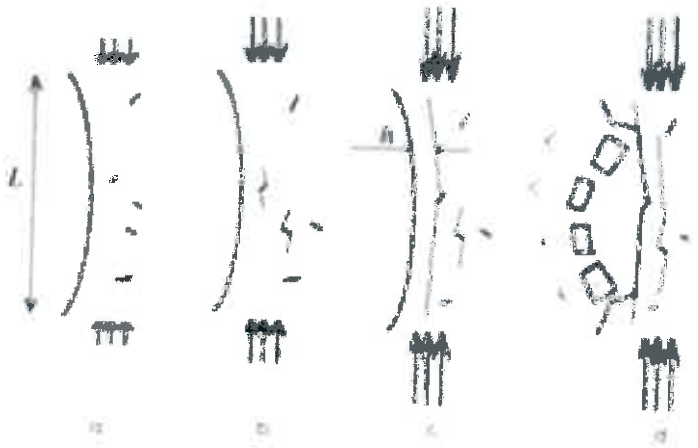

Figure 2.15: Illustration of buckling process in excavation surface when only maximum compressive stress is considered (Dyskin and Germanovich, 1993)

Morissette (2015) reconciled rockburst damage mechanisms reported by Kaiser *et al.* (1996) and Ortlepp (1992). In figure 2.16 it can be seen that strainbursts, buckling and bulking are grouped together. Common to these modes of failure is that they occur often in highly stressed rock. In summary, strainbursts could be the result of ejection or buckling of rock around the excavation in a violent manner.

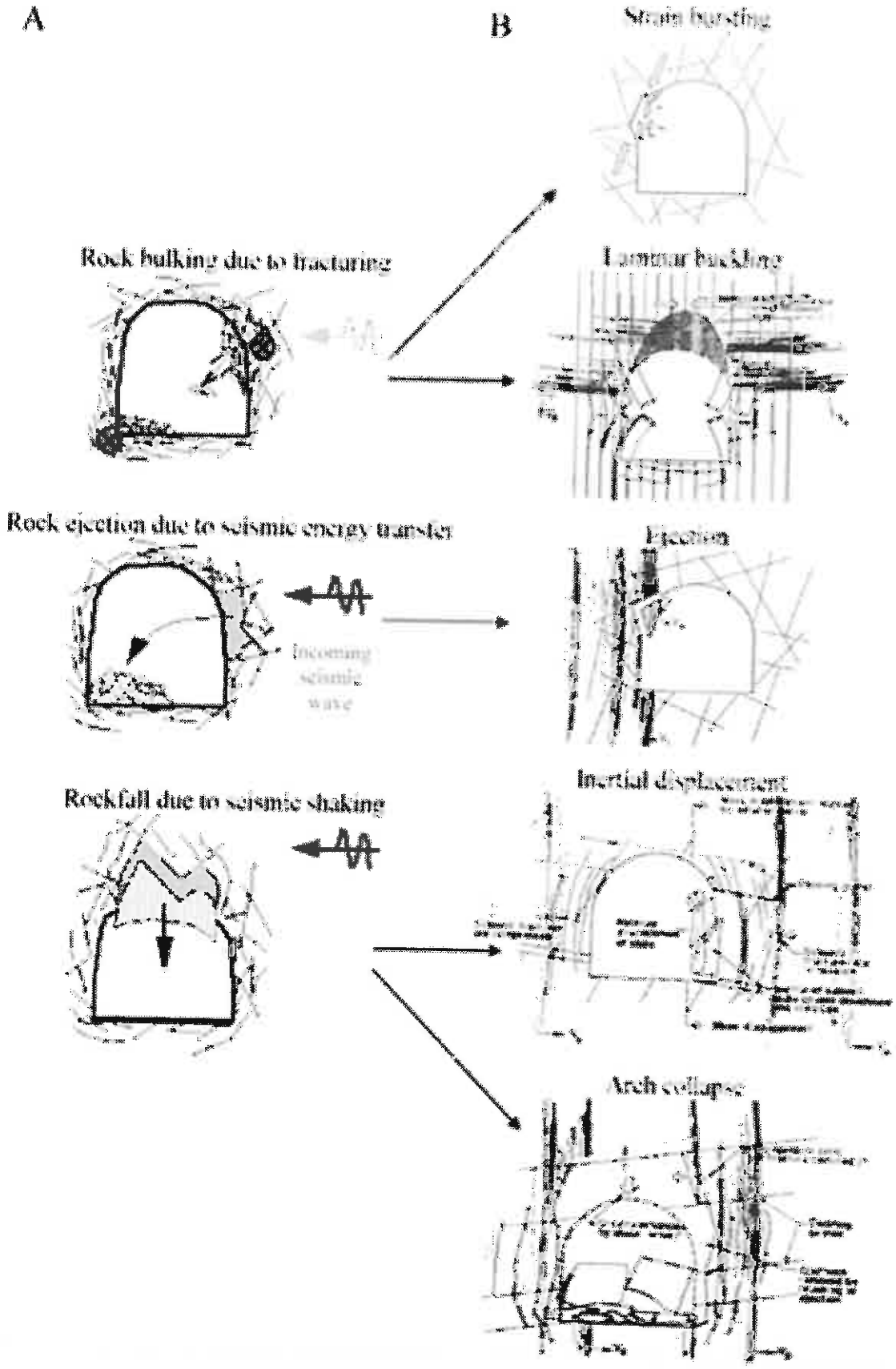

Figure 2.16: Reconciliation of rockburst damage mechanisms identified by (a) Kaiser et al. (1996) and (b) Ortlepp (1992) (modified by Morissette, 2015)

2.2.2.2 Rupture type rockbursts

Rupture type rockbursts involve seismic sources such as fault-slip and shear rupture (Ortlepp, 1992). The former involves re-activation of movement on existing geological structures such as dykes and faults, while the latter involves development of shear ruptures in intact rock masses. These two seismic sources can generate significant amounts of energy in the form of seismic/shock waves (P and S waves). It is not the passage of seismic waves in the rock mass which causes damage, but rather their interaction with mine excavations (Stacey, 2013). The damage caused by these waves can be devastating, both in surface and underground structures. Below are two examples showing severe damage experienced in a deep gold mine tunnel, and total collapse of a surface structure caused by mine-induced seismicity in South Africa.

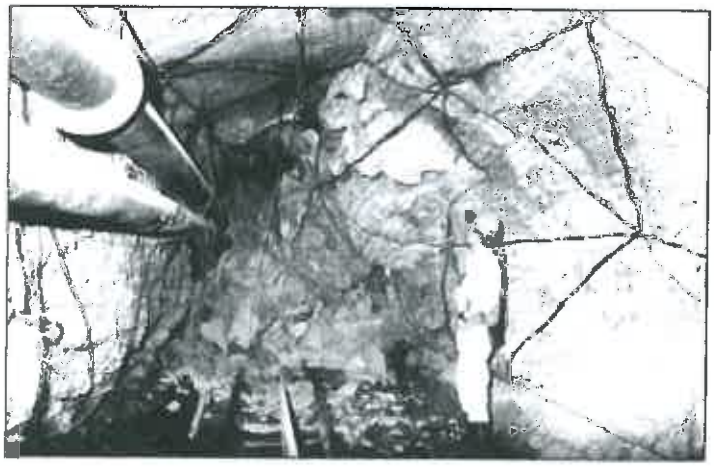

Figure 2.17: Total closure of a section in a tunnel caused by rockburst damage following $M_L = 3.6$ mine tremor occurrence (photograph W.D. Ortlepp, Durrheim 2010)



Figure 2.18: Six- storey building collapse in Welkom caused by $M_L = 5.2$ mine tremor (Durrheim, 2010)

The support method reported in this study aims to help combat the impacts caused by rupture type rockbursts, where the source of seismic event is distant from where rockburst is likely to occur. This section will address the following aspects:

- Identification of rupture-type seismic sources using seismic monitoring data
- Seismic/shock waves propagation in rock media, and rockburst damage caused by seismically-induced shock waves

a). Identification of rupture-type seismic sources

Mine-induced seismicity is not a random phenomenon, but a result of local and inelastic deformation within the rock mass associated with a distinct seismic source (Potvin, 2009; Potvin *et al.*, 2010a). Potvin *et al.* (2010a) defined seismic source as "a location where a mine induced change in the stress field combines with a geological feature(s), (it could be discontinuities or lithologies)

to produce a violent failure process." In addition, the violent failure process in the source may involve development of shear rupture in the intact rock mass (Ortlepp, 1997; Tarasov, 2014). This, together with the above, all form part of rupture-type seismic sources. As highlighted previously, these seismic sources have the potential to release significant quantities of seismic energy (large seismic events) with potential to cause catastrophic damage. *"Monitoring seismicity to identify and evaluate failure processes in the seismic sources of a mine is a valuable methodology for identifying and evaluating seismic risk"* (Hudyma, 2008). In this section, a statement by Hudyma is elaborated by an interesting case study extracted from a paper titled *"Interpretation of seismic data and numerical modelling of fault reactivation at El Teniete, Reservas Norte sector"* presented by Potvin and his co-workers (2010a). The case study provides means of detection and delineating rupture-type seismic sources, while the section following this focuses on wave propagation generated from these sources and the consequent rockburst damage in underground excavations.

Reservas Norte (RENO) sector, El Teniente Mine, started experiencing episodes of rockburst events since 2001, which negatively affected the rate of advance of caving. Following a major rockburst event in August 2005, the company was forced to revise current designs at the time in order to explore other viable options, aimed at enhancing mining efficiency and safety. A first step towards achieving the above was to identify possible seismic source/s responsible for seismic activities being experienced in the area. Seismic data from 2004 to 2008 was used to generate a seismic source model. A seismic source model is comprised of clusters of events grouped together, for instance, in terms of similarity of source parameters, spatial proximity of clusters and based on the correlations which exist between known geological structures or geometrical features *etc.* (Potvin and Wesseloo, 2013a). In-depth analysis and interpretation of clusters of seismic events in mines based on the Compre-

hensive Seismic Event Clustering technique (CSEC) is provided by Hudyma (2008). Figure 2.19 shows different cluster groups superimposed with a structural map comprised of major faults. It was found that 90% of seismic events clustered coincide with four faults encircled in figure 2.20 below.

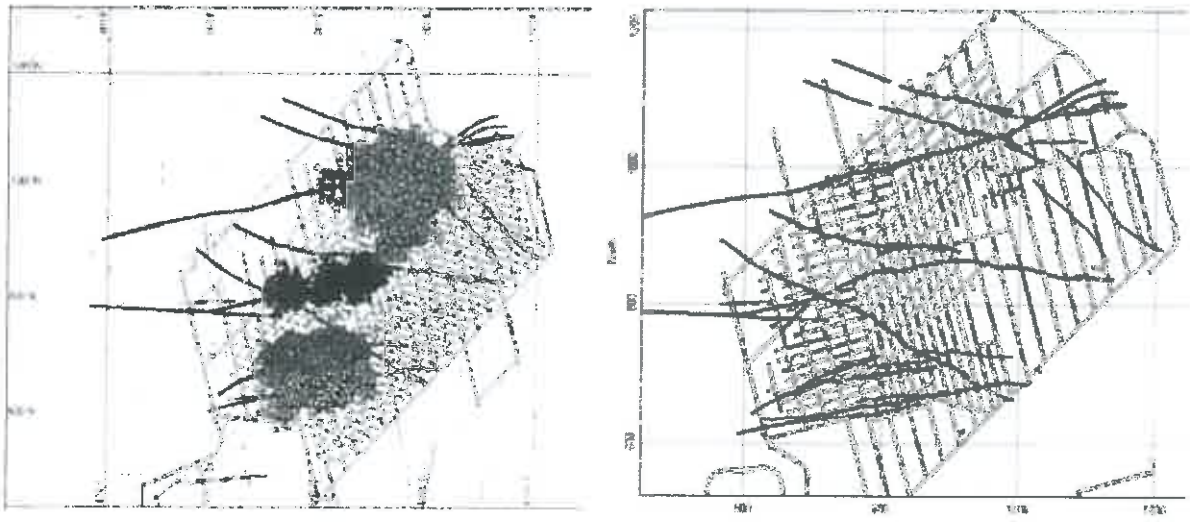

Figure 2.19: Plot of cluster groups (left) at RENO sector compared to location of faults (right) (Potvin *et al.*, 2010a)

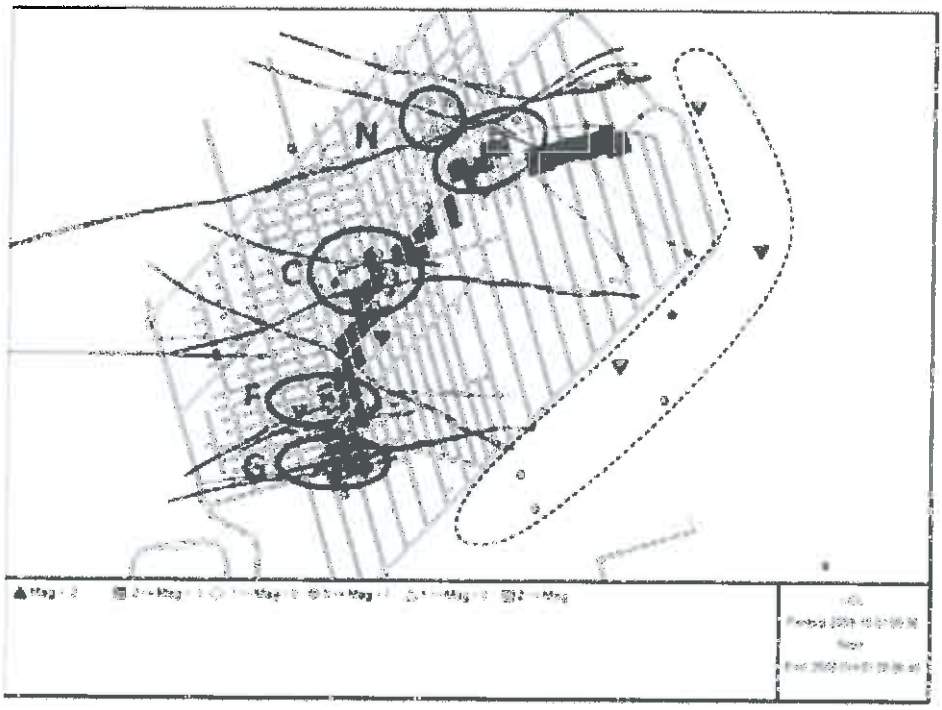

Figure 2.20: Superimposition of faults G, F, C and N1 with large seismic events (Potvin *et al.*, 2010a)

Three seismic source parameters were considered and analysed to assess seismic source mechanisms associated with the identified seismic sources.

Seismic energy

Seismic energy radiated by four seismic sources were estimated for both P and S waves using the following equation after Gibowicz and Kijko (1994).

$$E = 4\pi\rho c R^2 \frac{Jc}{Fc^2} \tag{2.6}$$

where,

E= radiated energy $(joules)$

ρ = rock density $\left(kg/m^3\right)$

c = velocity of the wave in rock (m/s)

R= the distance from seismic source (m)

J_c= the integral of the square of the ground velocity

F_c= an empirical radiation pattern coefficient

The velocity of wave in the rock for both P and S waves can be calculated using the following equations, respectively:

$$V_p = \sqrt{\frac{(1-v)E}{(1+v)(1-2v)\rho}} \tag{2.7}$$

$$V_s = \sqrt{\frac{E}{2(1+v)\rho}} \tag{2.8}$$

where,

ρ= density of rock $\left(kg/m^3\right)$

E= Young's modulus (GPa)

v = Poisson's ratio

Once quantities of energy carried individually by P (E_p) and S (E_s) waves are estimated, the E_s/E_p ratio is then used as an indicator to ascertain if there is any shearing at the source, and this is further discussed below for the sources dealt with in this case study.

Ratio of S-wave to P-wave energy

Potvin *et al.* (2010a) reported E_s/E_p ratio of about 23 for all the seismic events associated with the selected four faults of interest at RENO sector. They further added that 70 % of these events had E_s/E_p above 10. E_s/E_p ratio more than 10 has been suggested for the fault-slip mechanism (Gibowicz and Kijko, 1994), implying fault-slip shearing movement ahead of mining in this case, which was attributed to the advancing undercut. Seismic moment (M_o) was then used to specifically gain some insights into the size of the fault-slip.

Seismic moment

Seismic moment is widely used to estimate the size of fault-slip at the source related to the seismic event. Since this is difficult to measure in the field, the

use of the following equation is widely accepted to estimate seismic moment (Gibowicz and Kijko, 1994):

$$M_0 = 4\pi\rho c^3 R\frac{\Omega o}{Fc} \tag{2.9}$$

where,

M_0 = seismic moment (Nm)

ρ= density of rock $\left(kg/m^3\right)$

c = velocity of the wave in the rock (m/s)

R= the distance from the source (m)

Ωo = the low frequency plateau of the frequency spectrum of a waveform

Fc = an empirical radiation pattern coefficient

Figure 2.21 shows seismic response of three selected faults to undercut blasting estimated from cumulative seismic moment data for the period of five years considered in this study.

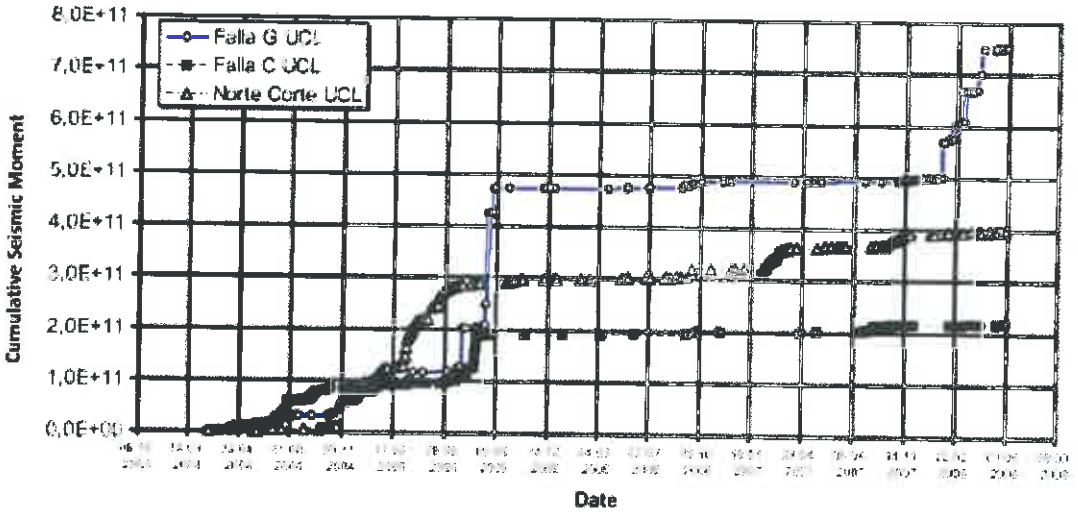

Figure 2.21: Cumulative seismic moment in selected faults at RENO sector (Potvin *et al.*, 2010a)

Numerical modelling was then conducted to simulate the fault-slip mechanism of the faults reported in figure 2.21. The model was calibrated against

seismic moment released by the faults. Mining steps were created corresponding to the five year span of seismic data analysed in the study. In order to calculate seismic moment from the model, Potvin *et al.* (2010a) related seismic moment with the displacement experienced by the fault, as appears in the following expression:

$$M_{0model} = GAD \tag{2.10}$$

where, G is the shear modulus, A is the area of slip and D is the mean shear displacement.

Despite challenges highlighted by the authors concerning complexities associated with modelling of block caving methods and the fault-slip process, which led to over simplification of the problem, seismic response of fault structures in terms of cumulative seismic moment (M_0) output was found comparable with cumulative seismic moment results in figure 2.21 calculated from waveform data using equation 2.9 (see figure 2.22 below). It was concluded that the calibrated model generated can be used to forecast future seismic responses, and that it can be used as a tool to rank different undercutting rates and geometries in terms of seismic hazard.

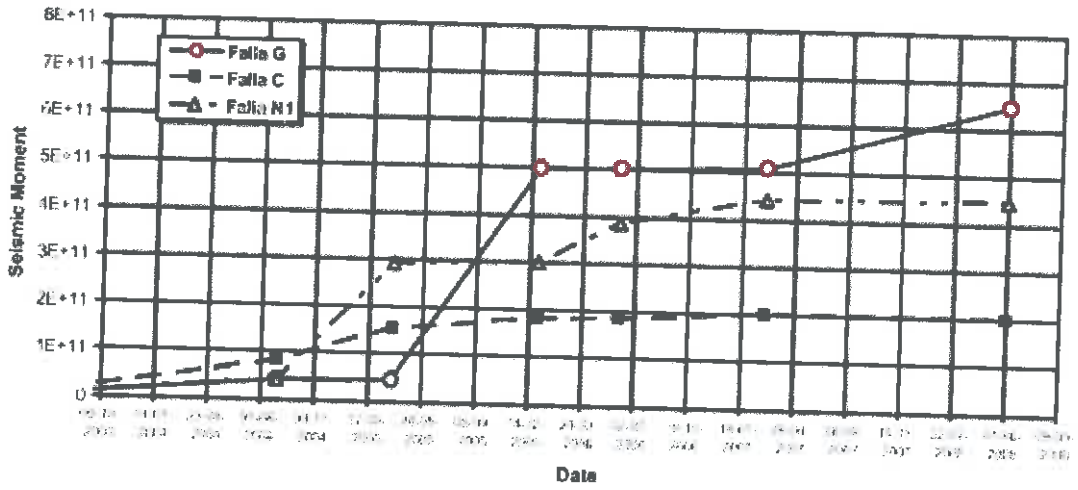

Figure 2.22: Cumulative seismic moment obtained using numerical modelling (Potvin *et al.*, 2010a)

Seismic monitoring is vital, especially in the early stages of mining (Potvin and Wesseloo, 2013a; Stacey, 2013). If seismic activities are detected early, mine design and planning can be optimized to help lessen seismic hazard. This will require a dense array of seismic sensors to obtain high quality data to help improve estimation of events location and their magnitude, and will also require in-depth knowledge about the geology of the area, particularly structural geology. In recent years, high resolution 3D seismic imaging has been successfully used in the Witwatersrand basin of South Africa to trace fault structures which might be potential conduits for water and methane in deep gold mines (Manzi *et al.*, 2012). These conduits were attributed to be corridors to transport water (water inrushes) and noxious gases in underground workings. There is no doubt that a combination of high resolution 3D seismic mapping and seismic source model interpretation could help to delineate active seismic sources ahead of mining as part of a seismic hazard management programme. It is, however, regrettable that current seismic monitoring techniques are not capable of predicting when and where the next event will occur. Meaning that an attempt to predict rockburst damage occurrence is a far-fetched pursuit at present. The following section will address aspects of seismic wave propagation in rock media and rockburst damage caused by seismically-induced shock waves.

b). Seismic/shock wave propagation in rock media and rockburst damage caused by seismically-induced shock waves

Seismic wave propagation in rock media has been extensively studied using laboratory, analytical and numerical techniques. The wave propagation phenomenon is complex since the rock mass is characterized by significant variability. Such complexity will be demonstrated in this section through relatively simple examples to complex scenarios.

Figure 2.23 shows theoretical radiation patterns of P and S waves around the hypocenter.

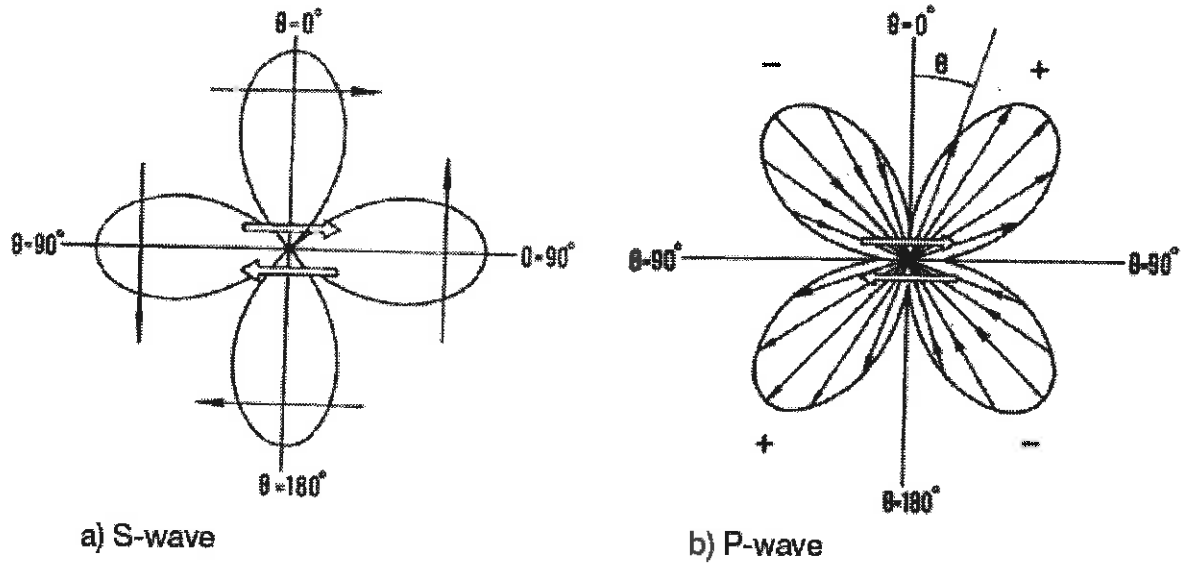

Figure 2.23: Illustration of theoretical radiation patterns of P and S waves around the seismic source (Aki and Richards, 1980))

When either of these waves encounter an interface such as a joint or crack, two things are possible: reflection and transmission of wave will take place at the interface. The coefficients of reflection and transmission at the contact depends on the fracture specific stiffness (k) and acoustic impedance ($Z = \rho C$). In the following example (figure 2.24), a wave is propagated across a vertical single fracture, while varying the fracture specific stiffness. For low values of specific fracture stiffness, the wave is slowed (measured change in time (ΔT) of wave arrival), and attenuated. When the specific fracture stiffness is infinite the transmitted wave becomes identical to the input wave. When more fractures are introduced, the problem of wave propagation becomes more evident (figure 2.25), presenting limitations to implement analytic solutions. Figure 2.25 shows wave propagation in a model without cracks (figure 2.25 (i)) against models with varying crack density (*i.e.* number of cracks in a model) and length (figure 2.26 (i) and (ii)). There is significant delay in wave arrival

time as the crack density and length increase. Information on delay in arrival time and attenuation of seismic waves has been used to diagnose the quality of the rock mass, specifically in this case to infer the state of rock fracturing around highly stressed excavations (Hildyard *et al.*, 2005).

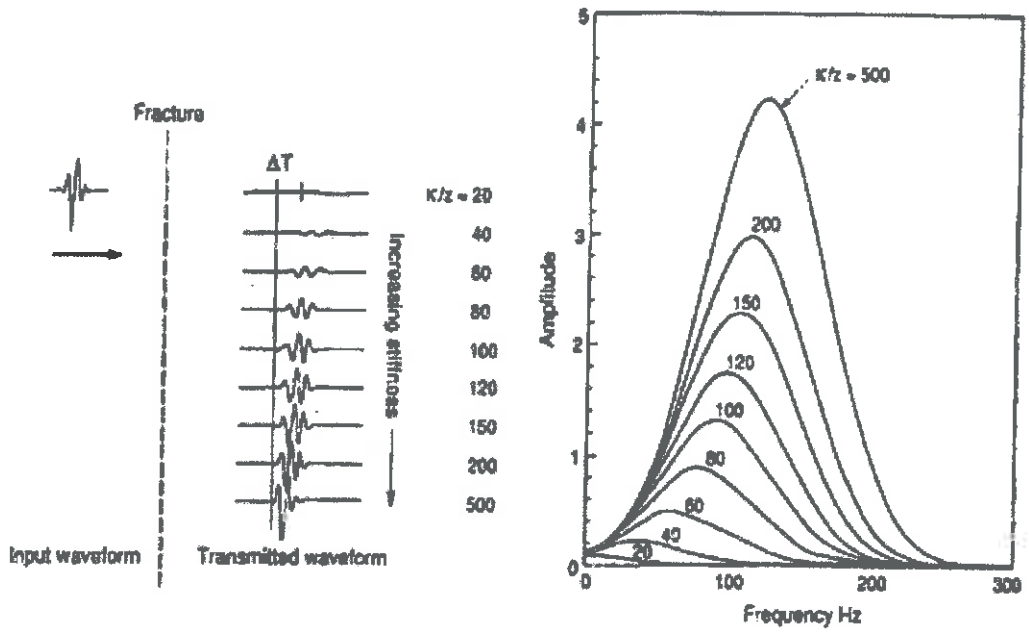

Figure 2.24: Illustration of the effects of a single fracture on the transmitted waveform and corresponding amplitude spectra (Myer *et al.*, 1990)

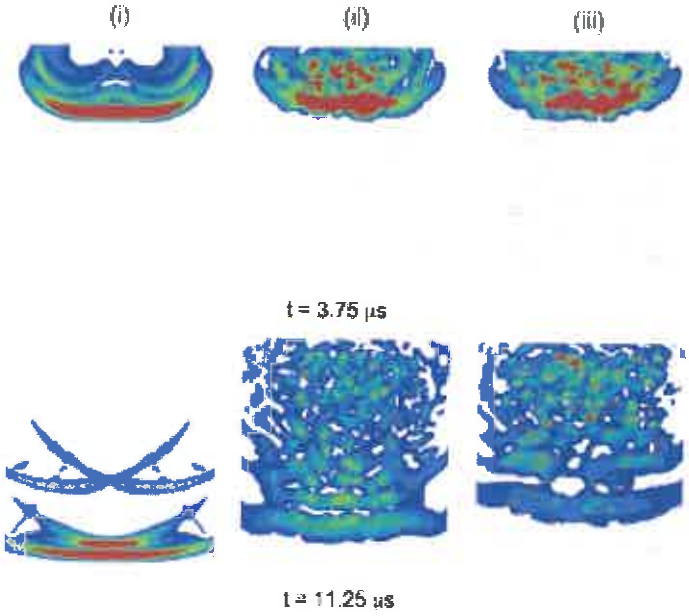

Figure 2.25: Wave propagation patterns expressed by snapshots of peak velocity at earlier time and latter time for different crack models. (i) Elastic (ii) Crack density 0.05, crack size 2 mm (iii) Crack density 0.10, crack size 3 mm (Hildyard *et al.*, 2005)

In the following example, 2D numerical modelling was conducted to study the propagation of P-waves generated by a blast load at the top left corner of the model. In figure 2.26 (a), a P-wave is propagated through a base model without any mining activity taking place, and the wave propagates without disturbance. In figure 2.26 (b), mine excavations (i.e. stopes) are introduced, resulting into strong wave reflection as the wave interacts with mined out areas. When the mined out areas are sealed with cementitious backfill material, the wave exhibit complex patterns around backfilled stopes (figure 2.26 (c)).

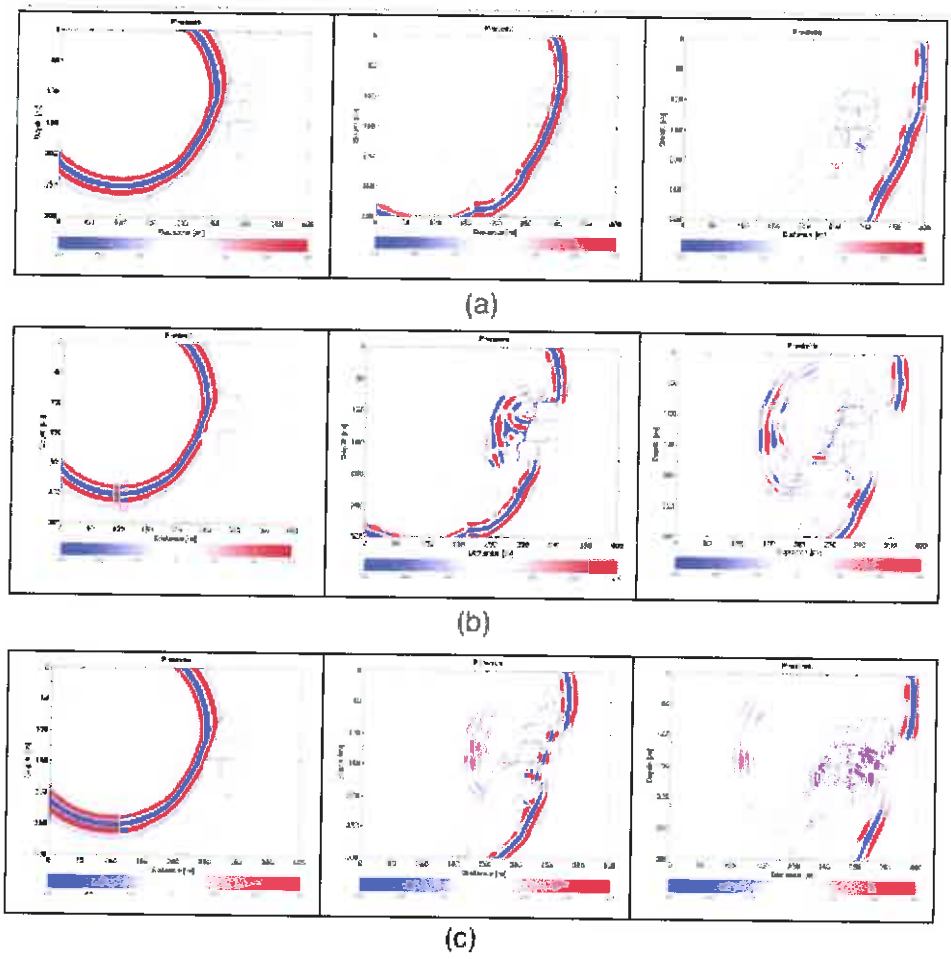

Figure 2.26: Snapshots of seismic wave propagation in (a) base model (b) model with mined out area areas (c) model with stope areas backfilled with cementitious materials (Saleh *et al.*, 2015)

The last example in demonstrating some of the complexities associated with wave propagation in rock media involves photoelastic experiments carried out by Daehnke (1997) to investigate seismic waves propagation and their interaction with narrow stopes common in South African gold mines (figure 2.27). A blast wave was induced at the top left corner, as shown by the origination of seismic wave propagation direction in the photoelastic physical model (figure 2.27 (a)). The wavefront in the direction of propagation is well pronounced in figure 2.27 (a), while figure 2.27 (b) displays chaotic wave propagation due to reflection and refraction of waves caused by artificial joints in the model,

bounding the stope from the top and bottom part. The matter could be exacerbated if sections of the model, separated by the two parallel discontinuities, were characterized by different mechanical impedance. If all the examples presented herein were to be combined to formulate a single scenario, it is obvious that the degree of wave propagation complexity will heighten to another level.

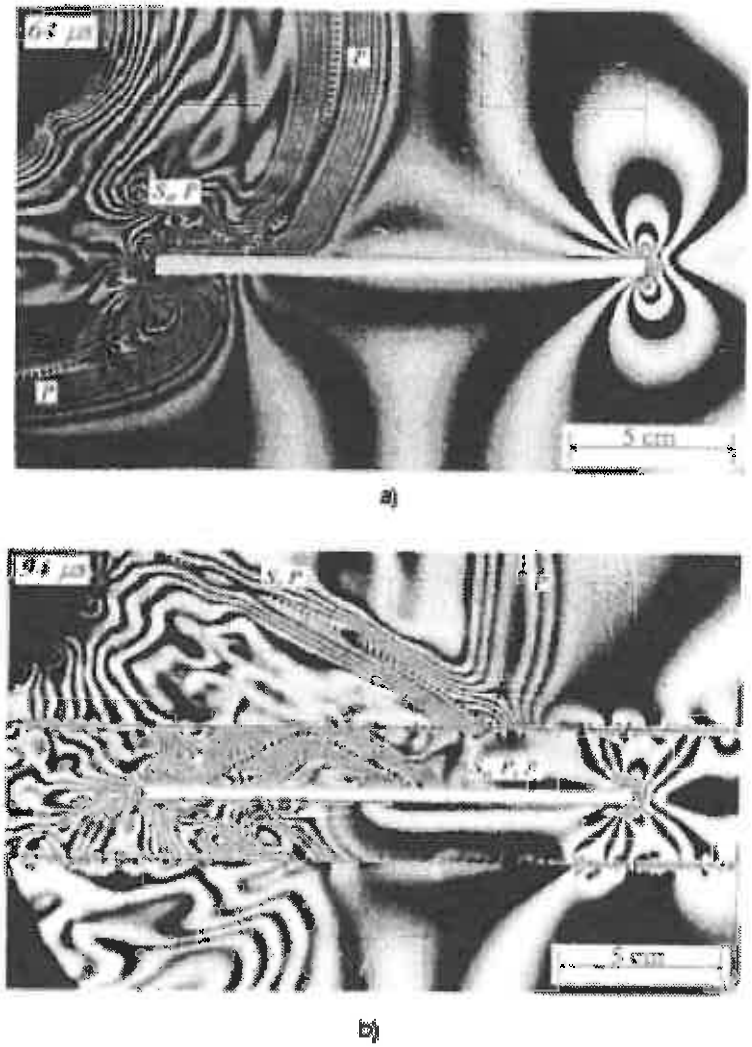

Figure 2.27: Photoelastic analysis of stress wave propagation when (a) wave interacting with a long narrow opening, and (b) when interacting with similar opening but bounded by two discontinuity plane above and below the narrow stope (Daehnke, 1997)

As mentioned previously, it is not the passage of waves in the rock mass which causes rockburst damage, but rather their interaction with mine exca-

vations. For this reason, this section will now be devoted to interaction of seismic waves with mine excavations and their consequent damage.

When the radiated waves from a seismic source encounter a void created by mining, wave reflection will take place upon reaching the free surface as demonstrated earlier (for example, figure 2.26). The reflected wave may cause rock fracturing near excavation surface, which might result in violent ejection of rock fragments (rockburst damage). The damage can be severe if the rock surrounding the excavation is highly fractured, but the presence of fractures is not a pre-condition for damage, as has been observed by the heave of unstressed concrete in rockbursts. Other waves than P and S waves could also be generated as the waves interact with excavations or with one another. According to Potvin and Wesseloo (2013b), the main factors which influence severity of rockburst damage include the magnitude of seismic event and the distance from the source. Other factors which may contribute to rockburst damage include the geometry of the excavation, the degree of rock fracturing, stress conditions around the excavation, the orientation of rock mass deformation and excavation, and the capability of dynamic rock support designed to resist rockburst damage (Hagan *et al.*, 2001; Heal 2010; Potvin and Wesseloo, 2013b). These have been categorized as "site effect" factors and this can vary from one environment to another.

Having highlighted some of the factors which might influence the severity of rockburst damage, there are fundamental questions which somehow challenge these factors as far as our understanding of rockburst phenomena is concerned. Stacey (2011) posed the following thought provoking questions based on field observations of several cases of rockburst damage:

- "Why is such damage (i.e. rockburst damage) often very localized?
- Is this localization a function of the rock support, type of support elements, quality of installation, and strength of grout?

- Is it a function of the seismic waves, their interactions, and their interactions with the excavation surface?

- Why is greater damage often associated with small magnitude events than with large magnitude events? Is it because of the proximity of the event? Is it because of direction of wave propagation? Is it because of magnification effects?"

Even with thorough forensic analysis of rockburst case studies, it is difficult to discern which factor, or combination of factors in particular, have contributed more to the occurrence of a particular rockburst incident. Without any attempt to provide answers to the above questions, it is arguable that for a rockburst to occur, seismic waves must at least interact with the excavation surface. The question of how ground motions generated by seismic waves translate into rockburst damage at the walls of mine openings has not been answered satisfactorily to date. Attempts have been made to assess the potential for rockburst damage caused by seismic wave interaction with mine excavations, and such rockburst damage criteria today form the fundamental basis for most of the design work geared towards designing a rockburst resistant support system to withstand dynamic loads (Kaiser *et al.*, 1996; Kaiser and Cai, 2012; Kaiser and Cai; 2013; Heal *et al.*, 2006). These criteria are, however, fundamentally flawed to a certain extent due to their ignorance of site amplification factor of ground motion on the surface of excavations, which could be a result of a variety of factors. The concept of seismic wave interaction with excavations and its influence in consequent rockburst damage is as complex as seismic wave propagation within rock media. This is perhaps due to lack of understanding of interrelationships which exist among factors highlighted above, and which influence rockburst damage.

2.3 Design considerations to help reduce rockburst damage in underground excavations

To date, numerous studies have extensively addressed the subject of support system design under dynamic loading conditions (Wagner, 1982; Ortlepp, 1983; Roberts and Brummer, 1988; Ortlepp, 1992a; Kaiser, 1993; Ortlepp and Stacey, 1994; Kaiser *et al.*, 1996; Cai and Champaigne, 2009; Potvin, 2009; Heal, 2010; Stacey, 2011; Durrheim, 2012; Kaiser and Cai, 2012; Mikula, 2012; Kaiser and Cai, 2013; Stacey, 2013; Stacey and Rojas, 2013; Morissette, 2015; Stacey, 2016a). This subject, like the rockburst phenomenon, has perplexed researchers for years. The continuing occurrence of rockburst damage is an indication that some deficiencies still exist in the current design rationale in burst prone environments. However, significant strides have been made to help stabilize underground excavations prone to bursting. This section focuses on the broad spectrum of design measures to ameliorate rockburst damage. First, the role of the engineering design process is highlighted.

A satisfactory engineering design is one which involves a series of steps (*i.e.* a design process) in this case presented in the form of a design wheel as shown in figure 2.28 (Stacey, 2009). Any design aims to provide a solution to a given problem and the objectives of such design need to be clearly defined earliest in the design process in order to achieve a desirable outcome. The first four steps in the design wheel under "Defining the design" are considered crucial since this phase involves collection of relevant data to help carry out the design. From the support design standpoint, comprehensive knowledge and understanding about anticipated mechanisms of loading; mechanisms associated with the rock and rock mass that the support is being designed to combat; and mechanisms of action of the support components, and their interaction, as an integrated support system is of paramount importance (Stacey, 2011).

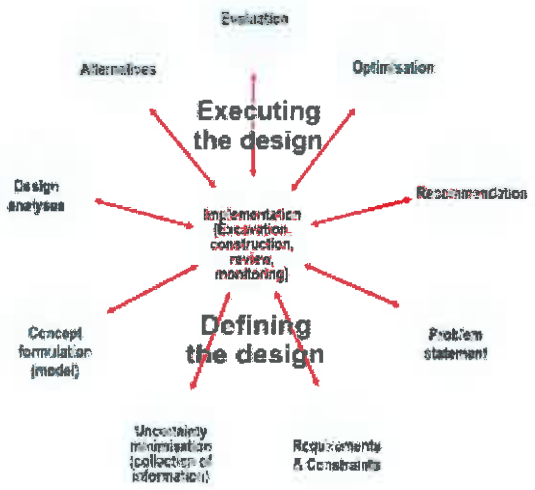

Figure 2.28: The engineering wheel of design (Stacey, 2009)

Stacey (2017) remarked that in rockbursting situations, the design must aim to fulfill the following objectives:

- *"To prevent strainbursts and rockbursts if possible.*
- *If this is not possible, to reduce the potential for rockbursts by introducing ameliorating measures.*
- *If neither of the options are satisfactory possible, to design rock support measures that will contain rockburst damage."*

It is generally accepted that neither seismic hazard, nor consequent rockburst damage can be totally eliminated. This implies that achieving the first objective in the above is seldom possible. As a result, ameliorating measures in place must at least aim to lessen seismic hazard significantly. A seismic hazard was defined by Hudyma (2008) as the occurrence of a seismic event with the potential to cause rockburst damage. Potvin and Wesseloo (2013a) and Stacey (2013; 2017) recognize three key design measures that can be implemented to help reduce the sources of seismic events and their consequent damage:

- Design of the geometries of excavations, mine layout geometry and mining sequence.
- Design of ameliorating measures to reduce seismic hazard by "changing" rock mass conditions.
- Design of suitable rock support to contain rockburst damage.

2.3.1 Design of the geometries of excavations, mine layout geometry and mining sequence

Design of geometries of the excavations, mine layout geometry and mining sequence has been regarded perhaps as an important step towards minimization of seismic hazard in the design process (Stacey, 2017). Care must be taken in the design of individual geometries of excavations and the mine layout geometry in entirety. In the case of individual geometries of excavations, circular excavations are generally considered to be more stable, whereas, square or rectangular excavations facilitate build up of stresses at the sharp corners of excavations which might initiate damage (Stacey 2017, Kasuka *et al.*, 2013, Read *et al.*, 1998).

As highlighted by Stacey (2013), the size of an excavation also matters as far as the occurrence of strainbursts is concerned. Large excavations usually expose enough surface area to be conducive to the release of high quantities of strain energy stored in the rock and rock mass. To overcome this, sizes of excavations which limit the build up of stresses around excavation walls must be designed and optimized. Long-straight surfaces, due to their susceptibility to strainbursting, could be avoided by doming both roof and sidewalls to reduce strainbursts (Stacey, 2017). Close proximity of one excavation to another also influences stress concentrations in adjacent excavations (Stacey, 2017), with more adverse impacts if the area is characterized by high horizontal stress con-

ditions (Read *et al.*, 1998). This must be taken into account during the design in order to avoid stress concentrations in the overall mining geometry. It has been observed that the overall geometry of mining can largely influence the occurrence of rupture type rockbursts as well. In order to minimize the seismic response of geological structures such as faults or dykes ahead of mining, Adams (1995) and Stacey (2017) indicated the need to modify mining layouts when mining towards geological structures by reducing the size of the mining face and the orientation of the face relative to the fault strike. Integration of numerical modelling and seismic monitoring data in this regard could be very beneficial in designing mining layouts and mine sequences aimed at reducing seismicity caused by fault or dyke structures (Mendecki *et al.*, 2001; Potvin *et al.*, 2010a). Case studies on the influence of mining geometry and sequencing in reducing the occurrence of seismicity in Australia, for instance, are documented by Potvin and Wesseloo (2013a). Handley *et al.* (2000) demonstrated the benefits of using the sequential grid mining method in minimizing seismic hazard compared with the traditional longwall mining method in South African gold mines.

Several authors have highlighted some practical challenges associated with reducing seismic hazard with a more favourable mining geometry (de Frey *et al.*, 2002; Vieira and Durrheim, 2002; Potvin and Wesseloo, 2013a; Stacey, 2017). This is because there are several factors which dictate the geometry of excavations and the ultimate mining layout geometry such as excavation usage, the nature of orebody being mined, mining method, efficiency and costs of ventilation, cleaning, face advance rates, gully dilution, and transportation of men, materials and rock *etc.* In view of this, Potvin and Wesseloo (2013a) mentioned that *"compromises must be assessed to deliver maximum value to the mine with an acceptable risk."*

Vieira and Durrheim (2002) stated that identification and quantification

of risk and optimization of mine plans is not sufficient. There is a need for continuous monitoring as part of systematic design process or holistic risk management through continuous improvement in competence, auditing of mining practice, monitoring of rock mass response (*i.e.* seismic and geotechnical monitoring), as well as quality control (Vieira and Durrheim, 2002; Stacey, 2013). The following section further presents possible design ameliorating measures to help reduce strainbursts and rockbursts, since one approach is never sufficient to help address the problem of this nature.

2.3.2 Design of ameliorating measures to reduce seismic hazard by "changing" rock mass conditions

In an interview, Stacey (2011) emphasized the fact that *"rock is about the only thing that you can't change as far as mining is concerned. You can change the ventilation....you can change the processes....you can pick the mining method and so on, but you have to do with geology and the orebody you've got...."* (https://www.youtube.com/watch?v=GuOkOHnsAc). From the rock mechanics point of view, there is however a window of opportunity to influence the behaviour of rock by implementing favourable mining geometry, as discussed in the previous section. This section presents another means of reducing rockbursts by "changing" rock mass conditions.

Preconditioning has been reported to have the potential to alter the capacity of rocks and rock masses to store strain energy and therefore, reduce the chances of strainbursting. This method has been used for years successfully as a practice to pre-fracture highly stressed stope pillars by destress blasting in order to reduce seismicity (Blake, 1972). Early experimental work on destressing was conducted in South Africa in the 1950s as a control measure to reduce facebursts in the stopes (Roux *et al.*, 1957). From figure 2.29 below, destressing reduces the stress intensity in the immediate vicinity of excava-

tion boundary by creating new fractures which reduce non-violent release of strain energy by softening the rock. Preconditioning of stope faces is now common practice in South African gold mines, to prevent hazardous face bursts (strainbursts) from the stope face (Toper, 2003).

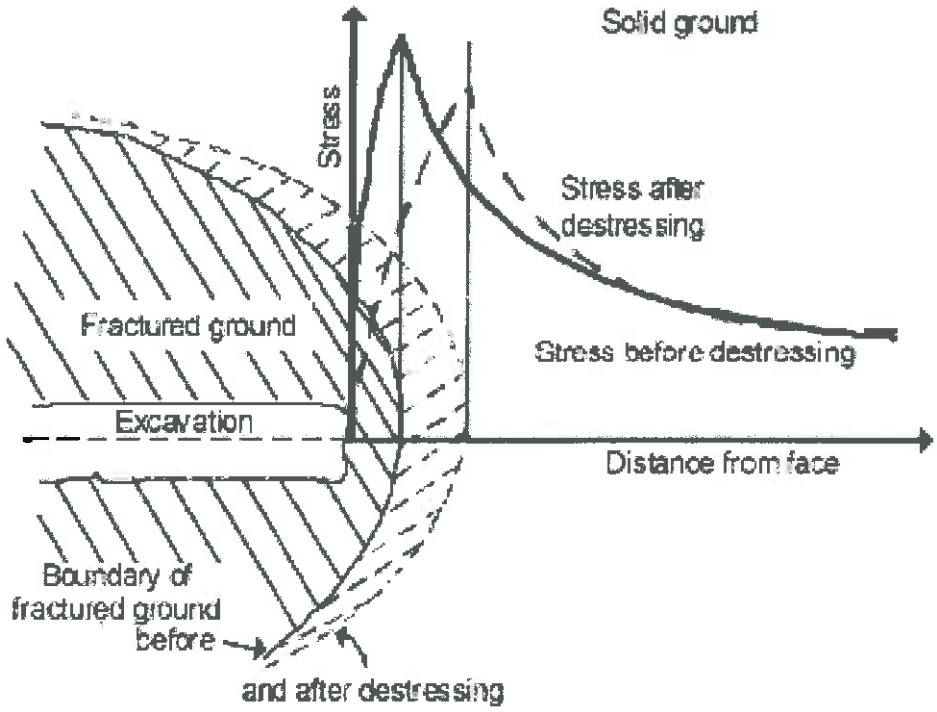

Figure 2.29: Illustration of the effect of destressing around excavation (Roux *et al.*, 1957)

Preconditioning can also be achieved through hydraulic fracturing in a huge mining operation (Araneda and Sougarret, 2007). Figure 2.30 provides an example of different mining environments where destress blasting could be applicable. Potvin and Wesseloo (2013a) emphasized the need for further research to better understand these techniques and their limitations. The following section covers aspects of rock support design to counter drastic impacts of rockburst damage, as part of a systematic design process.

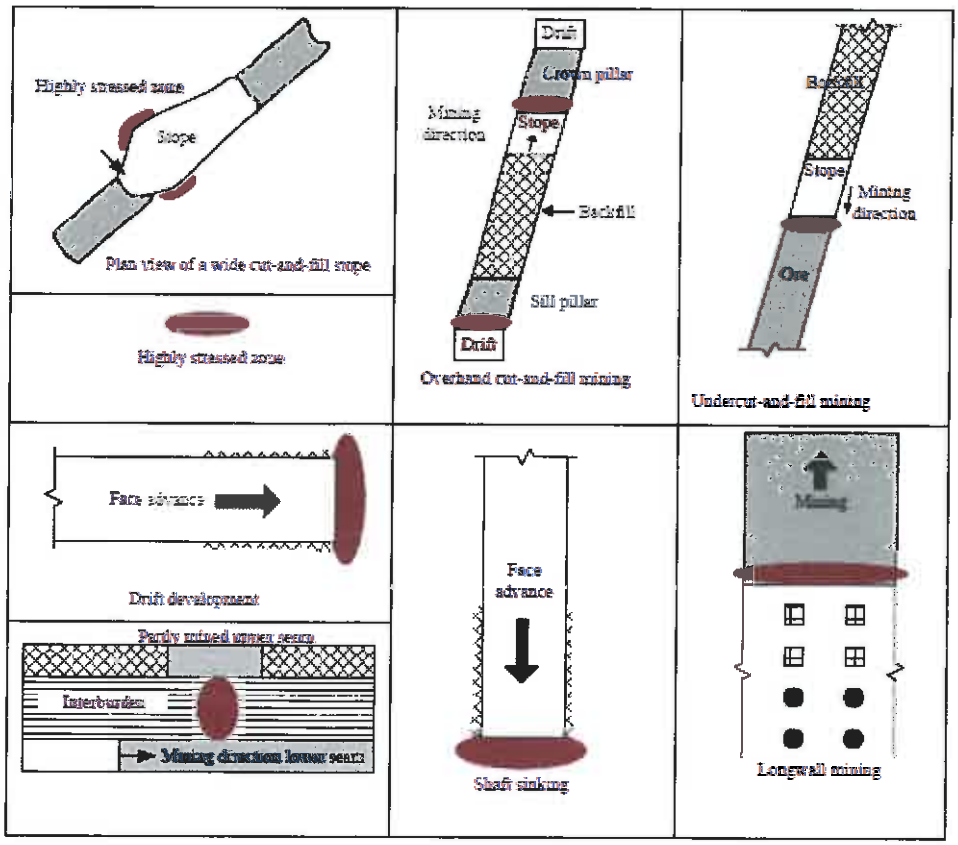

Figure 2.30: Potential areas to reduce strainbursting using destress blasting (Mitri, 2000)

2.3.3 Design of suitable support systems to cater for dynamic loading conditions

Design of ground support to prevent underground instability primarily aims to provide a match between the support system capacities and the demand imposed by failing rock acting on the rock support. If that is achieved, selection of various support elements and systems to provide stability in underground excavations can be done, and this exercise has been achieved successfully under static conditions. Mikula (2012) stated that the choice of ground support in rockbursting situations needs to contend with a myriad of factors such as complexities of seismic event mechanisms, the varying susceptibility of excavations to damage, the different damage mechanisms, the complex behaviour

of ground support systems, as well as the imprecise nature of much of the available data. This, on its own, summarily shows how complex is the design of rock support systems under dynamic loading conditions.

Three design approaches have been used in seismically active mines around the world, either individually or in combination, and these include deterministic, numerical and empirical methods. Mikula (2012) noted that there exist commonalities among these approaches as far as design methodology is concerned. The common steps involve the following:

- Define expected seismic event locations and source parameters.
- Define a ground motion relationship for the mine.
- Define damage criteria.
- Define a specification to guide selection of a scheme that would "survive the dynamic occurrence."

The first three points are combined and further discussed below under the topic "defining of seismic events and their potential corresponding damage." The discussion is followed by rock support specification for dynamic loading conditions.

2.3.3.1 Defining of seismic events and their potential corresponding damage

In recent years, estimation of seismic location, magnitude, and source parameters, is possible with some level of confidence due to increased quantity and high quality of seismic data. Clustering techniques as highlighted previously are available to group seismic events which exhibit distinct seismic sources. However, it is still not possible with the current knowledge to predict what magnitude of the next event would be, nor if it will result in rockburst dam-

age. Researchers for several years have resorted to implement the frequency-magnitude relationship to forecast the most probable event that could result in rockburst damage. Figure 2.31 shows Gutenberg-Richter frequency-magnitude relationship showing two different groups of seismic events. From the charts, a so called b-value can be obtained by fitting a straight line to the slope of the curve. Such information about the b-value has been used for deciphering of different seismic sources being experienced within the rock mass. For instance, a b-value, less than 0.8 as shown in the left chart, has been attributed to fault-slip seismicity (Hudyma, 2008).

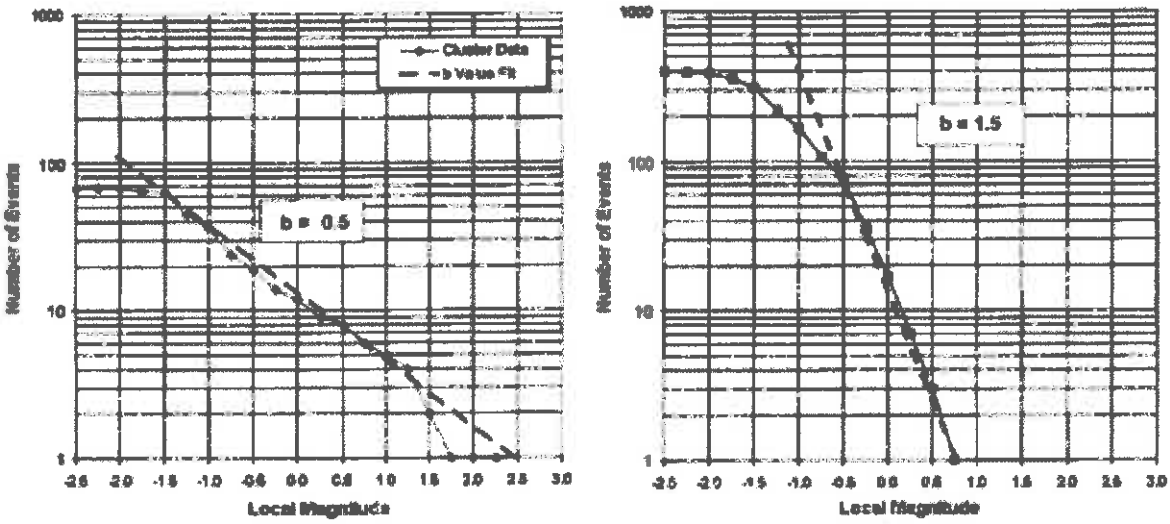

Figure 2.31: Gutenberg-Richter frequency-magnitude relationship showing two distinct groups of seismic events (Hudyma, 2008)

From frequency-magnitude relationship data, it is possible to generate seismic hazard maps based on the probability of occurrence of the largest expected seismic events. This approach requires the availability of seismic data gathered by seismic monitoring sensors deployed in and around the mine. Figure 2.32 depicts seismic hazard rating ranging from the least to the largest expected seismic event magnitudes. The current challenge, however, associated with seismic hazard rating, independent of which parameter used, is the lack of verification in retrospect to relate if the identified high hazard zones correlate

with resulting severity of rockburst damage.

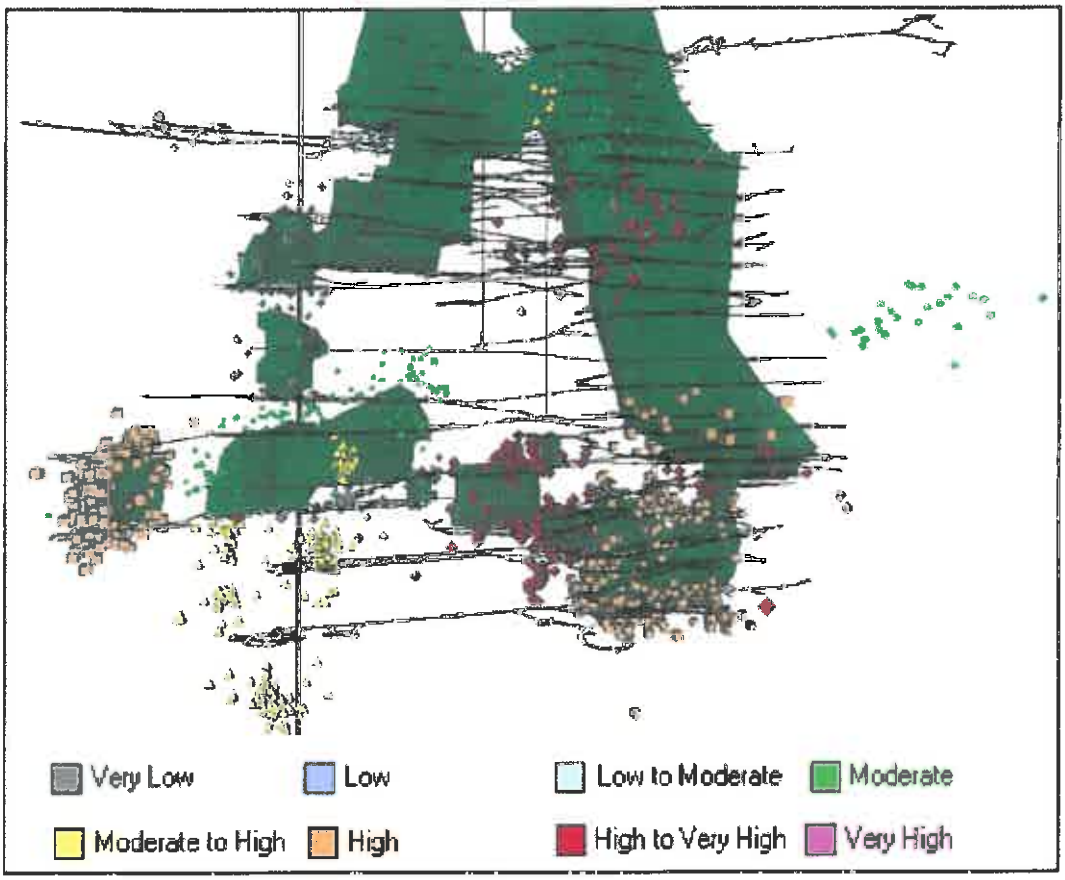

Figure 2.32: Seismic hazard map generated from clusters of seismic events (Potvin, 2009)

Once the largest expected seismic event/s has been examined for design purpose, the next step usually involves estimation of seismic energy associated with the seismic event and corresponding rockburst damage. The relative strength of waves propagating from the seismic source has been characterized by some as peak particle displacement, peak particle velocity and peak particle acceleration. Peak particle velocity (*ppv*) is preferred in characterizing the ground motion at the excavation surfaces following a seismic event. This parameter is used often around the world as a damage criterion to assess the potential of rockburst damage. To put this into perspective with rockburst damage, if a certain threshold value of *ppv* is reached at the excavation wall,

rockburst damage must be anticipated. Scaling laws are implemented to estimate *ppv* from the source of seismic event to the desirable location in the excavation (McGarr *et al.*, 1981; Hedley, 1992; Kaiser *et al.*, 1996; Potvin, 2010b). The ejection velocity of rock at the excavation boundary is equated to the *ppv* value obtained by the scaling law at the same location. With this information on expected ejection velocities, seismic demand imposed by the displaced rock during rockbursting can then be determined. The energy demand associated with seismic event at rock failure can simply be obtained by using the kinetic energy equation. However, the shortfall of equating *ppv* with ejection velocity is that ejection velocities far greater than *ppv* values estimated from seismic event magnitude and scaled-distance have been determined both experimentally and through back analysis of ejected rock fragments after rockburst events, as indicated in the table below (Piper, 1983; Ortlepp, 1992; Ortlepp, 1993; Ortlepp and Stacey, 1994; Stacey and Rojas, 2013).

Table 2.3: Ejection velocities obtained through back analysis and experimentally

References	Estimated ejection velocities (m/s)	Back analysis	Experimental analysis
Piper (1983)	≥ 55		✓
Ortlepp (1992)	10		
Ortlepp (1993)	$\geq 8; \geq 50$	✓	
Stacey and	9; 10	✓	
Rojas (2013)		✓	

In a recent study, Stacey and Rojas (2013) examined the rockburst damage dataset of Bacco (2010), who conducted back analyses of ejection velocities from observations of rockburst damage resulting from about 60 events, which occurred over a 12 years period. They reported large amplification factors for six selected events which ranged between 8 and 52, with an average value of 32. Such high amplification factors between the ejection velocities obtained by

back analysis and ejection velocities predicted from *ppv*, must be accounted for when calculating the seismic demand, as this could significantly affect the capability of rock support to resist dynamic loading. This implies that a multiplication factor must be incorporated in the kinetic energy equation to cater for amplification, and studies by Ortlepp and Stacey (1994) and Stacey and Ortlepp (2007) are good examples.

It is still debated whether *ppv* is the suitable parameter to assess the potential for rockburst damage (*e.g.* Mikula, 2012; Potvin and Wesseloo, 2013b). In addition, the use of scaling laws to estimate *ppv* has been challenged because scaling laws do not take into account the complexity of the rock mass through which the seismic waves propagate, and the influence of excavation orientation relative to seismic source, for instance, is often neglected when estimating the *ppv* (Potvin and Wesseloo, 2013b; Sahayi, 2013). The phenomenon of ground motion magnification at the excavation walls, possibly resulting from site effect, is not well understood to date.

2.3.3.2 Support specification for dynamic loading conditions

Knowledge of support system capacity and the dynamic demand imposed by accelerated rock strata during rockburst event forms the fundamental basis of support design in rockbursting environments. Before embarking on characteristics of suitable support system to withstand severe rockburst damage, this section will first discuss evaluation of support system capacity. Evaluation of demand has already been covered above.

Two common methods are used for physical testing of rock support to evaluate the support system performance under dynamic loading and these are: drop weight tests and blast experiments. Drop weight tests are used to quantify the capacity of individual support components by directly impacting the support element in the axial compression direction. Under static loading condi-

tions, pull tests are used both in laboratory and underground to determine the capacity of support components such as rock bolts. The capacity of a tendon for instance could also be inferred analytically if some mechanical properties are known.

Figure 2.33 summarizes results of surface support component capacities obtained using different drop weight test rigs, expressed in terms of their energy absorption capacities. One of the shortcomings of drop weight tests is that only individual and limited combinations of support components can be tested, and not the entire support system (which is a combination of various support components). In addition, the load applied to impact the support is only in the "axial" compression direction, which is not necessarily the case during a rockburst event. Stacey (2011) noted that a rockbolt during rockbursting can be subjected to various loads such as compression, tension, shear and torsion, or a combination of these loads. Figure 2.34 shows shear loading of rockbolts during a rockburst event. There also exists a lack of knowledge in terms of load transfer among support elements constituting a support system in an actual rockburst, making it impossible to determine the overall capacity of the support system. Blasting experiments are also used to evaluate the performance of support under dynamic loading. These two methods are further detailed in the following chapter.

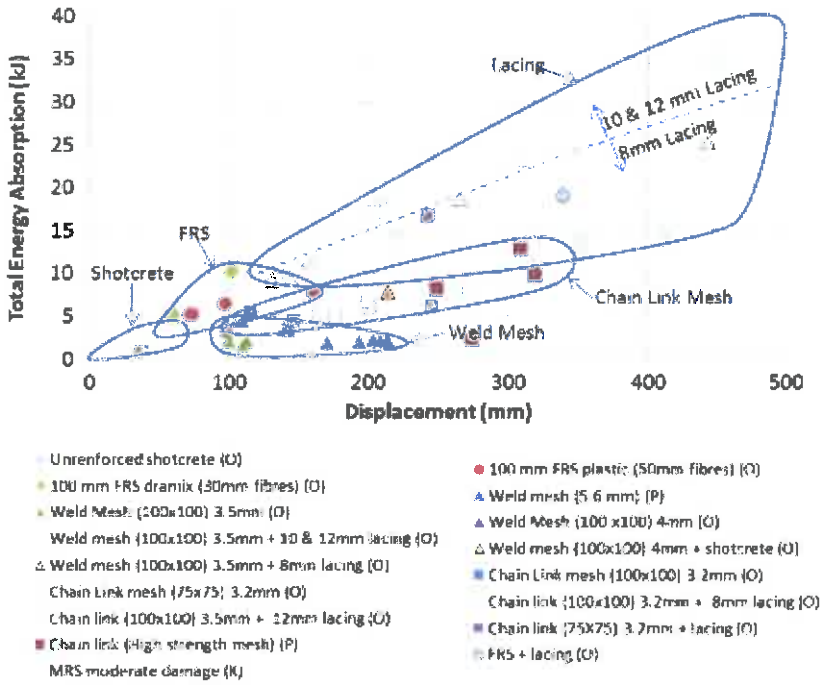

Figure 2.33: Performance of surface support systems under dynamic loading (Potvin *et al.*, 2010b)



Figure 2.34: Naked rockbolts indicating shear loading in a rockburst ejection (Stacey and Rojas, 2013)

Evaluation of the demand imposed on rock support in rockbursting condi-

tions is also a difficult undertaking as reported in the previous section. Designing a rockburst-resistant support therefore appears to be "impossible", considering the complexities associated with quantifying the capacities of support systems and the demand imposed by accelerated rock strata under dynamic loading conditions. Stacey (2011; 2012) attributed the continuing failure of support systems in burst-prone conditions to be a result of design indeterminacy resulting from a lack of understanding of support system capacity and the demand imposed by ejected rock strata in a dynamic loading environment. The problem of support design in rockbursting environment has been pronounced as a "Gordian Knot problem" (Stacey, 2013). As a result, Stacey (2011; 2013; 2016a) suggested an alternative approach to circumvent the design problem, which involves classification of rockburst type and specifying yielding support systems in a conservative manner.

Taking cognisance of the complexities associated with quantifying the support element system capacity and the demand, a number of studies have demonstrated the capability of various support elements to resist rockburst damage based on their yieldability. According to Ortlepp (1992), support subjected to dynamic loading must be able to withstand severe loading and accommodate large deformations at the same time. Figure 2.35 demonstrates the mechanical behavioral principles of a novel bolt (*i.e.* Negative Poisson's Ratio (NPR) bolt) characterized by high energy absorbing capacity and large deformation during dynamic rock fracturing (He *et al.*, 2014). Numerous rockbolts with large yield capabilities have been designed, and used in mining operations. These include Conebolts (Jager, 1992), modified Conebolts (as used by Simser *et al.*, 2007), D-bolts (Li, 2010) and Garford bolts (Varden *et al.*, 2008) to mention a few.

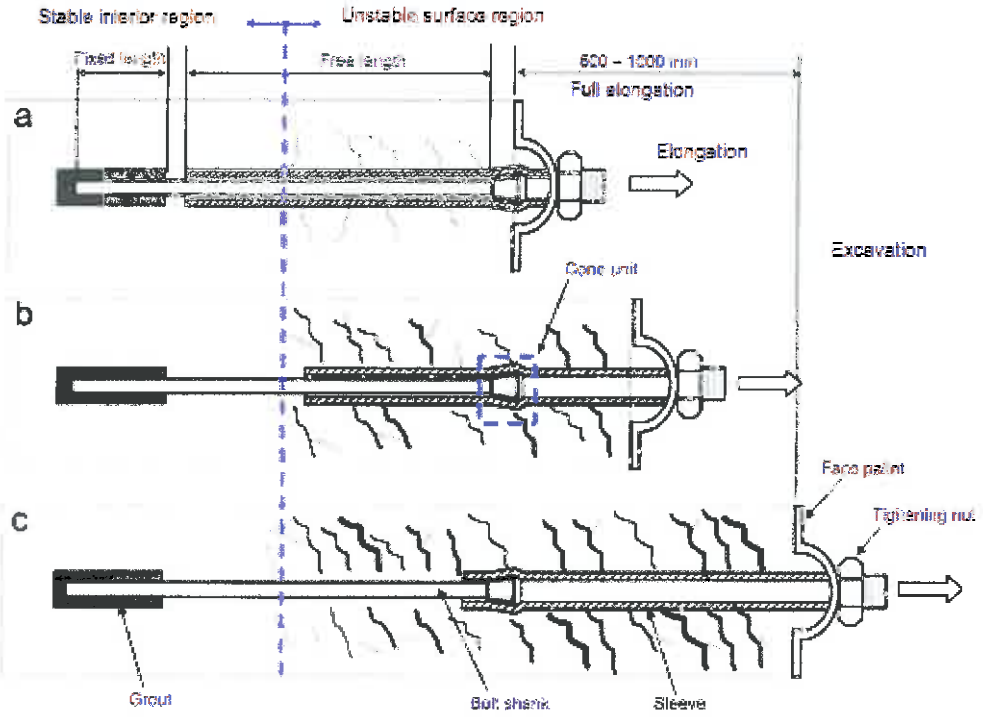

Figure 2.35: Mechanical behavioral principles of NPR bolt under dynamic loading (He *et al.*, 2014)

Stacey and Ortlepp (2007) utilized the results obtained from physical testing of rock support to demonstrate the effectiveness of using yielding support. In a chart they have created using a scaling law by McGarr *et al.* (1981), which appears in figure 2.36, yielding support has much greater capability of absorbing large amounts of energy due to seismicity than non-yielding, rigid rockbolts. Their chart considered an amplification factor which might give rise to high ejection velocities as opposed to the charts produced by Heal *et al.* (2006) and Mikula (2012).

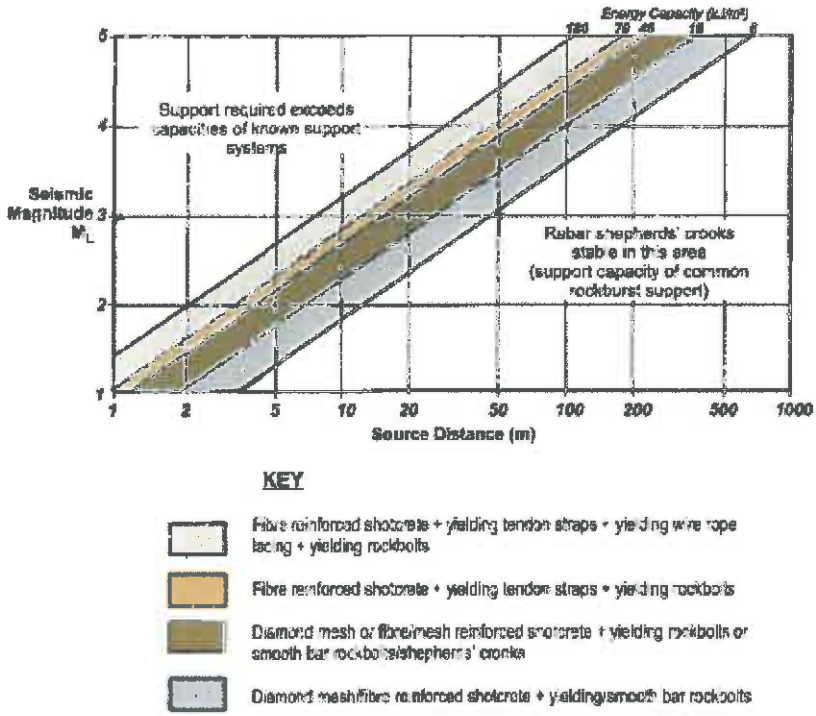

Figure 2.36: Correlation of support systems with seismicity (Stacey and Ortlepp, 2007)

As highlighted above, Stacey proposed a conservative approach to "bypass" the current support design deficiencies in rockbursting situations by specifying yielding support per rockburst type. The characteristics of ideal support to contain severe rupture type rockbursts damage are well described by the following extracts from Stacey (2016a):

- "Yielding rockbolts with proven yield capability in tension over their full length, and at significant velocity, certainly greater than 5 m/s, and preferably greater than 10 m/s.

- Additional yielding bolts, oriented at different angles, to reduce the risk of failure of bolts under shear loading. If this is done, at least some bolts will be more suitably oriented to resist shear failure.

- High capacity chain link mesh, with apertures typically of 50 mm. Fibre

reinforced shotcrete can be used in addition, and is essential in mechanized environments to protect the mesh from equipment damage.

- Heavy weld mesh straps, or tendon straps, or wire lacing, linking between bolts/nuts/faceplates and wire mesh/shotcrete.
- 0.5 m faceplates, preferably circular, without sharp edges. Their design must ensure that their capacity exceeds that of the mesh, bolts and nuts.
- Nuts on bolts must have greater capacity than the bolts, so that nuts are not a weak link."

Stacey (2016a) commented that, *"the combination of these support elements is likely to be able to contain damage from even a very severe rockburst. Containment of damage will ensure that safety is maximized, that consequential costs are avoided or at least reduced, that the risk is minimized and therefore that value is created for the project."*

Another method which has been suggested to help combat the effects of rockbursts caused by seismically-induced shock waves termed "sacrificial support" is described in detail below, and further investigated in this study. Some of the innovative and controversial support methods to contain rockburst damage are reported by Stacey (2016b) and Rizwan and Stacey (2014).

2.4 The sacrificial support concept – an alternative method to enhance safety in rockbursting environments

This section presents, at conceptual level, an additional alternative potential method to help combat rockburst damage. A case study based on recent observations made by Stacey and Rojas (2013) on support behaviour after rockburst

events, which match the concept of sacrificial support, is also presented.

Sacrificial concept was proposed more than two decades ago (Stacey, 1991). After a study of shock waves in blasting and their application, Stacey (1991) proposed the wave trap mechanism approach to help tackle the problem of rock damage associated with rockbursts. He was motivated by the promising results obtained by Hino (1959), which demonstrated the potential to alleviate the impact of reflected shock waves and thus reduce damage. The following section presents details of the original concept of the tensile wave trap as a possible means of inhibiting rockburst damage when a patent application was registered by Stacey (1991). The following section is given a similar title as appears in the patent application.

2.4.1 Method of and means for inhibiting rockbursts

The primary goal of the method was to provide a means for inhibiting rockburst damage. The proposed method involves application of a thin layer of some "substance" on the free surface of a tunnel, shaft, stope *etc.*, characterized by low tensile strength. It was suggested that low strength liner material has the capability to facilitate debonding of the support layer from rock surface upon reflection of compressive wave from the free surface, whilst at the same time preventing rock damage from occurring.

The wave trap mechanism of the thin layer is demonstrated by the following two sketches. Figure 2.37 shows propagation of a compressive shock wave (16) through jointed rock media (12) generated by a seismic source (14) situated near the bottom part of the sketch. When the compressive shock wave reaches the upper boundary free surface (10), the compressive wave is reflected back as a tensile wave, causing ejection of a block of rock (20) in direction 22. In figure 2.38, a thin layer of "substance" (24) is introduced at the free surface (10). When the compressive shock wave reaches the contact (10), minor reflection

takes place while the remainder of the wave propagates further through the layer followed by reflection of the wave at the free surface. The substance in the liner/layer, as shown in the figure, is ejected, leading to dissipation of reflected wave (16) trapped in substance (24) and in turn preventing damage to the rock (*i.e.* rockburst).

It is important to highlight that the proposed support method does not aim to replace the existing rock support commonly used in burst prone mines. Instead, the support could be used in conjunction with the type of support described in the previous section by Stacey (2016a).

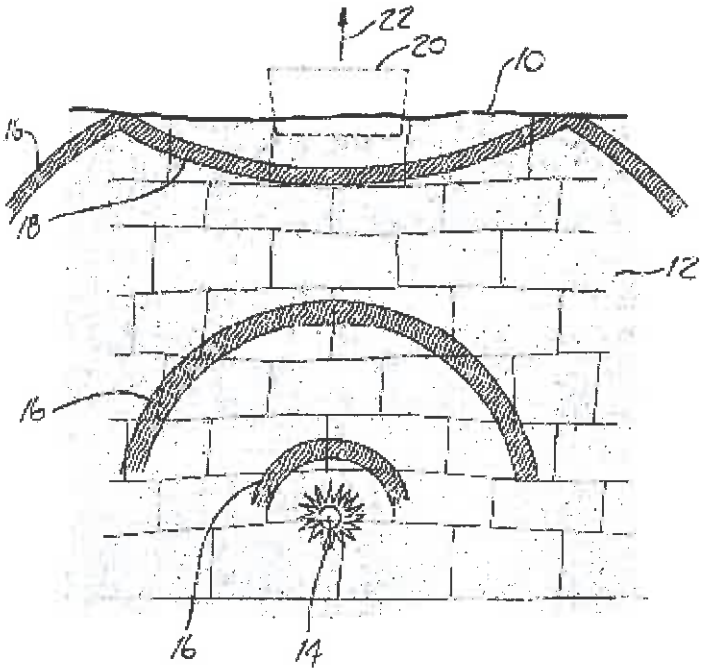

Figure 2.37: Propagation of compressive wave in jointed rock mass media (Stacey, 1991)

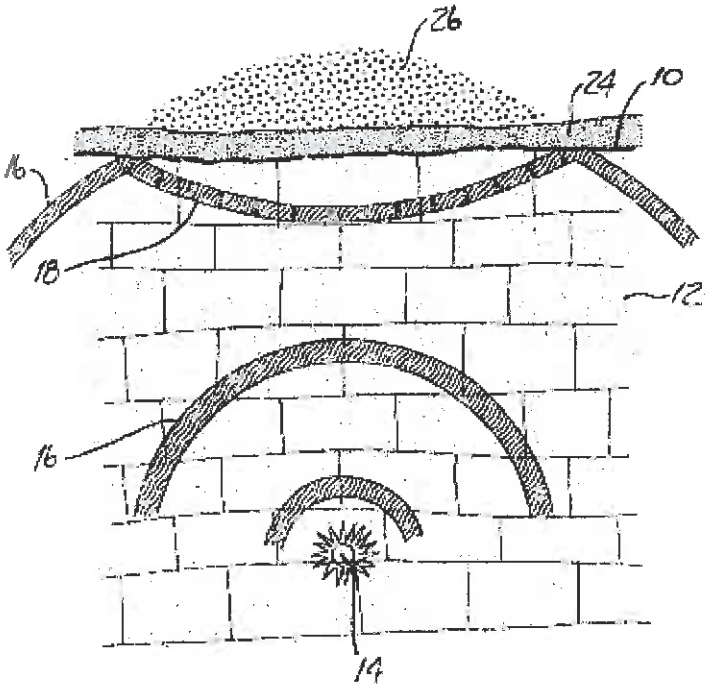

Figure 2.38: The mechanism of sacrificial layer behaviour in resisting rockburst damage (Stacey, 1991)

Recently, a case study to "validate" the behaviour of sacrificial support described above has been reported, based on the observations of support made in a real rockburst event, and this case study is covered in the next section.

2.4.2 Behaviour of sacrificial support in rockbursting environment – a case study

The experience gained in a rockburst event reported in a Chilean mine has presented possible evidence of the effectiveness of the sacrificial support concept suggested above to help reduce rock wall damage induced by shock waves. Figures 2.39 and 2.40 show rock and support damage in tunnels as a result of a rockburst event. Figure 2.39 shows ejected rocks from both sidewalls of the tunnel, and the failure of support can easily be noted. In figure 2.40, heave of the floor, which the authors (Stacey and Rojas, 2013) referred to as clean concrete, is apparent from the figure. In addition, the concrete is referred to

as clean because it was not covered with water or mud before the rockburst event. The interesting feature that one can notice from both the figures is that where the floor is covered with water or mud there appears to be no damage to the rock. This raises the question as to whether the presence of the water or mud layer influenced the failure in some way.



Figure 2.39: Rockburst damage in lower sidewalls of tunnel (Stacey and Rojas, 2013)



Figure 2.40: Rockburst damage caused by floor heave (Stacey and Rojas, 2013)

Apart from the incidents presented above, Stacey and Rojas (2013) further present a fascinating case pertaining to support behaviour in a dynamic loading environment. Figure 2.41 depicts some concrete panels, which initially were designed to provide stability to the tunnel walls, now lying on the floor of the tunnel. A close scrutiny of the figure shows that the wall rock was apparently undamaged after rockburst event. This type of support was termed a sacrificial support because it saved the rock from damage, with failure only experienced by the support itself. The sacrificial support concept can also be applied to the previously presented case. Both cases led the authors to develop a conceptual model to explain possible mechanisms of sacrificial support behaviour.



Figure 2.41: Concrete support panels ejected during rockburst event (Stacey and Rojas, 2013)

2.4.2.1 Tensile wave trap mechanism – a possible explanation of sacrificial support behaviour

To understand the conundrum presented by the two incidents reported above, Stacey and Rojas (2013) developed a simple conceptual model, which is referred to as a tensile wave trap mechanism. The conceptual model assumes a seismic compressive wave generated from a point source which is distant from the excavation boundaries. In figure 2.42, a seismic compressive wave is propagating through a rock medium lined with a concrete/shotcrete layer at the upper boundary, which, in this case, is representing the tunnel excavation surface. Due to differences in stiffness or mechanical properties between rock/concrete medium, part of the propagating wave will be reflected (possible minor reflections) at their interface, and then propagation will take place through the concrete until reflection takes place at the concrete/air boundary. This is because air cannot support the passage of the compressive wave and thus the compressive wave will be reflected as a tensile wave. The reflected tensile wave will now travel back to rock/concrete interface, and, owing to the fact that the interface has limited tensile strength, the tensile wave will

remain trapped within the concrete and ejection will take place as shown in figure 2.43.

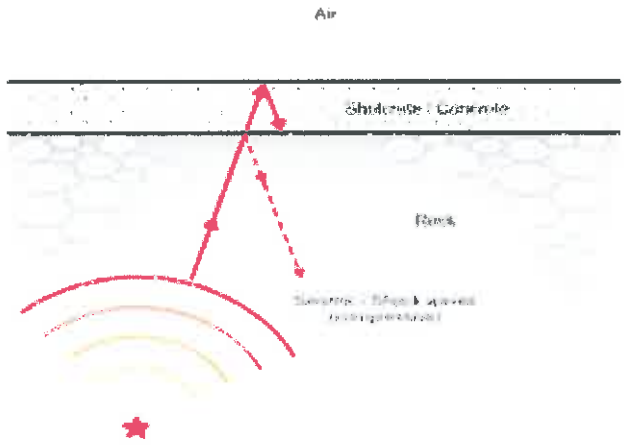

Figure 2.42: Passage of a compressive wave and reflection at the concrete/air interface creating a tensile wave (Stacey and Rojas, 2013)

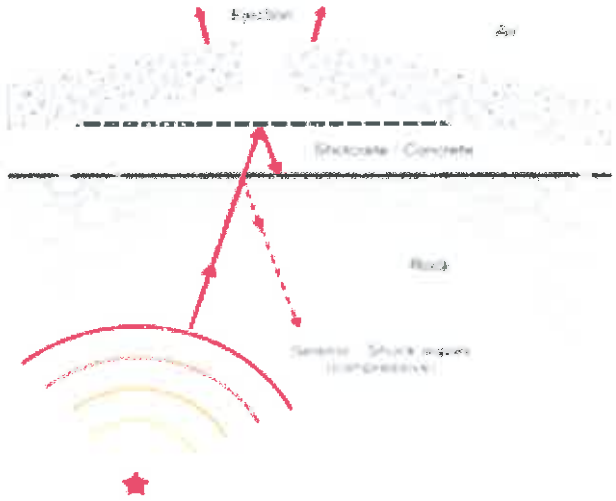

Figure 2.43: Ejection of the concrete due to the tensile wave (Stacey and Rojas, 2013)

In order to interpret the mechanism for the incidence wherein the tunnel floor was covered with water or mud (figures 2.39 and 2.40), a rock medium supported with concrete was now superimposed with a thin layer which is

indicated as a gel, *i.e.* a thin layer of gel representing water or mud (see figure 2.44). A similar wave trap mechanism was also assumed in this regard. The seismic compressive wave will also take a similar path of motion from the point source, and the compressive wave will be reflected as a tensile wave at the interface between the air and water/mud. As a result of inability of water or mud to sustain tensile stresses, the wave is trapped and dissipated as a spray of water and mud (figure 2.45), leaving the concrete and rock undamaged. On the other hand, it can now be easily be inferred how floor heave had taken place in the area covered with fresh concrete. The ejected support concrete panels shown in figure 2.41 were rehabilitated following the rockburst event, and these were held against the tunnel wall by cables grouted within the rock mass as part of new support practice. In addition, wire mesh was added to help catch the ejected panels in case a rockburst was to occur. With this new support arrangement in place, a seismic event was experienced in the area without rockburst damage.

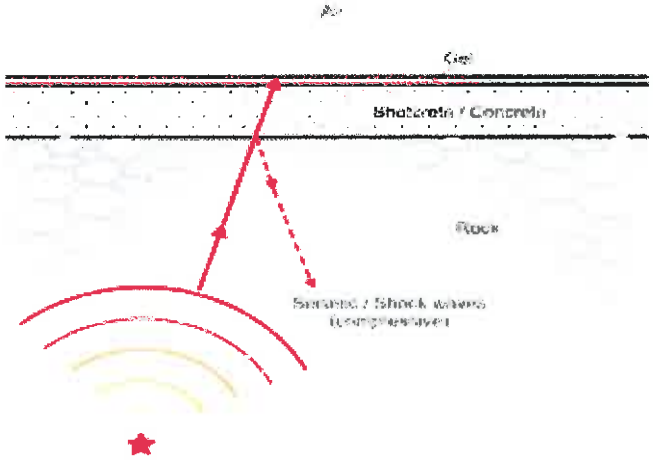

Figure 2.44: Propagation of a compressive wave through rock, concrete, and water/mud (Stacey and Rojas, 2013)

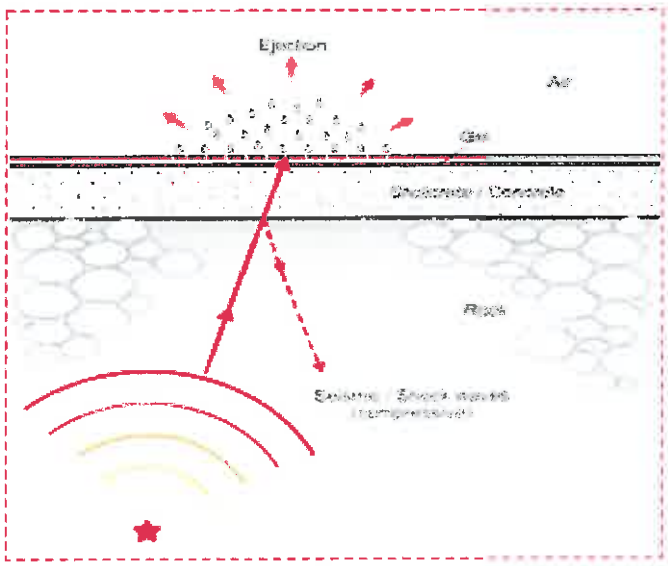

Figure 2.45: Reflection of a compressive shock wave at the interface between the air and the water/mud (Stacey and Rojas, 2013)

The study by Stacey and Rojas (2013) left some important questions unanswered pertinent to "sacrificial support" behaviour. The present study is aimed at providing answers to the following questions pertaining to different support layers of the materials investigated:

- Is a minimum thickness required for the layer (*i.e.* support layer) to effectively resist dynamic rock failure (*i.e.* rockburst damage)?
- What are the effects of different stiffnesses of support layers/liners on their capability to combat the effects of stress waves?

2.5 Objectives and aims of the study

The general objective of the study is to identify and investigate support method/s designed to alter the strength of shocks waves in order to reduce the drastic impacts induced by shock waves, which cause damage both to the underground mining excavations and support system itself. After the literature survey, it has been noted that a support in the form of a layer/liner interface may help to

ameliorate the problem of rockbursts more than does a conventional support system on its own.

2.5.1 Specific objectives

The specific objectives of the study aim to provide possible answers to the questions posed above. The aspects will be investigated experimentally and numerically. The specific objectives are to:

- Evaluate the performance of support liners consisting of materials with differing mechanical properties under dynamic loading;
- Investigate the effects of varying the thickness of different support liners on the overall behaviour of the support liner;
- Investigate some aspects of sacrificial support behaviour using numerical modelling, and make comparisons with experimental results where possible.

Some of the research related to these objectives is described by Mudau *et al.* (2016), who attempted, for the first time, to provide answers to the questions, and the outcomes of such study are covered comprehensively in this thesis.

2.6 Chapter summary

This chapter has comprehensively reviewed relevant literature addressing fundamental aspects of rockburst phenomena such as various seismic source mechanisms responsible for rockburst occurrence, and design measures to help alleviate the ensuing rockburst damage. A thorough review was also conducted to gain in-depth knowledge about the identified method with potential to help combat the effects of rockbursts caused by seismically-induced shock waves. This review yielded positive results as far as identifying gaps in knowledge is

concerned, warranting the need for further research, which is the main objective of this study.

The following chapter describes details of the experimental programme designed to investigate the effectiveness and behaviour of what is so called "sacrificial support" in resisting dynamic rock failure, under a controlled laboratory environment, using the split Hopkinson pressure bar (SHPB) technique. The chapter begins by providing a review of previous studies on physical testing of rock support under 'rockburst' conditions.

3 Experimental programme for testing the performance of sacrificial support under dynamic loading

In the previous chapter, a comprehensive review of rockburst damage mechanisms and design measures to ameliorate drastic impacts caused by rockburst damage in mine excavations was conducted. An identified sacrificial support concept with potential to help reduce rockburst damage was reviewed in detail in order to identify the gaps in knowledge, which warrant further research investigation.

This chapter first presents a review of past studies on physical testing of rock support under simulated rockburst conditions. The remainder of the chapter covers the experimental programme established to investigate the behaviour of sacrificial support under dynamic loading conditions using the split Hopkinson pressure bar (SHPB) technique.

3.1 Review of previous studies on physical testing of ground support elements and systems under "simulated" rockburst conditions

An insight into the performance of rock support systems is of paramount importance from a stability and support design point of view in rockbursting environments. To date, there is no standardized procedure for physical testing of rock support under dynamic loading conditions. It is difficult, if not impossible, to simulate real rockburst conditions, either in the field or the laboratory. Most of the studies conducted in the past on rock support performance have been through drop weight tests or blasting experiments and these are discussed below.

3.1.1 Drop weight tests

Drop weight tests have been carried out around the world by several research engineers to evaluate the performance of individual support elements and combinations of support elements (Yi and Kaiser, 1994; Ortlepp and Stacey, 1997; Guler *et al.*, 2001; Stacey and Ortlepp, 2001; Stacey and Ortlepp, 2007; Kuijpers *et al.*, 2002; Stacey and Ortlepp, 2002; Gaundreau *et al.*, 2004; Player *et al.*, 2004; Thompson *et al.*, 2004; Ansell, 2005; Ansell, 2006; Charette and Plouffe, 2008; Player *et al.*, 2008a; Player *et al.*, 2008b; Plouffe et al., 2008; Player *et al.*, 2009; Li, 2010; Wu and Oldsen, 2010; Li and Doucet, 2012, *etc.*). A critical examination of various test facilities based on drop weight tests conducted in Australia, Canada and South Africa is reported by Player *et al.* (2009) and Hadjigeorgiou and Potvin (2011). The following table summarizes some of the mechanical details and types of support components tested using different test rigs.

Table 3.1: Comparison of the dynamic loading simulation methods for each trial (reproduced from Hadjigeorgiou and Potvin, 2011)

Rig #	Common name	Individual reinforcement units	Support systems (panels)	Props	Max. drop weight (kg)	Maximum height of drop (m)	Maximum energy available (kj)	Maximum impact velocity (m/s)
1	Terratek	Short bolts up to 1.6 m	N/A	Props up to 1.6 m		N/A		3
2a	SRK drop weight test facility Set-up #1	N/A	1.6 x 1.6 m		1,048 (2,706)	4	41.12 (81.5)	8.8 (7.3)
2b	SRK drop weight test facility Set-up #2	Rockbolts and cablebolts	N/A		1,048 (2,706)	4		20
3	SIMRAC Dynamic Stope Test Facility	N/A	3 x 3 m	Props up to 2 m (with extensions)	10,000	3	300	7.7
4	GRC-Laurentian	Steel rod	N/A	N/A	48.494	0.3	0.14	2.43

5	GRC-Greighton	2.44 m long N/A	1.2 m x 1.2 m diamond; shotcrete panels	N/A	565	4	21.9	8.8
6a	NTC	Bolts up to 1.7 m long	1.5 x 2.75 m N/A	N/A	1,000	2	20	1.5
6b	NTC-CANMET	Bolts up to 1.7 m long	N/A	N/A	3,000	2	58.86	6.26
7	WASM	Bolts and cables up to 2.4 m long	1 x 1 m	N/A	4,500	6	225	10
8	Wedge-block loading device	Bolts and cables up to 5.5 m long	No	No	10,000	4	390	8.9

9	MIRARCO	N/A	1.5 m x 2.7 m screen	N/A	565	3	16.63	7.67

Drop weight testing is self-explanatory–it involves release of a suspended weight to directly impact the support components being tested, with certain desired kinetic energy (Figure 3.1). The size and configuration of test rig depends on the objective of the study.

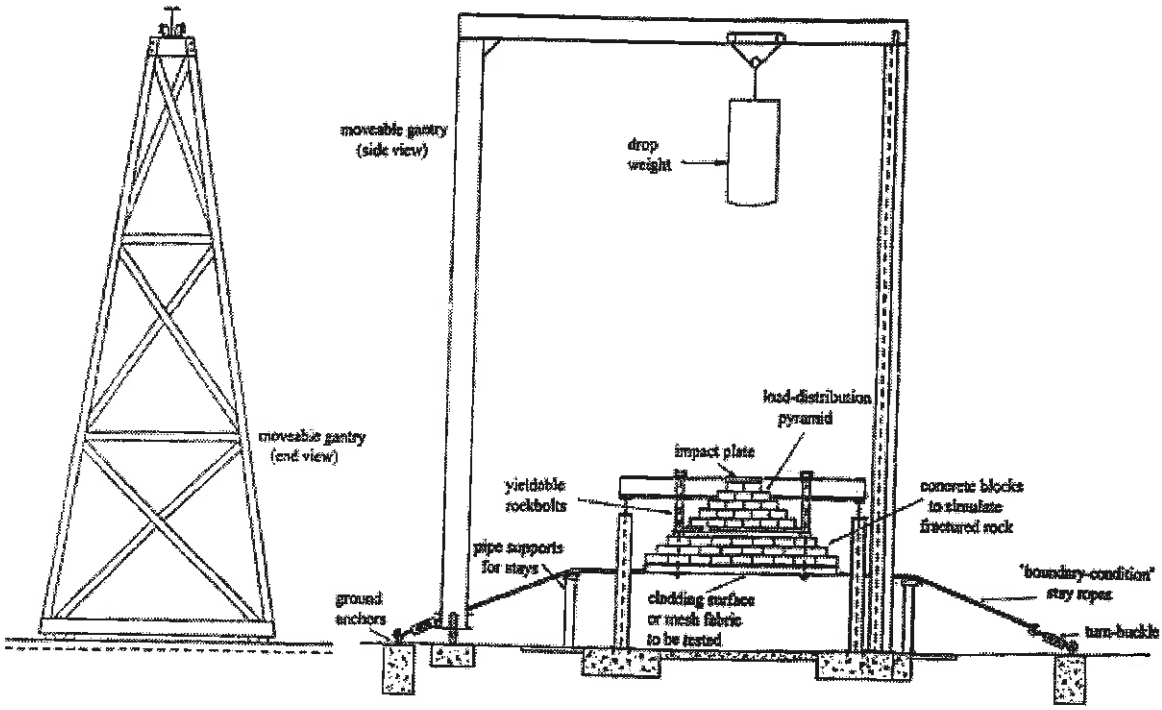

Figure 3.1: Illustration of drop weight test facility (After Ortlepp and Stacey, 1997)

Stacey (2012) provides a philosophical overview regarding physical rockburst testing of rock support for both drop weight tests and blasting experiments. Below are some of the merits and demerits of drop weight tests.

Merits

- *"Relatively simple and quick to perform*
- *Can provide repeatable results*
- *Suitable for comparative testing and quality control testing."*

Demerits

- *"Impact loading may not be representative of rockburst loading*
- *Direct impact on surface support is not considered to be representative of rockburst loading*
- *When impact via a load spreader is used, the load/energy to which the support is actually subjected is unknown*
- *Appropriate representation of lateral continuity of support is unlikely to be achieved*
- *The effect of the stress in, or confinement of, the rock mass is usually not taken into account*
- *The methods published have generally not achieved satisfactory testing of support systems involving both retainment and containment elements. A probable exception to this is the large-scale facility described by Ortlepp et al. (2001) for tabular stope support system testing."*

3.1.2 Large-scale blasting experiments

Before drop weight tests were used as test methods to evaluate the performance of support under dynamic loading conditions, blasting experiments had already been used for physical rock support testing under blast loads since 1960s. Ortlepp (1969), working in South Africa, probably conducted the first underground blast experiments to evaluate the performance of conventional and yielding bolts in deep-level gold mines. The yielding rockbolt showed superior performance compared to conventional rockbolt in terms of stabilizing the ground under extreme blast loads (figure 3.2). In a separate study, Ortlepp (1992) noted the poor performance of non-yielding, but a yielding bolt reduced the ejection velocity of a block of rock from 10 m/s (as experienced in area supported by conventional bolt) to 0.5 m/s without the bolt failing.

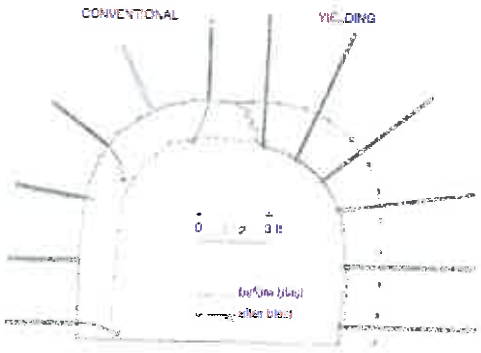

Figure 3.2: Profile of the tunnel after the blast test (Ortlepp, 1969)

Apart from underground blast experiments, Ortlepp (1994) further undertook surface direct blast experiments in a quarry mining environment to assess the response of different support tendons. To achieve this, concrete blocks, retained at same surface level by different rockbolt elements grouted into the granite foundation, were blasted upward to assess the performance of the support tendons in tension. Cone bolts showed better performance by yielding at high ejection velocities, up to about 12 m/s, with displacements in order of 0.5 m. Non-yielding, rebar bolts, on the other hand, failed due to their low energy absorption and yield capacity.

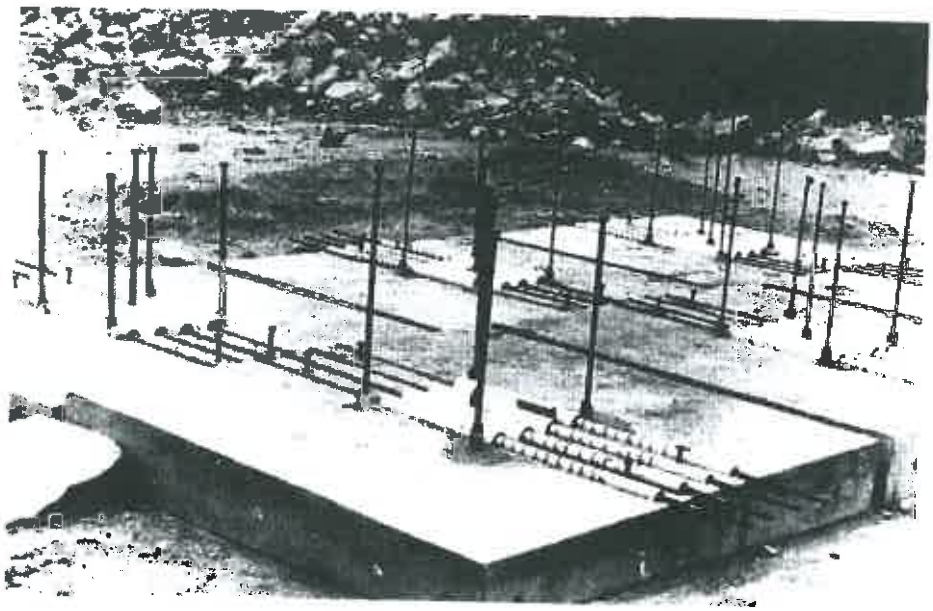

Figure 3.3: Photograph of concrete panels and the test studs grouted in position ready for testing

Recent blast experiments in South Africa were conducted, for instance, to compare measured ground velocities (*i.e.* peak particle velocities) within the rockmass and on the skin of excavations. The aim was to correlate rockburst damage intensity with *ppv* values recorded by sensors installed on the surface of excavation, and monitor ejection velocities by high-speed filming (Milev *et al.*, 2001). Reddy and Spottiswoode (2001) investigated the influence of geology on simulated rockburst experiments, while Haile and Le Bron (2001) in the same series of investigations, evaluated the performance of rockbolt reinforcement. A layout of underground blast experiments used for these tests is shown in figure 3.4. Explosives were charged in blastholes drilled in a drift parallel to the main drift where observations were to be made. A similar geometry was used in the blast experiments reported below.

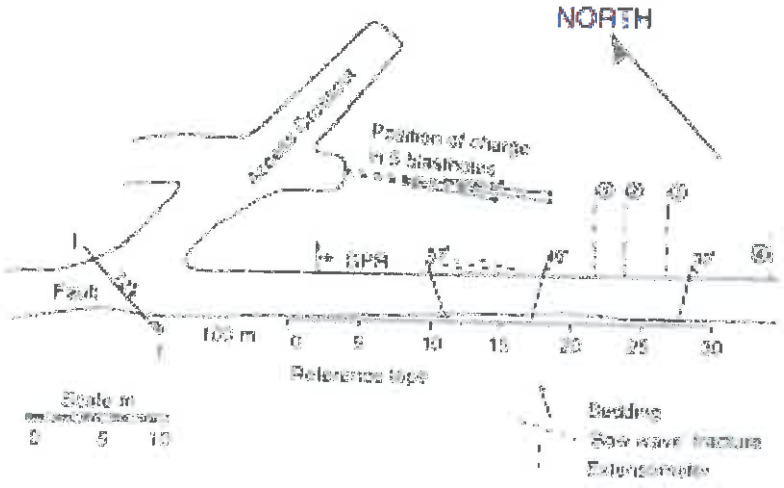

Figure 3.4: Geometry of underground blast experiment (Haile *et al.*, 2001)

In Canada, both surface (*i.e.* direct blast test) and underground blast experiments have been performed to assess the performance of support systems ranging from blast response of thin spray-on liners (e.g. Archibald *et al.*, 2003; 2006), thin spray-on liners and shotcrete (Espley *et al.*, 2002), shotcrete and wire mesh to fibre reinforced shotcrete (Tannant *et al.*, 1994a), and rockbolts (Tannant *et al.*, 1994b; 1995).

The most comprehensive large-scale underground blast experiments perhaps ever conducted to measure the performance of a range of ground support systems was arguably the one conducted by Heal (2010) in Western Australia, and this is evident in table 3.2 below.

Table 3.2: Ground support systems tested using blasting experiemnts in Western Australian mines (reproduced from Heal, 2010)

Ground Support System	**Test Site(s) (Date Tested)**	**Range of PPVs Generated (m/s)**	**Description**
Split Sets and Mesh	Long Shaft Rhondo North Access (June 2004)	1st blast: 0.3 – 1.3 2nd blast 0.1 – 1.0 3rd blast: 2.0 – 3.5	2.4 m SS47 Split Sets (1.2 – 1.5 m spacing) and weld mesh (2.4 x 3.0 m

	Mt Charlotte 1155 Access (April 2005)	1st blast: 0.1 – 0.6 2nd blast: 0.2 – 0.8 3rd blast: 1.1 – 1.6	sheets, 100x100 mm, 5.5 mm galvanized steel).
Split Sets and Mesh with cone Bolts and Fibrecrete	Long Shaft 13/2 Access (April 2004)	1st blast: 0.4 – 0.8 2nd blast: 0.4 – 0.7 3rd blast: 0.4 – 2.4	2.4 m grouted Cone Bolts (1.0 – 1.5 m spacing), 75 mm fibrecrete (Dramix steel fibres), 2.4 m SS47 Split Sets (1.2 – 1.5 m spacing) and weld mesh (2.4 x 3.0 m sheets, 100x100 mm, 5.6 mm galvanized).
High Desnity Split Sets and Mesh with Fibrecrete	Long Shaft 13/2 Access (April 2004)	1st blast: 0.3 – 0.6 2nd blast: 0.3 – 0.5 3rd blast: 0.6 – 2.0	2.4 m SS47 Split Sets (0.6 – 0.75 m spacing), 75 mm fibrecrete (Dramix steel fibres) and weld mesh (2.4 x 3.30 m sheets, 100x100 mm, 5.6 galvanized steel).
Widely spaced Split Sets and Mesh	Long Shaft Rhondo North Access (June 2004)	1st blast: 0.3 – 1.1 2nd blast: 0.1 – 1.0 3rd blast: 2.1 – 3.5	2.4 m SS47 Split Sets (1.5 m – 2.4 m spacing) and weld mesh (2.4 x 3.0 m sheets, 100x100mm, 5.6 mm galvanized steel
Split Sets and Masterseal	Mt Charlotte 1155 Access (April 2005)	1st blast: 0.1 – 0.5 2nd blast: 0.3 – 0.7 3rd blast: 1.3 – 1.7	2.4 m SS47 Split Sets (1.2 – 1.5 m spacing) and Masterseal 845A thin spray-on liner

			(4 mm thickness).
Split Sets and Fibrecrete	Darlot Walters 1240 Access (August 2006)	1st blast: 0.7 – 1.7	2.4 m SS47 Split Sets (1.2 – 1.5 m spacing) and 50 mm fibrecrete (Synmix synthetic fibres)
Securabolts and Fibrecrete	Darlot Walters 1240 Access (August 2006)	1st blast: 0.6 - 1.9	2.4 m R27 Securabolts (1.2 – 1.5 m spacing) and 50 mm fibrecrete (Synmix synthetic fibres).
Split Sets and Mesh with Fibrecrete	Darlot Walters 1240 Access (August 2006)	1st blast: 0.7 –1.8	2.4 SS47 Split Sets (1.2 – 1.5 m spacing), weld mesh (2.4 x 3.0 m sheets, 100x100 mm, 5.6 mm galvanized steel) and 50 mm fibrecrete (Synmix synthetic fibres).
Securabolts and Mesh with Fibrecrete	Darlot Walters 1240 Access (August 2006)	1st blast: 0.6 – 1.9	2.4 R27 Securabolts (1.2 – 1.5 m spacing), weld mesh (2.4 x 3.0 m sheets, 100x100 mm, 5.6 mm galvanized steel) and 50 mm fibrecrete (Synmix synthetic fibres)
Split Set and Tunnelguard with Cone Bolts	St George 8 Level Stockpile (January 2007)	1st blast: 0.4 – 3.1 2nd blast: 2.7 – 3.2	2.4 m SS47 Split Sets (1.25 m – 1.1 m spacing), 3 m grouted Cone Bolts (1.25 m – 1.1 m spacing) and 100 thick Tunnelguard

			thin spray-on liner.
Split Sets and Mesh with Cone Bolts	St George 8 Level Stockpile (January 2007)	1st blast: 0.7 – 2.7 1st blast: 2.4 – 3.1	2.4 SS47 Split Sets (1.25 m – 1.1 m spacing), weld mesh (4.0 m x 2.4 m sheets, 100x100 mm, 5.6 galvanized steel) and 3 m grouted Cone Bolts (1.25 m – 1.1 m spacing).
Cone Bolts and High Energy Absorption (HEA) Mesh	Long Shaft 14L Eimrock Access (May 2008)	1st blast: 0.3 – 2.4 2nd blast: 0.8 – 3.0	2.4 m grouted Cone Bolts (1.2 m – 1.5 m spacing), HEA Mesh (3 m x 2.4 sheets, 100x mm, galvanized steel weld mesh with high tensile cable
Cone Bolts and Mesh with Fibrecrete	Long Shaft 14L Eimrock Access (May 2008)	1st blast: 0.3 – 2.2 2nd blast: 0.6 – 1.9	2.4 m grouted Cone Bolt (1.2 m – 1.5 m spacing), weld mesh (100x100 mm, 5.6 mm galvanized steel) and 70 mm fibrecrete (Synthetic syntehtic fibres).

In Sweden, in situ tests to assess the vulnerability of shotcrete to blast vibrations during underground tunnel construction have been well studied (*e.g.* Ahmed, 2012; Ahmed and Ansell, 2014). Shirzadegan *et al.* (2016) conducted large scale blasting tests of a rock support system, consisting of Swellex rockbolts, reinforced shotcrete and welded mesh, at LKAB Kiirunavaara underground mine, to evaluate the response of the rock support system subjected to strong dynamic loading.

Most recently, in China, He *et al.* (2016) conducted underground blasting tests to evaluate the performance of the NPR yielding bolt and an ordinary anchorage cable under repeated blasting loads. The NPR bolt, as expected, endured more impact loading and provided greater stability to the tunnel than the ordinary cable.

Blast experiments are probably the closest simulations of conditions to induce violent dynamic rock fracturing comparable with rockburst damage. These tests mostly provide qualitative results about the performance of different support components and support systems. It is, however, acknowledged that real rockburst damage cannot be simulated (Stacey, 2012). In blasting experiments, it has been noted that gas expansion plays a significant role in causing rock fragmentation, rather than rock failure being only a result of reflection of shock waves from a free surface, as would be expected in real rockburst situations. Some of the disadvantages of conducting blasting experiments include the high costs involved, the need for a special environment (*e.g.* underground space), difficulty of conducting visual monitoring, and poor experiment repeatability (Ortlepp, 1994; Stacey, 2012).

The following section details the experimental programme for testing the performance of sacrificial support under dynamic loading.

3.2 Experimental programme for testing the performance of sacrificial support under dynamic loading

The above section discussed physical testing of rock support under dynamic "simulated" rockburst conditions. Owing to some challenges associated with blast experiments for instance, it was essential to search for an alternative

testing methodology that would enable dynamic rock fracturing to be studied in a controlled laboratory environment. The split Hopkinson pressure bar (SHPB) is one of the popular and well-established techniques used to test a range of materials at high strain rates. For this reason, the technique was adopted in this study. This section will, however, first present a descriptive summary of earlier experimental work conducted to investigate the behaviour of sacrificial layer using plate impact tests.

3.2.1 Plate impact tests

Before SHPB testing was identified as a suitable method to investigate the behavior and mechanism of sacrificial support, initial tests carried out involved the use of a plate impact test. The test set-up was in-house designed and is shown in the figure 3.5. The primary goal of this test was to generate shock waves within a finite body and study the effect of reflected shock waves on sacrificial layer behaviour at the boundaries thereof. To achieve this, a hammer was used to impact the plate at the bottom to generate a compressive shock wave that would propagate outwards to the boundaries of the plate. Strain gauges were cemented near the bottom and top parts of the plate, as shown in the illustration below. An accelerometer was mounted at the centre of the plate (Figure 3.5b).



(a)

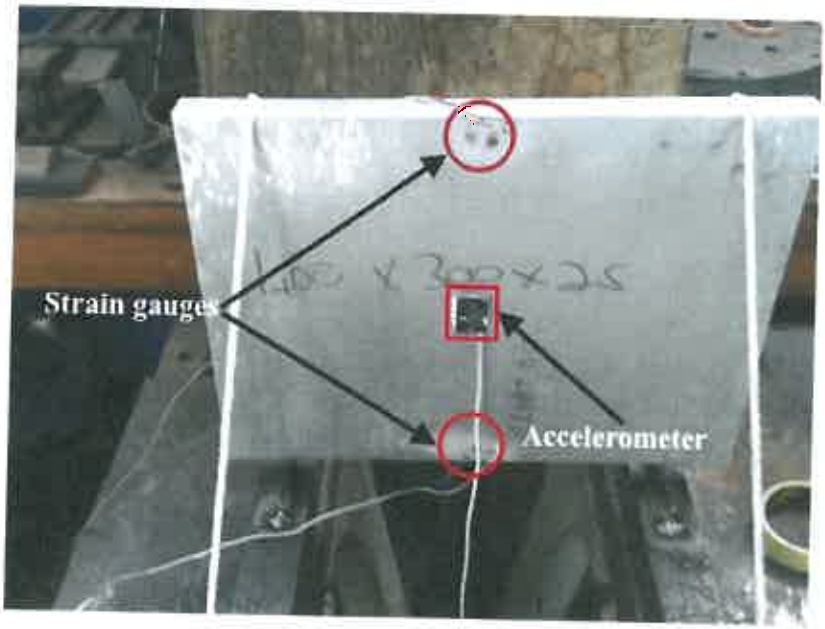

(b)

Figure 3.5: (a) A side and (b) front view of plate impact test set-up

It was realized early during testing that this set-up was inappropriate to address the task at hand. Among identified challenges, the chosen loading

condition was not sufficient to generate high impact energies, and this, combined with damping of the aluminum plate, augmented the problem. As a result, all sensors were not sensitive enough to detect the passage of generated wave. As far as testing of sacrificial layer behaviour is concerned, a transparent water containment made of perspex plastic was machined and fitted at the top boundary of the plate. The dimensions of the containment were similar to those of the plate but with different depth. The containment was filled with water and the plate was struck at the bottom to generate a shock wave. In this case, the plate represents the wave transmitting "rock mass" and the top boundary of the plate represent the floor of the tunnel filled with water in this regard. There was no movement of water noticed in the containment after the impact as would have been expected, and it was not possible to deduce the amount of shock wave energy dissipated by the water due to ineffective sensors. In a separate test, a strip of aluminium was placed at the top boundary to assess possibility of a tensile wave trap mechanism exhibited by the liner, but unfortunately, there was no displacement of the liner noticed. Assuming that the loading condition was sufficient to generate detectable wave signals with potential to cause the ejection of the support liner material, such results will be unsatisfactory since only the mechanism of behaviour of the liner would be observed. The influence of reflected tensile wave on the mechanical behaviour of the plate will be neglected, considering that the strength of reflected waves would not be sufficient to induce plastic deformation of the plate. However, in rockburst situations, the effect of reflected shock waves from the surface of excavation may be to cause significant dynamic rock fracturing in the form of rockburst damage. This unsatisfactory experimental set-up was abandoned, and the SHPB technique was adopted for the reason/s mentioned previously.

3.2.2 Split Hopkinson Pressure Bar tests

Today's version of the traditional split Hopkinson pressure bar (SHPB) for compression strength tests is the early work by Kolsky (1949). Initially, Hopkinson (1914) studied the shape and evolution of stress pulses propagating in long cylindrical rods under dynamic loading events. A detailed historic account of Hopkinson bar tests can be found in Gama *et al.* (2004) and Chen and Song (2001). According to Field *et al.* (2004), the use of SHPB as a test method to determine dynamic mechanical properties of a variety of materials gained momentum in the 1970s. Today, different configurations of the Hopkinson pressure bar exist, which allow measurement of the dynamic stress-strain response of a wide range of materials at high strain rates. Figure 3.6 shows the range of high strain rates that split Hopkinson pressure bar tests can achieve. In simple terms, strain rate (ϵ) is defined as the change in strain with time (Gray, 2000). From figure 3.6, it is also evident that the dynamic strength of materials increases at high strain rates compared with the quasi-static strength, which is conducted at low strain rates.

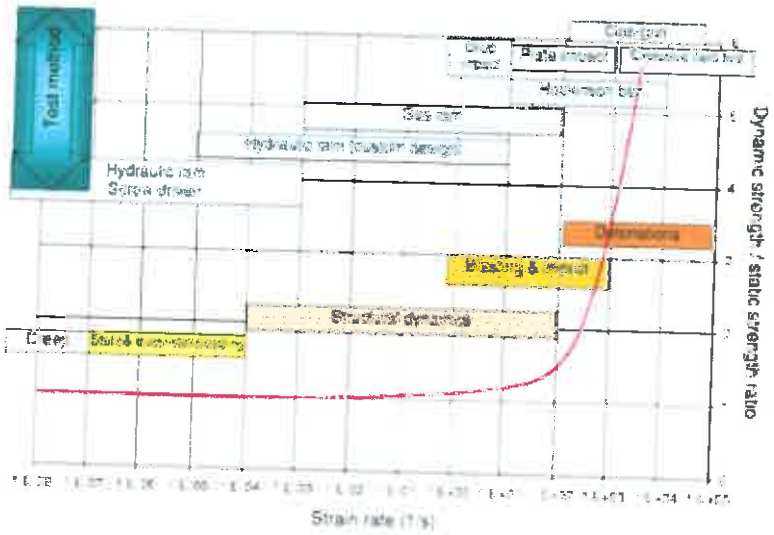

Figure 3.6: Classification of loading techniques and an overview of material's response at high strain rates (Cai *et al.*, 2006)

A comprehensive list of references pertaining to major developments in the split Hopkinson bar as a test method for characterization of rock materials is provided by Zhang and Zhao (2014) in their review paper.

As highlighted, the SHPB technique was chosen due to its capability to study dynamic fracturing of rock at high strain rates. The theoretical aspects and mechanical details of SHPB tests configured for spalling are presented below. Some experimental results of compressive strengths are reported.

3.2.3 A test methodology to demonstrate the mechanism of sacrificial support

It is difficult, if not impossible, to simulate real rockburst conditions, either in the field or laboratory. Most of the studies conducted in the past on rock support performance under dynamic loading conditions have been through underground blasting experiments or drop weight tests as discussed earlier in this chapter. With blasting experiments, it has been noted that gas expansion plays a significant role in causing rock fragmentation, rather than rock failure being only a result of reflection of shock waves from free surfaces, as would be expected in real rockburst situations. In drop weight tests, there is no interaction between a rock mass and the tested support system, since testing is done by releasing a suspended mass with certain kinetic energy to directly impact the support system. Both of these test methods should, however, be credited with providing some insights on support performance under dynamic loading conditions, but not on the basis of simulating real rockburst conditions (Stacey, 2012).

In light of the difficulties associated with simulating rockburst conditions, it was found essential to search for a simple, yet robust, testing methodology, with the capability of studying dynamic rock fracturing in a controlled laboratory environment. The Split Hopkinson Pressure Bar (SHPB) is one of the popular

and well-established techniques used to test a range of materials at high strain rates.

3.2.3.1 Theoretical and mechanical details of SHPB test configured for spalling

In order to study spall failure phenomena, a single Hopkinson pressure bar may be used instead of the two bar configuration often used for classic SHPB compression tests. Such a configuration has allowed the dynamic tensile strength of a variety of materials such as ceramics to be determined at high strain rates (Najar, 1994; Johnstone and Ruiz, 1995; Galvez *et al.*, 2000; Diaz-Rubro *et al.*, 2002), concrete (Diamaruya *et al.*, 1997; Klepaczko and Brara, 2001; Brara and Klepaczko, 2006, 2007; Schuler *et al.*, 2006), composites (Govender *et al.*, 2009, 2011) and rocks (Zhou *et al.*, 2007).

Govender *et al.* (2011) demonstrated the spall damage phenomenon for a long rod specimen directly impacted by a projectile. Specimen failure occurs at a location when the resultant stress between the incident compressive stress wave and reflected tensile stress wave exceeds the tensile strength of the material (figure 3.7). This failure mechanism is common in situations wherein the source of stress waves is distant from where failure is realized, *e.g.* failure observed in a tunnel remote from the seismic source. High ejection velocities in rockbursts often exhibit spall fragments, and this is a serious issue of concern from safety point of view.

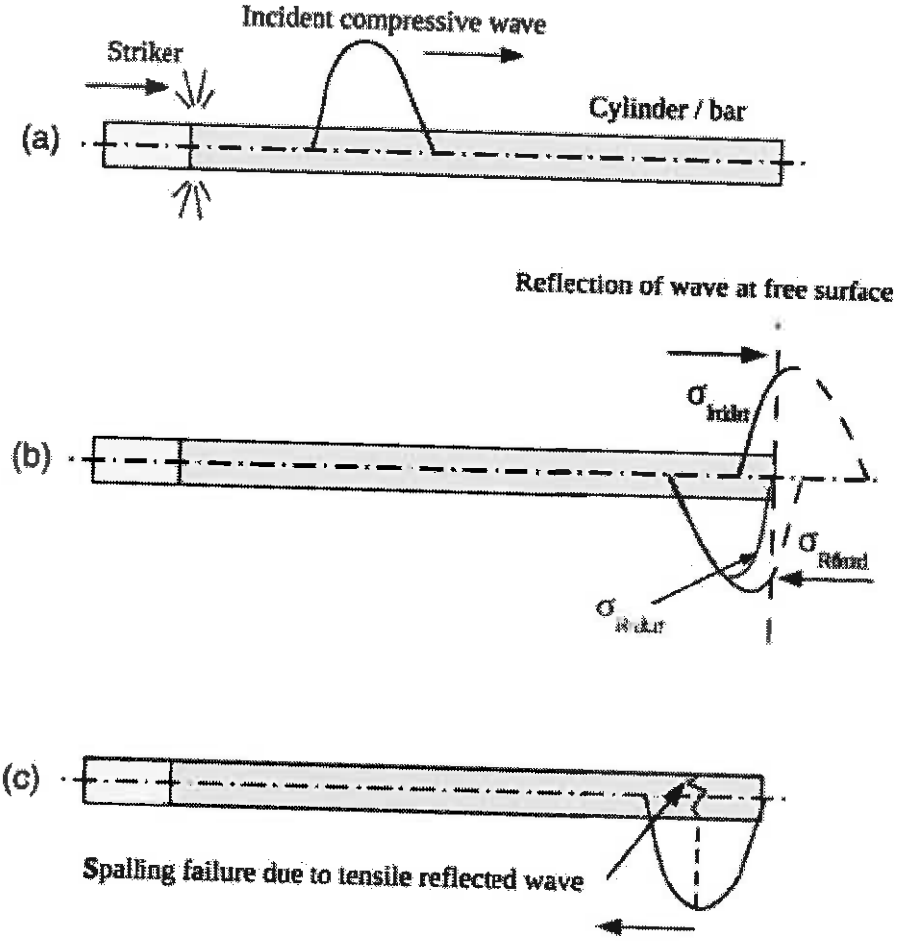

Figure 3.7: A schematic representation of spall failure in a long cylindrical road loaded by impact (Govender *et al.*, 2011)

Shock/stress waves generated from a seismic event in a mining environment are complex to understand and simulate, as demonstrated previously. As a result, a one-dimensional stress wave propagation approach was adopted for simplicity. Spalling phenomena described herein also assume a 1D theory of stress wave propagation in elastic media, which can be represented by the following equation:

$$\frac{d^2u_z}{dt^2} = C^2\frac{du_z}{dz^2} \tag{3.1}$$

where, u is the displacement, t being time and C the wave velocity.

Figure 3.8a shows a SHPB set-up for a spalling test of a long cylindrical

specimen attached at the right hand end of the Hopkinson pressure bar, while figure 3.8b is a modification of the SHPB set-up with a liner (*i.e.* sacrificial liner) attached to the specimen. Both the input bar and specimen are supported by bushings in order to minimize friction, and their movement is restricted to one degree of freedom in the x-direction. The bushings are aligned beforehand to ensure that the striker, input bar and specimen are co-linear at the start of the test. Before testing of specimens, the input bar is calibrated for wave speed and stress level.

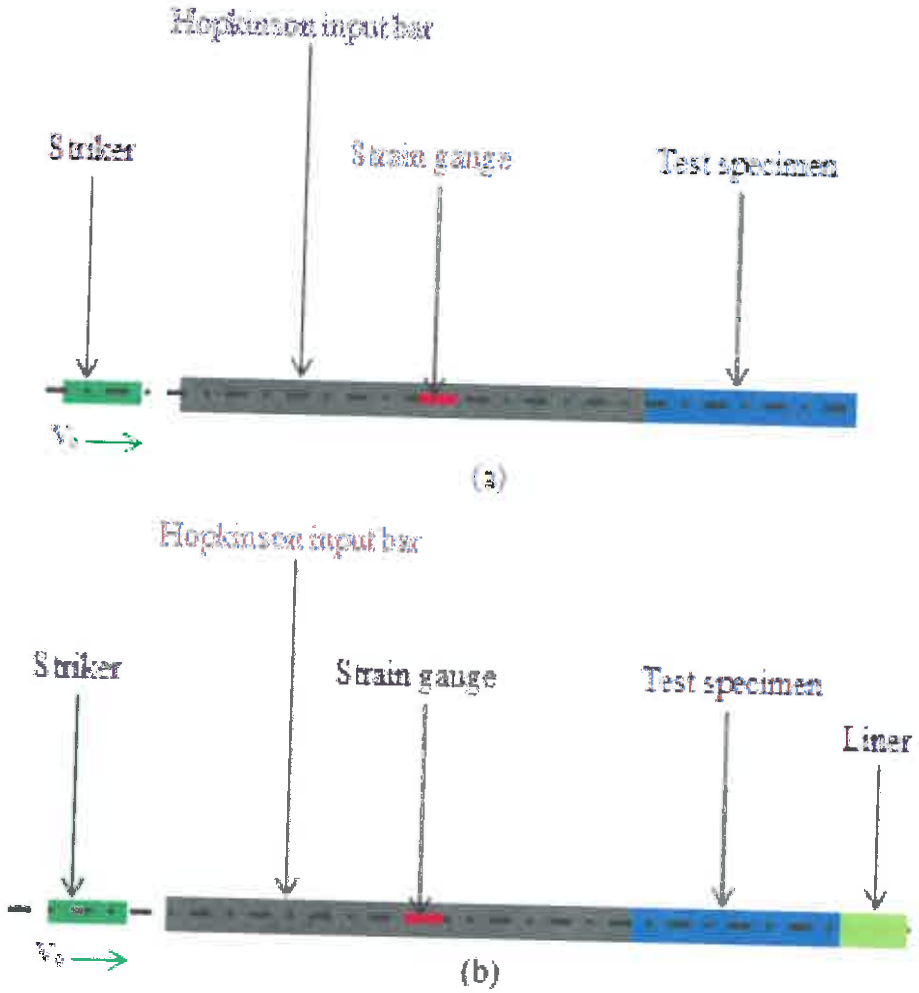

Figure 3.8: Schematic experimental set-up for spalling test (a) without liner and (b) with liner

In order to induce a stress wave, a gas gun is used to propel the striker to

impact the input bar. The generated transient strain pulse will then propagate down the input/transmitting bar as a longitudinal compressive stress wave, and on arrival at the bar/specimen interface, part of the compressive stress wave will be reflected back as a tensile stress wave due to bar/specimen impedance, whereas the remainder of the compressive stress wave will travel through the specimen and be reflected back at the specimen free end. The transmission of stress waves at the contact between two-layered media is governed by their mechanical impedance. To achieve satisfactory wave transmission at bar/specimen interface in the SHPB, grease is often applied at the contact. The contact tensile strengths between the input bar/rock test specimen and the rock/support liner is considered to be zero. A pair of strain gauges, cemented diametrically opposite at the mid-length of the input bar, is used to measure the amplitudes of incident and reflected waves. A calibration factor is then used to convert the recorded output voltage into stress. The dynamic stress pulse can be shifted in time from the centre of the bar to the bar/specimen interface using a time shift based on one dimensional wave propagation.

Centreless ground silver steel was used for the input bar. The input bar used had a nominal diameter of 25 mm and was 2000 mm long. The centreless ground bar ensures that uniformity in terms of cross-sectional area and straight neutral axis of the bar are attained throughout the entire bar length (Gama *et al.*, 2004). Kyowa^{TM} strain gauges with length of 2 mm were bonded at the mid length of the bar. SHPB tests require a data acquisition system with high sampling rate (Zhou *et al.*, 2012). The stress wave signals measured as output voltage in two strain gauge stations were amplified before they could be recorded by a 16 bit data logger at 10 MHz. A calibration factor was used to convert voltage into stress. A profiled striker was machined from the same material as that of the input bar. A short striker was used as projectile in order

to induce a short pulse duration, which is ideal in the context of a spalling test, wherein a short pulse with short wavelength less than the specimen length is a pre-requisite in order to induce spall damage. Since the generated pulse could contain some oscillations, a pulse smoother was used to eliminate the Potchammer-Chree mode high frequency oscillations. Regarding the impact of the input bar with a striker, it was ensured that the bar was always loaded within its elastic limit. Table 3.3 summarizes selected properties for silver steel used in this study.

Table 3.3: Selected properties of silver steel

Parameter	Value
Yield strength	600 MPa
Density	7817 kg/m^3
Wave speed	5250 m/s

3.2.3.2 Spall test specimen preparation

Test specimens of anorthosite, norite and marble rock types were prepared for both quasi-static and dynamic tests. Cylindrical rock specimens were obtained through laboratory core drilling. Figures 3.9a and 3.9b indicate drilling of core samples from a block of rock and existing core sample, respectively. Spall testing requires relatively long cylindrical specimens as compared to quasi-static size specimens. The diameter of specimens is the same as the diameter of the Hopkinson pressure bar to be used, to facilitate even loading across the specimen face. In this study, an input bar with nominal diameter of about 25 mm was used, hence all the spall test specimens were prepared with a similar diameter to the input bar. The range of lengths of tested rock specimens was between 285 mm and 350 mm. All test specimens used were free from cracks or vein-structures and fairly homogenous.



(a)



(b)

Figure 3.9: Laboratory core drilling of spall test specimens from (a) a block of rock and (b) existing core sample

3.2.3.3 Liner material preparation

In the context of spalling phenomenon described in figure 3.7, the present study aim to combat dynamic rock fracturing (*i.e.* rockburst damage) by introducing a liner material at the free end of rock test specimens as shown in figure 3.8b. The choice of liner materials was governed by "sacrificial" liner materials involved in case study reported previously (Section 2.4.2). As a result, concrete and clay liners were chosen, following the behaviour of sacrificial layer in the real rockburst. A weak fine-grained concrete was used in this study, and it was allowed to cure for 14 days after casting (Figure 3.10). The concrete had a density of 2500 kg/m^3 and a p-wave velocity of 3440 m/s. The clay material of choice used in this study was Bentonite. Bentonite and water were thoroughly mixed in a container to produce a slurry-like consistency, as appears in figure 3.11a. Other liner materials used include a piece of silver steel with similar properties to the Hopkinson input bar



(a)



(b)

Figure 3.10: (a) Concrete liners with different thicknesses, and (b) liners with varying thickness attached to rock specimens



(a)



(b)

Figure 3.11: (a) Preparation of clay liner material, and (b) attached clay liner material contained in plastic tube

3.2.3.4 Quasi-static material characterization

It is necessary to determine the quasi-static rock mechanical properties before one conducts spall tests with the SHPB. One of the fundamental pre-requisites of spall testing is that the test specimen must not be loaded beyond its compressive strength. With that in mind, the dynamic stress pulse magnitude

in the SHPB can be controlled to fall below the rock material compressive strength by regulating the velocity at which the striker is fired. However, the reflected stress wave from the specimen free end must be sufficient to break the specimen in tension. Some of the results of dynamic compressive strength of rock materials used in this study were obtained using SHPB compression testing and the results are reported below.

Accurate data on the mechanical properties of rocks is of paramount importance in the fields of rock mechanics and rock engineering. At least five specimens per rock type were subjected to two quasi-static tests. Table 3.4 summarizes the uniaxial compressive strength data and deformation properties (i.e. Young's Modulus and Poisson's ratio) of anorthosite, norite and marble. Data for Brazilian Tensile Strength tests (BTS) are also included in table 3.4. In addition, an ultrasonic technique was used to measure the wave speeds in the tested rock materials to aid in determining the impedance mismatch of rock relative to the Hopkinson pressure bar.

Table 3.4: Mechanical properties of rocks tested

Rock type	**UCS (MPa)**	**BTS (MPa)**	**Young's modulus (GPa)**	**Poisson's ratio**	**Density** (g/cm^3)	**P-wave velocity** (m/s)
Anorthosite	239	11	93	0.30	2.78	4463
Norite	233	15	95	0.27	2.64	4640
Marble	104	4	78	0.32	2.88	5200

3.2.4 Dynamic compression testing with SHPB

Most recently, the International Society of Rock Mechanics (ISRM) has suggested SHPB as a test method for determining the dynamic uniaxial compressive strength of rock materials (Zhou *et al.*, 2012). A standard SHPB set-up consists of the following: a striker, loading (input) bar, and transmitting bar, a gas gun, stopper, as well as a data acquisition system. Figure 3.12 shows a complete SHPB set-up with a thin specimen sandwiched between long bars.

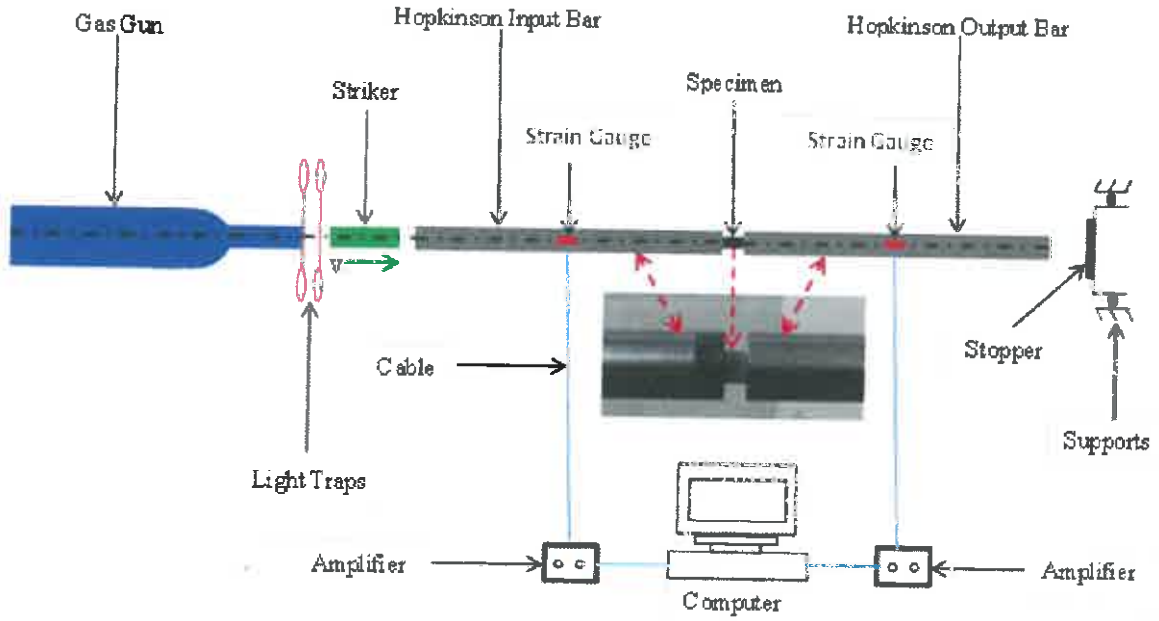

Figure 3.12: A schematic representation of SHPB set-up for dynamic compression

A gas gun is used to launch a striker to impact the input bar. The generated transient strain pulse will then propagate down the input bar as a longitudinal compressive stress wave, and on arrival at the input bar/specimen interface, part of the compressive stress wave will be reflected back as a tensile stress wave due to specimen/bar impedance, whereas the remainder of the compressive stress wave will travel through the specimen and be transmitted to the output bar. A pair of strain gauges cemented diametrically opposite at the mid length of the input and output bars is used to measure the amplitude of incident (ε_i), reflected (ε_r) and transmitted (ε_t) waves. Below is a typical graph showing strain gauge signals, with reflected and transmitted waves shifted to the respective bar-specimen interface.

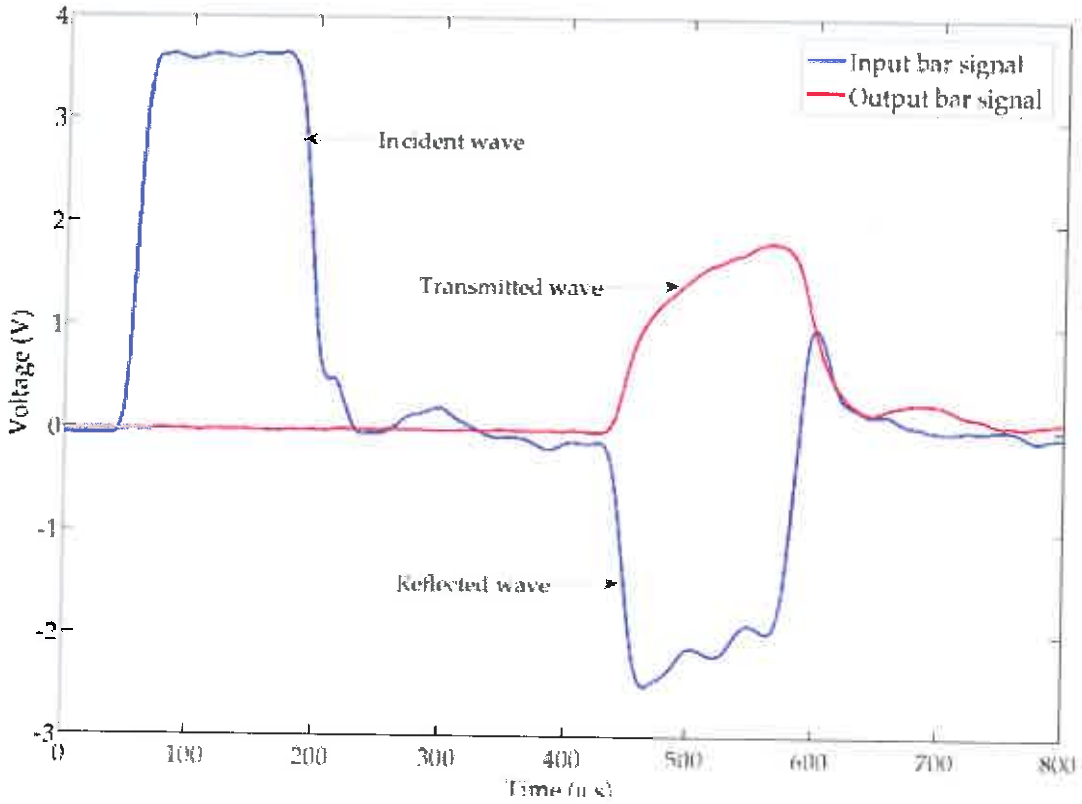

Figure 3.13: Typical strain gauge signals for SHPB test (of cast iron) (Govender, 2011)

Assuming one-dimensional theory of stress wave propagation, forces and velocities at the bar-specimen interface can be determined.

The forces (P_1 and P_2) at the contact of specimen and both input and output bars can be calculated by the following:

$$P_1(t) = A_{bar} E_{bar} (\varepsilon_i(t) + \varepsilon_r(t)) \tag{3.2}$$

$$P_2(t) = A_{bar} E_{bar} (\varepsilon_t(t)) \tag{3.3}$$

where, A_{bar} and E_{bar} are the cross-sectional area and Modulus of Elasticity of the bar, respectively.

Likewise, the velocities ($v_1(t)$ and $v_2(t)$) at the contacts of specimen of both input and output bars can be calculated by the following:

$$v_1(t) = C_o\left(\varepsilon_i(t) - \varepsilon_r(t)\right) \tag{3.4}$$

$$v_2(t) = C_o\left(\varepsilon_t(t)\right) \tag{3.5}$$

where, C_o is the wave velocity given by:

$$C_o = \sqrt{\frac{E_{bar}}{\rho_{bar}}} \tag{3.6}$$

The ultimate goal of a SHPB compression test is to determine the stresses and strains in the specimen. The strain rate, strain and stress experienced by the specimen are given by:

$$\dot{\varepsilon} = -\frac{2C}{L}\varepsilon_r \tag{3.7}$$

$$\varepsilon(t) = -\frac{2C}{L}\int_0^t \varepsilon_r dt \tag{3.8}$$

$$\sigma(t) = \frac{A_{bar}}{A_{specimen}} E\varepsilon_t \tag{3.9}$$

The above equations are valid if the specimen experiences uniform stress and strain during the test.

Centreless ground silver steel with similar properties reported in table 3.3 was used for both input and output bars. The bars used had a nominal diameter of 25 mm and were 2000 mm long. To avoid repetitive loading of the specimen, a 50 mm segment was trimmed from the output bar resulting in a nominal length of 1950 mm. According to Govender *et al.* (2012) *'this ensures that the reflected wave in the output bar unloads the specimen before the second transit of the wave in the input arrives, thus preventing repetitive loading of*

the specimen.' Kyowa^{TM} strain gauges with length of about 2 mm were cemented at the mid length of both the bars, and that is before the output bar was trimmed.

A conventional steel bar with a diameter of 19.05 mm and nominal length of 750 mm was used to impact the input bar. Since the generated pulse could contain some oscillations, a pulse smoother can be used to eliminate the Potchammer-Chree modes high frequency oscillations. The most fundamental aspect of SHPB tests is its calibration. Calibration of the SHPB set-up in entirety must be done systematically (Gray, 2000) and its purpose is that the measured strain signals at mid-bar strain gauges must precisely represent stress and strain in the bars. This implies that individual bars must be impacted by a projectile with known velocity separately and calibration must also be done for both bars (input and output) without the test specimen. Details on how calibration was done in this study are well documented by Govender (2011).

Fundamental to SHPB results is their validity. The stress equilibrium and constant strain rate for tested rocks were evaluated to validate the results. Before determining the average specimen stress, the expressions below are used to diagnose the balance between the specimen face stresses at the input and output bar interfaces.

$$\sigma_{input}(t) = \frac{A_{bar}E_{bar}}{A_{specimen}}\left[\varepsilon_i(t) + \varepsilon_r(t)\right] \tag{3.10}$$

$$\sigma_{output} = \frac{A_{bar}E_{bar}}{A_{specimen}}\varepsilon_t \tag{3.11}$$

Ideally, the specimen face stresses must satisfy stress equilibrium conditions for SHPB results to be considered valid and reliable. The few selected results show some difference between the peak stresses at input and output bars, and the trend has been recognized in other unreported results. In figure 3.14, a

face stress difference of 11 MPa was noticed at input and output bar interfaces for anorthosite rock material. The peak stress at input is slightly higher than than of output. A good example of stress equilibration is shown in figure 3.15.

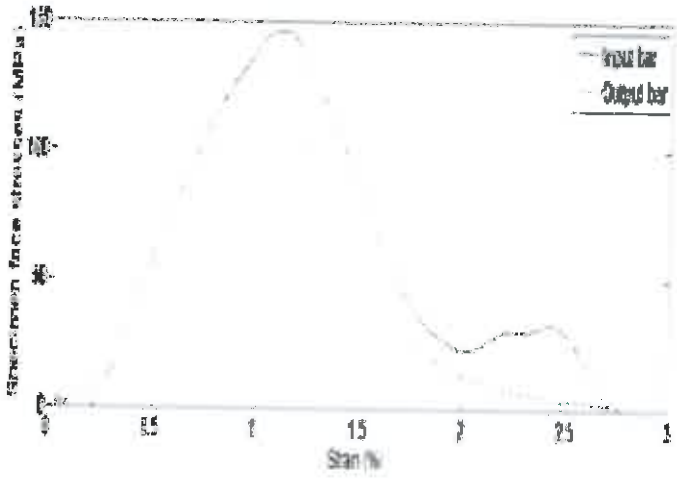

Figure 3.14: Example of face stresses for Anorthosite rock type under compression test with SHPB

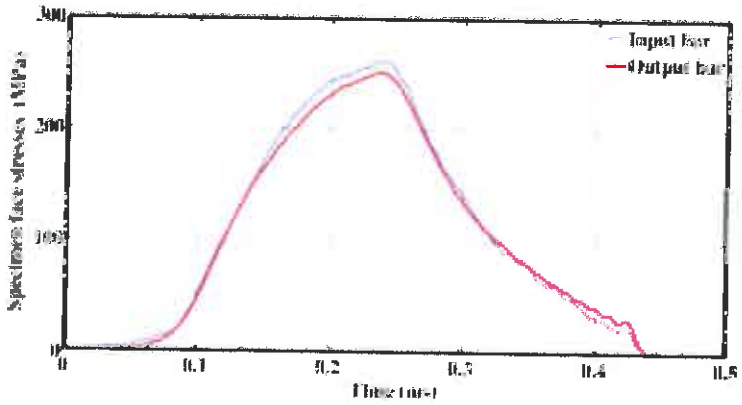

Figure 3.15: Example of face stresses showing good equilibration (Govender *et al.*, 2012)

While reasonable "stress equilibrium" based on the slight variation in peak stresses is recognized, there is a phase lag between input and output bar stresses immediately after the peak stress is reached. This offset could be the result of sensitivity of wave velocity values for individual bars used during the shifting of

stress signals from strain gauge stations to the bar-specimen interfaces (Lifshiz and Leber, 1994).

The rock materials tested were fairly brittle in nature. In SHPB testing, brittle materials are sensitive to small strain rates, which can lead to premature failure of material. Figure 3.16 shows strain rate results for an anorthosite test specimen. Unfortunately, a constant strain rate was not achieved in this regard. In SHPB testing as described in figure 3.6, the strength of materials increase with strain rate. However, the dynamic compressive strength of anorthosite obtained is even less than quasi-static UCS of anorthosite (see table 3.4). Figure 3.17 is an example of fairly constant strain rate achieved for glass fibre reinforced polypropylene (GFPP) material. Even though there is a slight drop of strain rate at peak failure, the strain rate nearly plateaus afterwards. Ideally, constant strain rate must resemble what is depicted as "exaggerated constant strain rate" in figure 3.17.

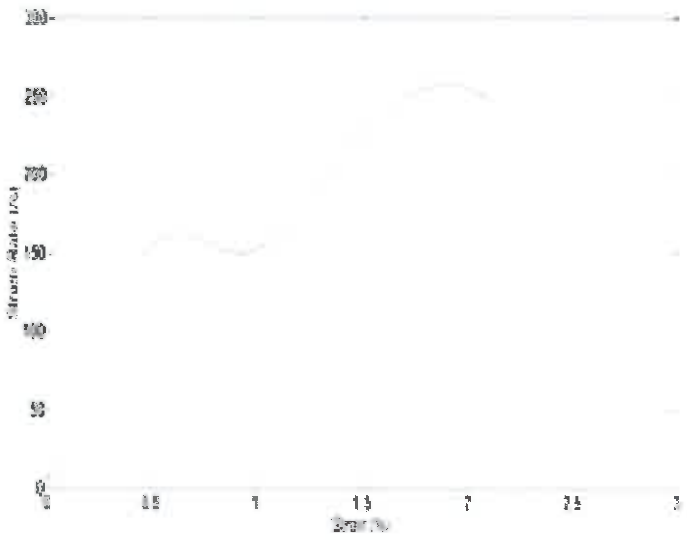

Figure 3.16: Strain vs true strain for tested rock material

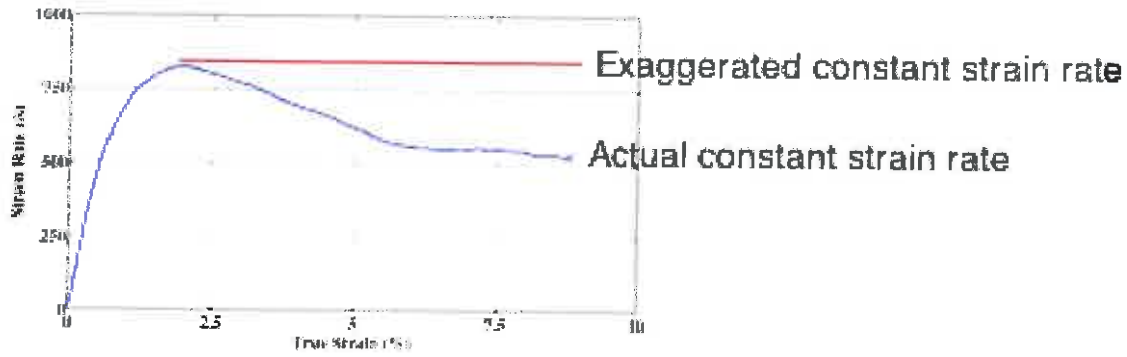

Figure 3.17: Strain rate for a typical SHPB test using a conical striker (modified after Govender *et al.*, 2012)

Poor stress equilibrium in Hopkinson bar tests can be the result of a number of factors (Govender *et al.*, 2012). Firstly, comparison of impedance mismatch between Hopkinson pressure bars and the test specimen was made. To achieve this, the density (ρ) and wave speed (C_o) in both the Hopkinson bar and rock material must be known. The impedance mismatch (ρC_o) for both anorthosite and norite were found to be equal (*i.e.* 12 MPa s/m), whereas ρC_o= 41 MPa s/m was determined for silver steel. Govender et al. (2012) tested Glass Fibre Reinforced Polypropylene under impact loading with low impedance ρC_o= 1.7 MPa s/m, and the bar impedance was similar to the one used in this study. The small specimens tested suffered equilibrium problems. In this study, high impedance mismatch reported is unlikely to have contributed to stress non-equilibrium situations. Specimen geometry is one of the possible factors which might have affected the stress equilibrium. It has been reported by Zhang and Zhang (2014) that the specimen/bar area mismatch ($D_S \approx 0.8 D_B$) must be considered before embarking on SHPB tests. All the test specimens tested in this study had a nominal diameter of 12 mm, and were prepared at a length to diameter ratio of one. By using the expression above for area/bar mismatch, specimens with diameter of 20 mm should have been used. High area mismatch between the specimen and bar increases the effect of friction and inertia, which causes specimens not to deform uniformly. Lastly and more importantly, the

size and configuration of striker chosen is of significant importance. A relatively long and profiled striker is recommended due to its capability to produce a low rise time stress pulse, which facilitates stress equilibrium. Unfortunately, profile strikers were only machined after this research work, and are shown below.

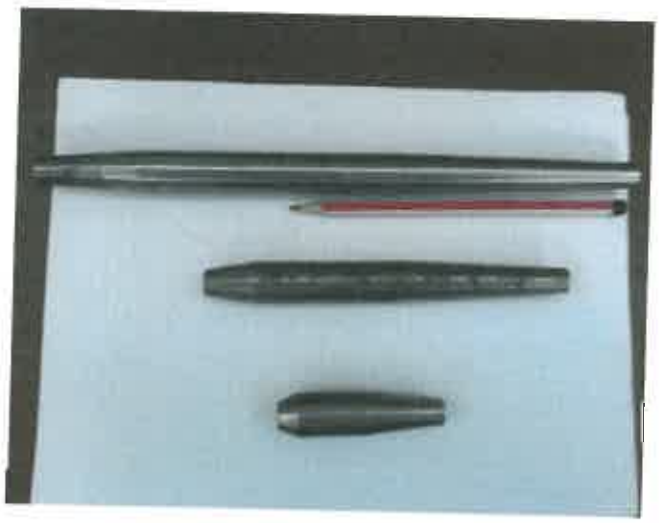

Figure 3.18: Photograph of profiled strikers

3.3 Chapter summary

This chapter covered a range of topics including a review of physical test methods to evaluate the performance of support elements and systems under dynamic loading conditions. The experimental programme aimed at investigating the performance of sacrificial support to resist rockburst damage was broadly covered. The following chapter reports experimental results on performance of sacrificial layers in resisting dynamic rock fracturing.

4 Dynamic rock failure containment using a sacrificial layer

The previous chapter dealt with two main topics: physical testing of rock support under dynamic loading conditions, and the experimental programme designed to evaluate the performance of sacrificial support.

In this chapter, spalling test results, based on the split Hopkinson pressure bar (SHPB) technique used to study some aspects of dynamic rock fracturing in tension at high strain rates are described. The role a sacrificial layer plays in combating such dynamic rock failure is presented. Qualitative results on the performance of sacrificial layers, captured by high-speed photography, are presented. Some useful insights into the effect of varying sacrificial liner thickness on dynamic rock failure are provided. The chapter also assesses the effect of impedance mismatch in layered systems and its influence on rock damage (*i.e.* rockburst damage).

4.1 General observations from spall tests conducted without support liners

Rock specimens were tested without any form of liner to allow the rock the freedom to fail dynamically due to the effect of the reflected tensile stress wave from the free end of the rock test specimen. These results are required before the performance of sacrificial various liners could be evaluated. Following this, different liner materials were then tested to evaluate their potential to prevent dynamic rock fracturing as reported in the following section.

Figure 4.1 exemplifies failed rock specimens for tests conducted without liners. All specimens were tested at relatively similar loading conditions by controlling the striker impact velocity. Common to all the test specimens is multiple fragmentation pattern, resulting from the reflected tensile wave from rock specimen free end. In the example presented below, all test specimens are characterized by three fragmentation pattern (as shown by encircled fracture zones), independent of rock type. Dynamic rock fracturing of spall test specimens generally initiates first at a certain location away from the specimen free end, progressing backward in the opposite direction as the reflected tensile stress wave interacts with the tail of the propagating incident compressive stress wave within the rock specimen. Multiple spallation could partly be the result of specimen length, *i.e.* long specimens are more susceptible to suffer from multiple spalling than short specimens.

As pointed out above, the following section will explore the effect of introducing various liner materials and liner combinations in inhibiting dynamic rock fracturing.

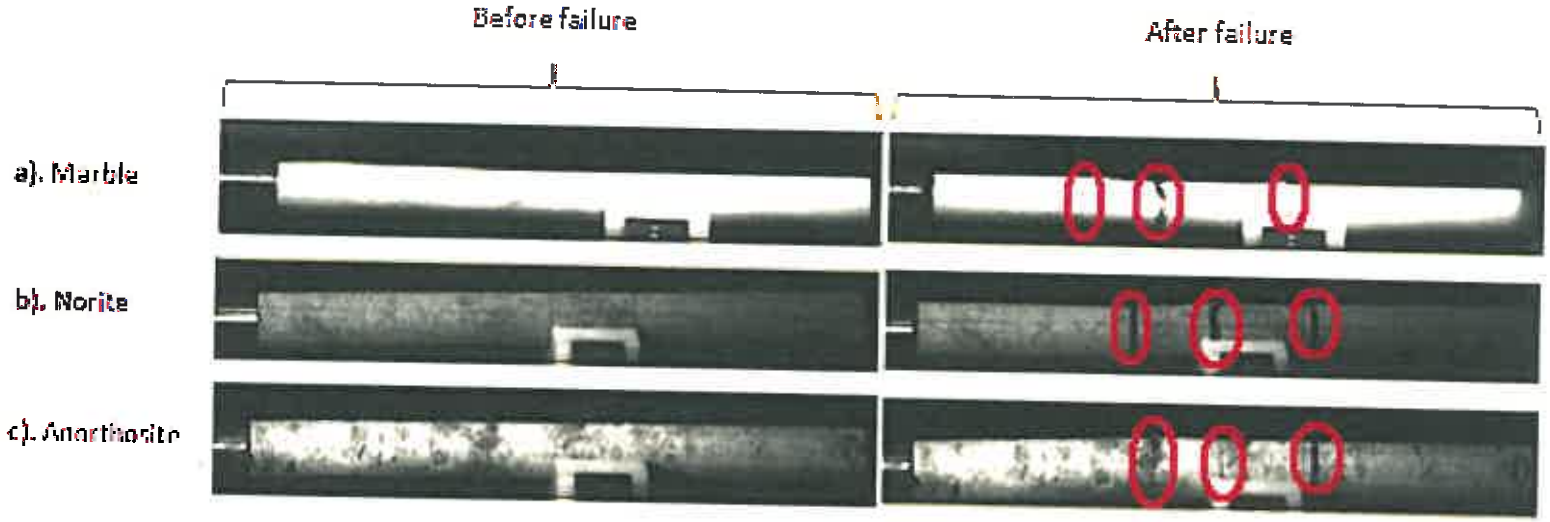

Figure 4.1: Frames of different rocks tested, before and after spalling

4.2 Evaluating the performance of support liners consisting of materials with differing mechanical properties

In this section, various liners and liner combinations, aimed at helping to reduce dynamic rock fracturing, are investigated. Concrete and clay liners were chosen, following the behaviour of sacrificial layers in real rockburst events, as previously reported. To achieve a fair representation of low to high impedance mismatch between rock specimen and support liner, a steel liner was used as one of the liners. The performances of various liner materials under dynamic loading are presented below.

4.2.1 Tests with minimum liner thickness per liner material type

Tests with minimum liner thicknesses per liner material type were conducted before liner thickness could be varied, with exception of silver steel, which had only a nominal thickness (length) of about 140 mm. The performance of concrete, clay, concrete/clay liner combination, and steel liners in preventing spall failure is presented in the following sections.

4.2.1.1 Tests with 45 mm thick concrete liner (concrete liner series)

A weak fine-grained concrete was used in this study as already mentioned. Initially, all the concrete liners were prepared at a nominal thickness of 45 mm as part of the trial runs. Figure 4.2 shows the behaviour of different rock types supported with concrete liners with this nominal thickness. There is relatively little difference in terms of rock fragmentation patterns, despite the introduction of the liners, as compared with the behaviours of rock specimens reported above without liners.

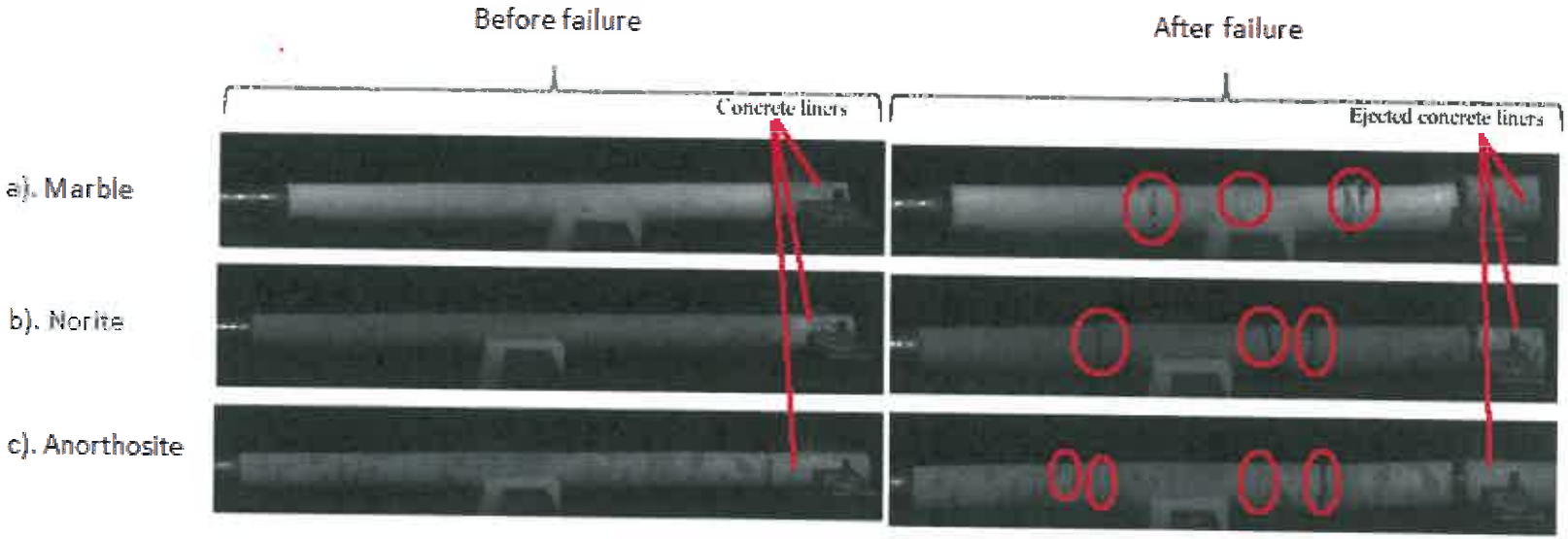

Figure 4.2: Different rock test specimens supported with 45 mm concrete liner

4.2.1.2 Tests with 10 mm thick clay liner (clay liner series)

The minimum thickness for the clay liner was 10 mm and a plastic tube was used to contain the clay. It was difficult, if not impossible, to fill the plastic tube containment beyond a thickness of 50 mm for the parametric study, due to difficulties associated with handling wet clay.

From the photographs in figure 4.3, marble specimens spalled at one location, resulting in two fragment pieces. In contrast, the anorthosite and norite cores are characterized by a two-spall fragmentation pattern. There is a noticeable decrease in spall fragmentation in this liner series as compared to the observations reported in the previous section.

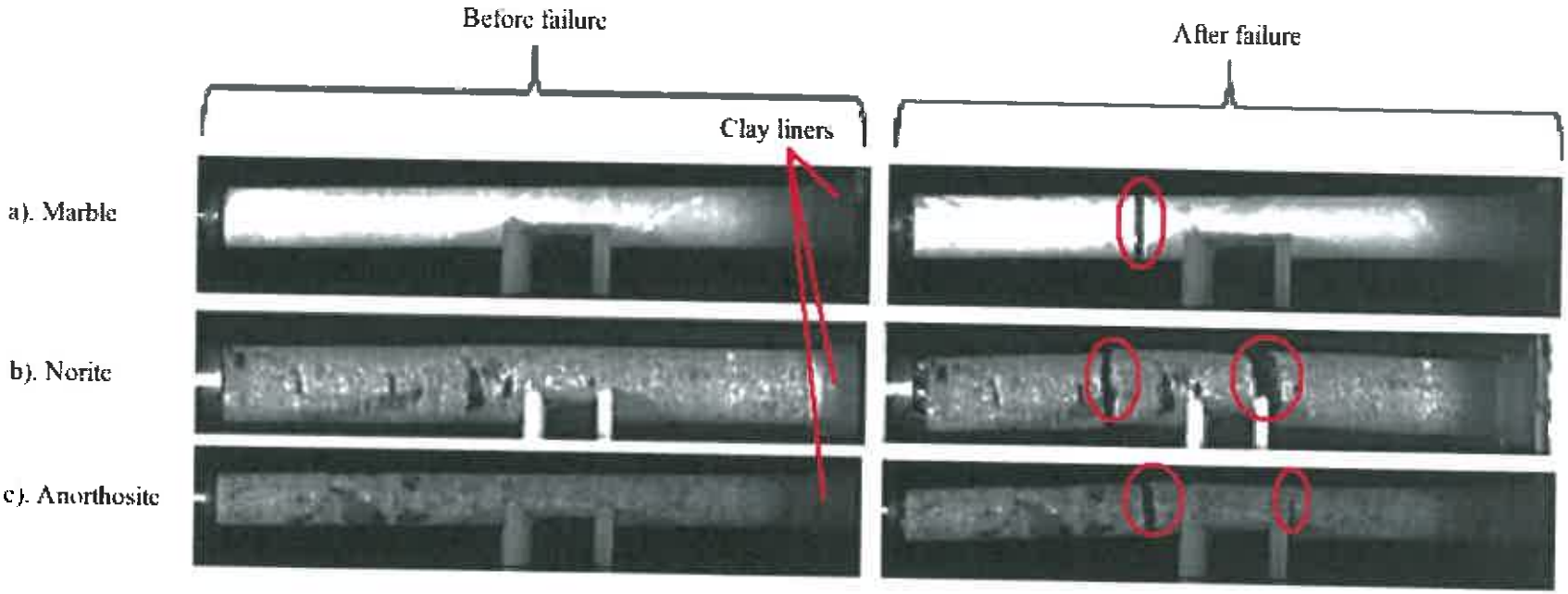

Figure 4.3: Different rock test specimens supported with 10 mm clay liner

4.2.1.3 Tests with 30 mm thick concrete/clay liner combination (concrete clay combination)

A combination of concrete and clay was used to assess its effectiveness in preventing dynamic rock failure. This composite of concrete/clay liner was made up of a 20 mm thick concrete liner, and a 10 mm thin clay liner. All the rock test specimens in these tests, as illustrated in figure 4.4, show a three-spall fragmentation pattern. Similar observations of behaviours of rock specimens were made for rocks supported with 45 mm thick concrete liners reported under sub-subsection 4.2.1.1.

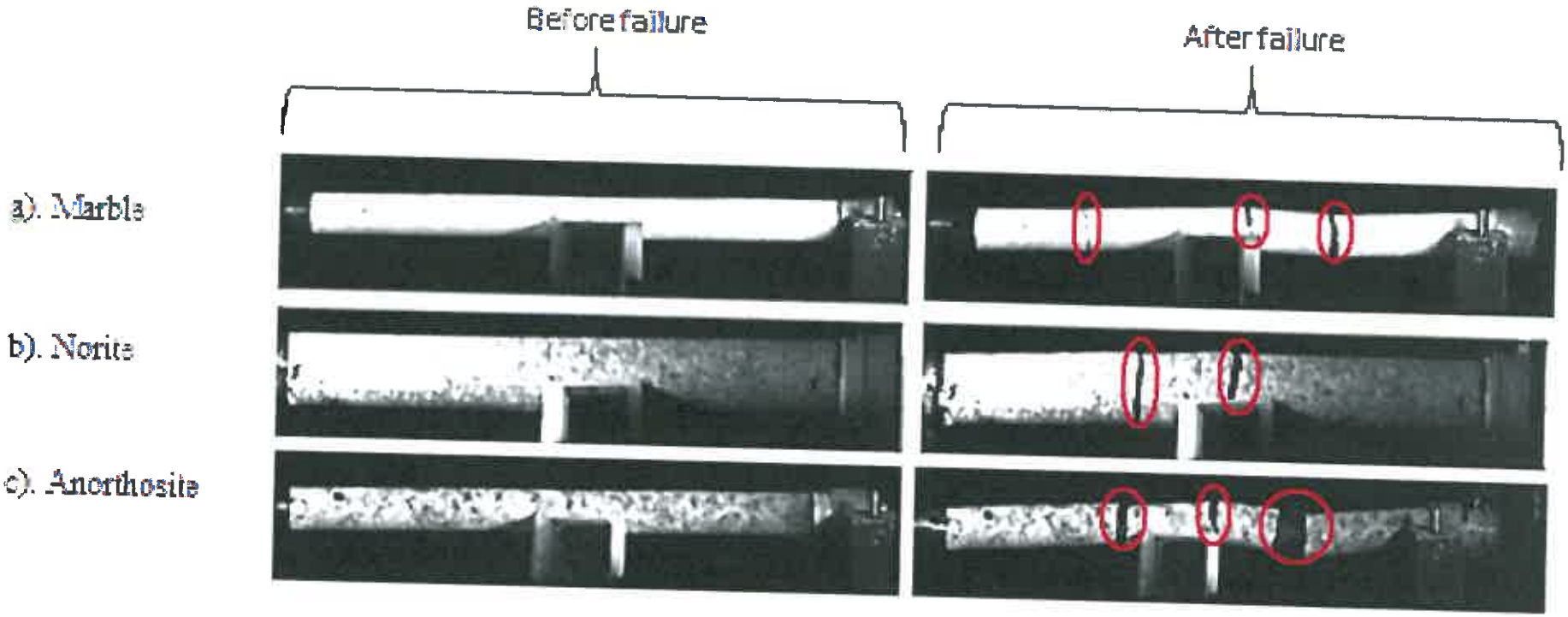

Figure 4.4: Different rock test specimens supported with 30 mm concrete/clay liner

4.2.1.4 Tests with a 140 mm thick steel liner (steel liner series)

The capability of steel in resisting the effect of the reflected tensile wave in rock was examined. Norite and anorthosite exhibited a two spall fragmentation pattern, while the marble test specimen spalled at one location, as shown in figure 4.5. Similar observations were made for the same rock types supported with a 10 mm thick clay liner, as reported above (see figure 4.3).

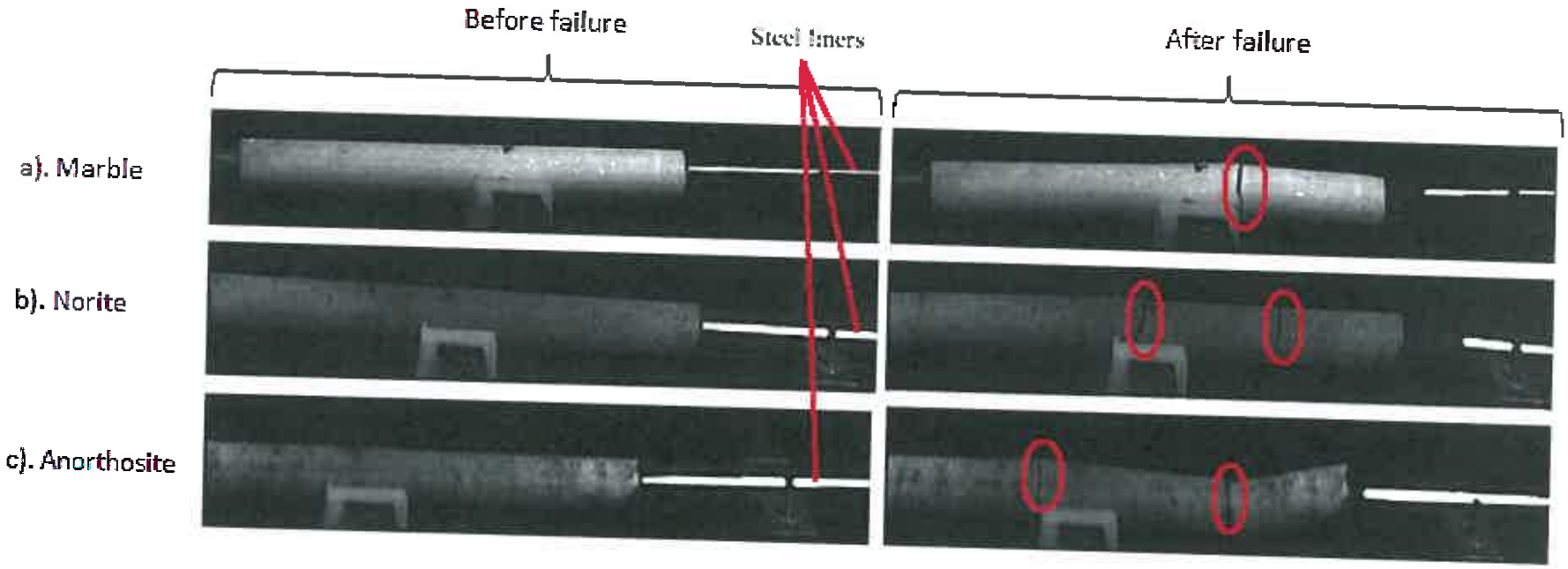

Figure 4.5: Different rock test specimens supported with 140 mm steel liner

In the following section, the effect of varying support liner thickness on dynamic rock failure is investigated.

4.2.2 Effect of varying liner thickness on dynamic rock failure

In order to study the effect of varying liner thickness (δ), it was decided to test respective liners with a constant thickness as an initial step toward examining their effectiveness to resist dynamic rock failure as reported in the previous section. Three series of liners, namely concrete, clay and a concrete/clay combination are discussed in this section.

4.2.2.1 Concrete liner series

Figure 4.6 depicts the behaviour of different rock types together with concrete, as the concrete liner thickness is varied. The initial thickness of concrete liner used was about 45 mm, which was then increased to 70 mm and 140 mm. Frames 1, 2 and 3, numbered in ascending order for all rock types in figure 4.6 (on the right hand side), indicate the decrease in rock fragmentation as the concrete liner thickness increases. Concrete liner thickness variation generally showed better performance in reducing spall damage, independent of rock type tested. Marble test specimens, with maximum thickness (~140 mm) of concrete liner, eliminated dynamic rock damage, and this is a good example of how a sacrificial support ought to behave under dynamic loading.

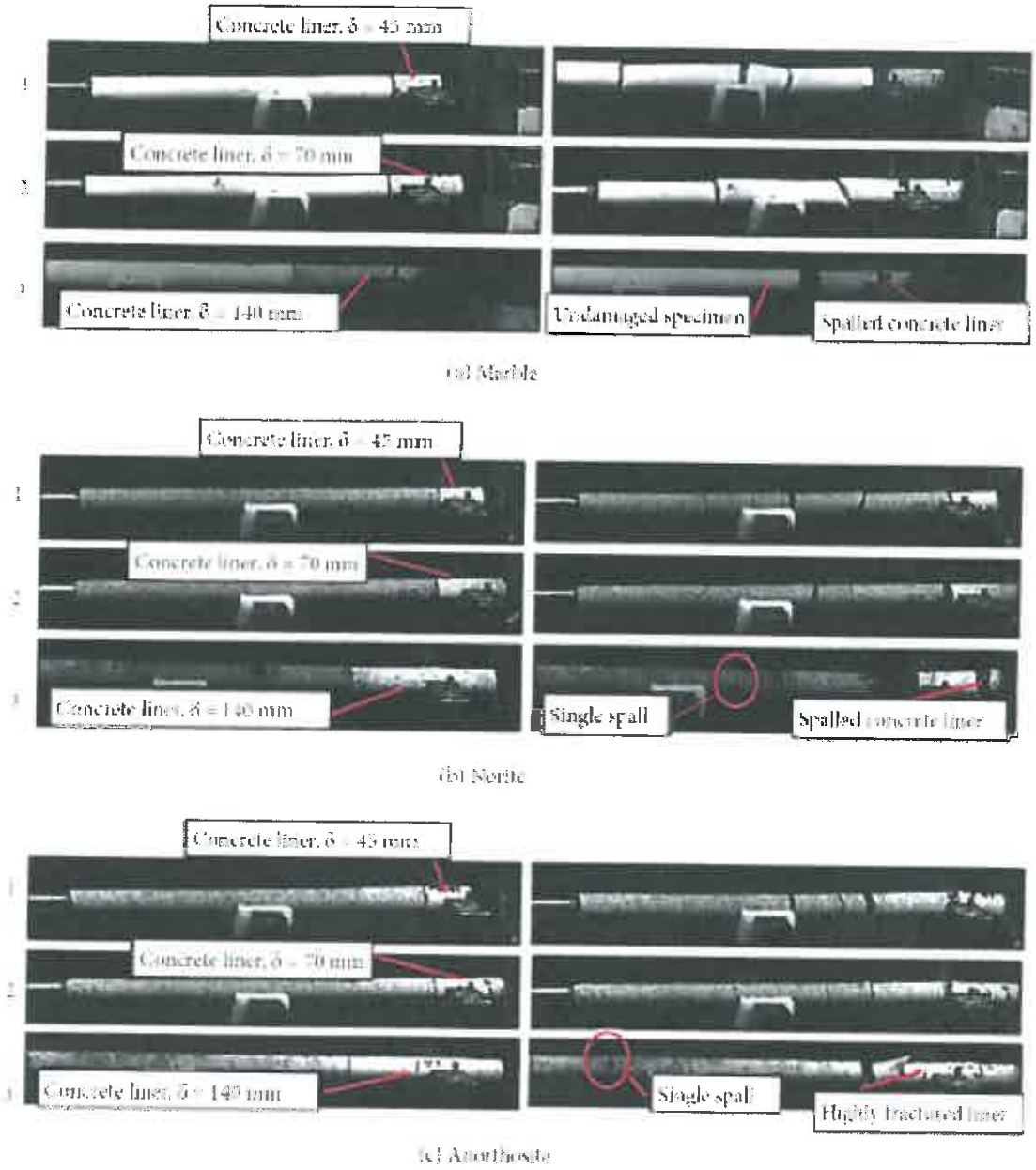

(a) Marble

(b) Norite

(c) Amphibolite

Figure 4.6: Dynamic behaviour of different rock types with various thicknesses of concrete liner

4.2.2.2 Concrete/clay liner combination

In this section, the thickness of concrete liner was varied while the thickness of the clay liner was kept constant at 10 mm throughout testing. Different thicknesses considered for concrete liner can be seen in figure 4.7.

For marble test specimens, failure was inhibited when the thickness of the concrete/clay liner was 110 mm and 120 mm. This indicates that the clay liner could have absorbed the stress wave at the concrete/clay liner interface, resulting in a decrease in the strength of the reflected tensile wave at the contact, thus reducing the potential to re-enter rock specimen again and cause rock damage due to stress wave superposition. Spall damage was prevented from occurring in both anorthosite and norite when the liner thickness was 200 mm long, and there are two possible reasons for such behaviour. Firstly, the duration of the transmitted stress wave in concrete would have been prolonged, decreasing the chances of cyclic loading of the rock specimen, resulting from the reflected tensile stress wave, which in turn may cause rock spall damage. In addition, spalling of the liner support itself, as observed in case of longer liners, might have helped in reducing the strength of the tensile wave reflected from the concrete/clay liner contact, through energy loss during the fracturing process. Secondly, damage was not apparent in any of rock types due to the presence of the clay liner, as explained earlier.

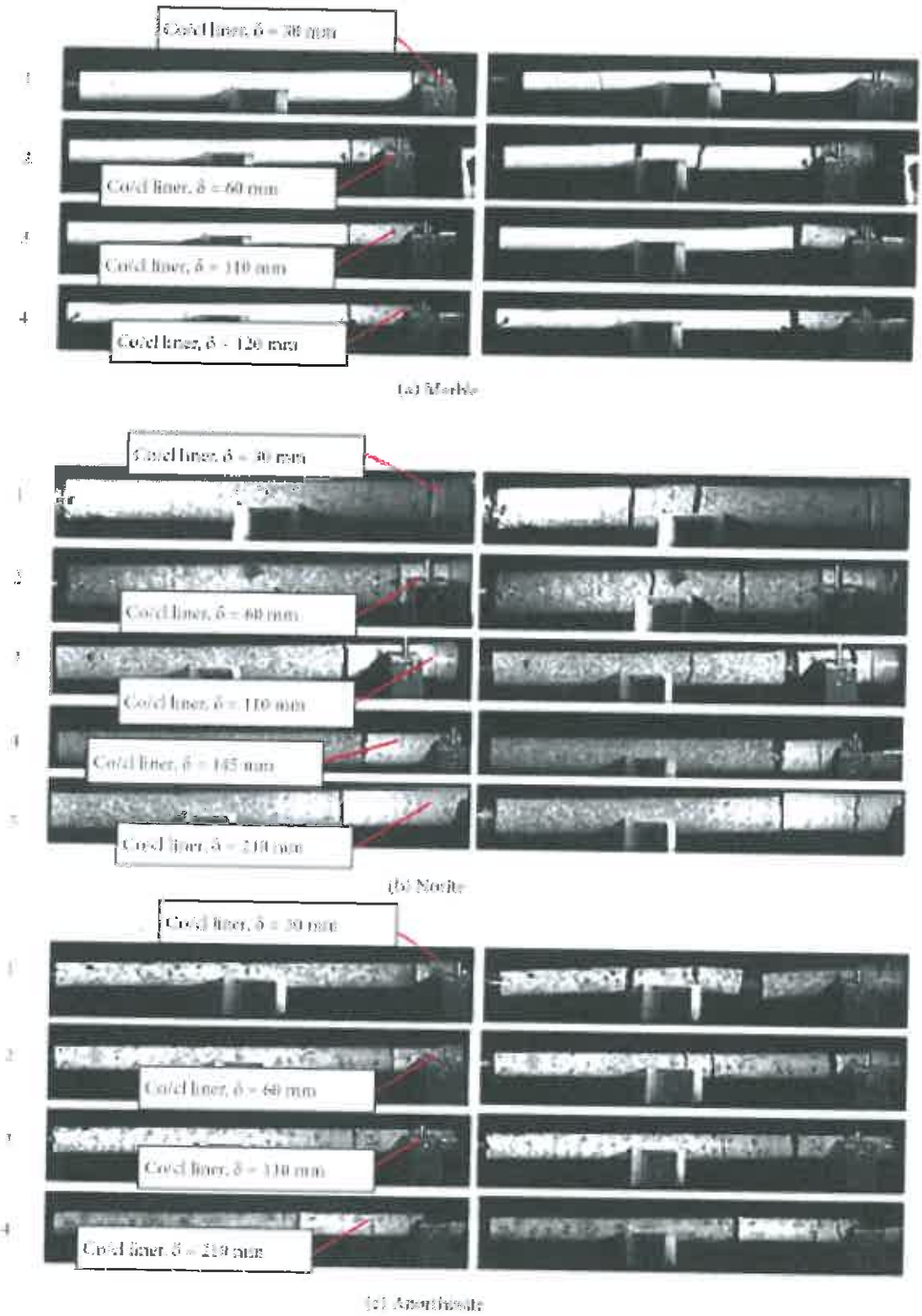

Figure 4.7: Dynamic behaviour of different rock types with various thicknesses of concrete/clay liner combination

4.2.2.3 Clay series

This clay liner series shows opposite behaviour in terms of its ability to help combat dynamic rock fracturing. The behaviour of marble specimens is erratic, considering that decreasing a liner thickness impacts positively in reducing the degree of rock damage, as learned previously. In this case, however, the number of fragments increased as the liner thickness increased. In brief, all test specimens failed despite an increase in liner thickness. This raises a fundamental question regarding the effectiveness of using "soft" liner materials as sacrificial support, and this is further interrogated in the following section.

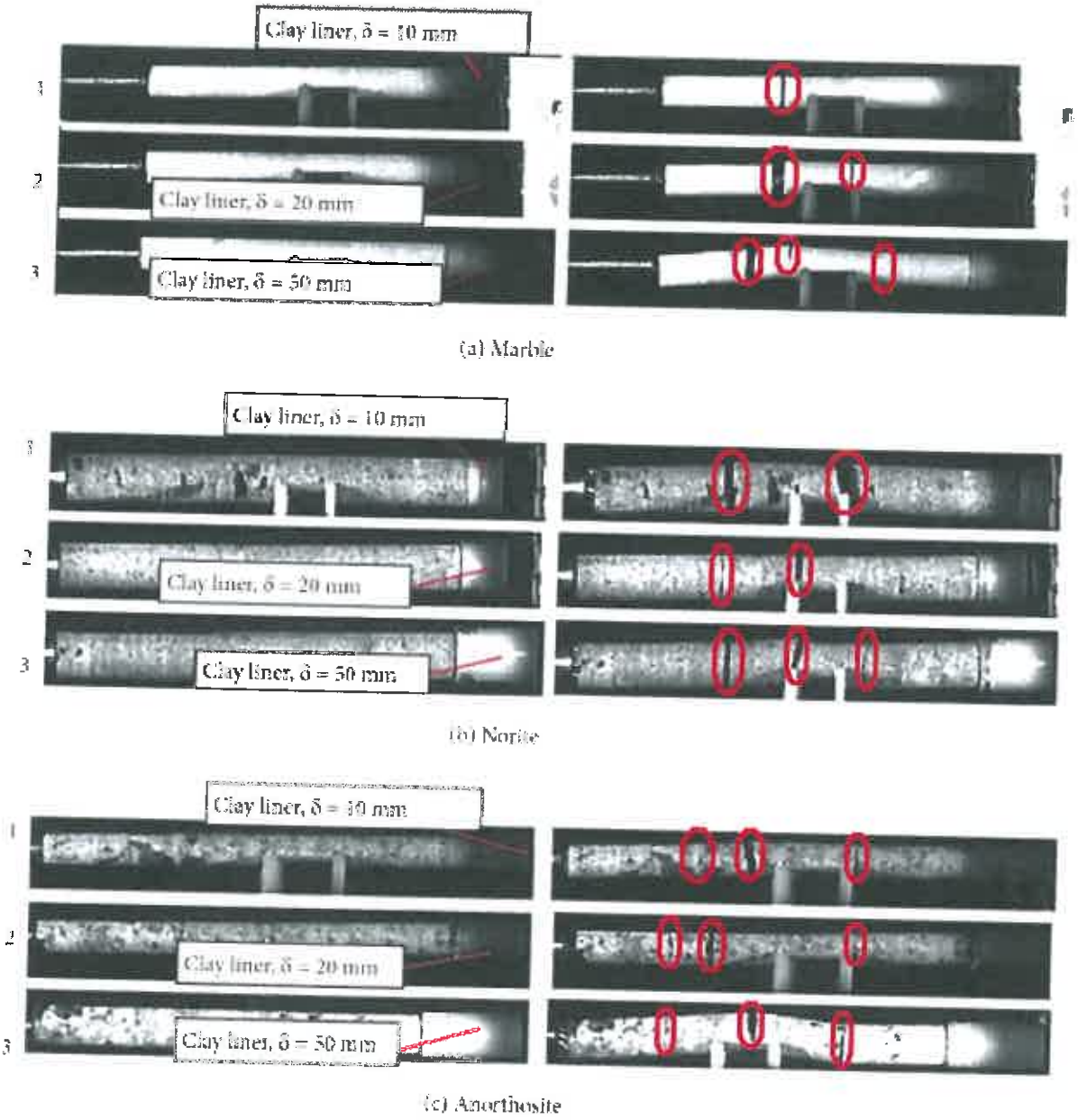

Figure 4.8: Dynamic behaviour of different rock types with various thicknesses of clay liner

4.2.3 Effect of mechanical impedance on rock damage in layered systems

It was not practical to cement strain gauges on both rocks and support liners tested in order to mirror the propagation of stress wave in the whole SHPB set-up. Instead, a basic analytical approach was used to determine the coefficients

of transmission and reflection respectively using the following equations:

$$\frac{\sigma_{trans}}{\sigma_{inc}} = \frac{2\rho_2 C_2}{\rho_1 C_1 + \rho_2 C_2} \tag{4.1}$$

$$\frac{\sigma_{refl}}{\sigma_{inc}} = \frac{\rho_2 C_2 - \rho_1 C_1}{\rho_1 C_1 + \rho_2 C_2} \tag{4.2}$$

The subscripts 1 and 2 denote Hopkinson pressure bar and rock specimen respectively. In cases when there are more than two liners, as in this study, equation 4.1 can be applied consecutively to determine the transmission ratio into the third layer.

$$\frac{\sigma_{trans}}{\sigma_{inc}} = \left[\frac{2\rho_2 C_2}{\rho_1 C_1 + \rho_2 C_2}\right]\left[\frac{2\rho_3 C_3}{\rho_2 C_2 + \rho_3 C_3}\right] \tag{4.3}$$

Subscripts 3 in this regard represent a support liner. The transmitted stress wave in the second layer can be used as an incident stress to the third layer from equation 4.3.

Tedesco and Landis (1989) reasoned that if the transmission and reflection of a stress wave in layered media is the function of impedance mismatch, then mechanical impedance could be manipulated to prevent internal damage of a layered structure subjected to external blast loads. Such an approach could also yield positive outcomes in trying to prevent rockburst damage to an excavation supported with a liner, when under dynamic loading. Generally, all the "layers" constituting HPB in this study had different mechanical impedance. For the input bar, rock materials tested, and the support liner materials (*i.e.* concrete and clay), the mechanical impedance relationship between these liners can mathematically be expressed as: $\rho_1 C_1 > \rho_2 C_2 > \rho_3 C_3$. In case of the steel support liner, this relationship changes to: $\rho_1 C_1 > \rho_2 C_2 < \rho_3 C_3$, due to the high impedance mismatch between steel and the rock materials. The Hopkinson pressure bar was dynamically loaded in the stress region between 80

MPa and 100 MPa. The percentage of transmitted stress wave in the first two media (*i.e.* Hopkinson bar and rock) without the liner (*i.e.* liner support) was sufficient to cause spall damage to rock upon reflection from the specimen free end. At least 46 % ($\geq$ 37 MPa) of the stress wave was transmitted to the rock test specimen for all rock types, while 54 % was reflected back to the steel bar. About 80 MPa was assumed as the input stress wave in the steel bar. Assessment of the effect of impedance mismatch between rock materials and different liner materials to dynamic rock failure is carried out below.

4.2.3.1 Impedance mismatch between rock materials and concrete liner

Assuming 37 MPa as the amplitude of incident stress wave in all rock specimens as established above, equation 4.1 can be used to calculate the coefficients of transmission and reflection at rock and support liner interfaces. It was found that at least 80 % ($\geq$ 30 MPa) of the stress wave was transmitted into the concrete for all rock types. To put this into perspective, the concrete used had high transmission ratios thereby preventing rock damage, since the reflected tensile wave was not strong enough to initiate rock damage, particularly in the case of marble test specimens with the thickest concrete liner. The concrete/clay liner combination can be added in this category.

4.2.3.2 Impedance mismatch between rock materials and clay liner

Literature values for density and p-wave velocity of saturated clays were used to define the impedance of clay. The density and p-wave velocity adopted for saturated clays in this regard are 2000 kg/m^3 and 1100 m/s, respectively. A simple calculation shows that at least 70 % of the stress wave was reflected at the rock/liner interface for all rock materials. This indicates that clay is a "reflective"[1] material, with high potential to induce significant damage due to

[1] A "reflective" material in this context is used to refer to a liner material characterized by wave transmission ratios less than 0.5.

high magnitudes of reflected tensile wave, making it an unattractive material to help prevent rock spallation, at least for the rocks tested in this study.

4.2.3.3 Impedance mismatch between rock materials and steel liner

A steel liner also exhibits a high coefficient of reflection, but less than that of a clay liner. At least half of the stress wave was reflected back into the rock specimens, resulting in the rock damage evident in figure 4.5.

4.3 Comments on experimental findings

The sections above explored the effectiveness of various support liners in helping to limit rock damage caused by reflected stress waves. This was achieved by using liners with different mechanical stiffness and varying support liner thickness. The results for the behaviour of clay and steel liners were perhaps easier to interpret, because failure of the rock test specimens under these two series was attributed to high coefficients of stress wave reflection at rock/liner interface. The effect of liner variation was considered for a clay liner up to 50 mm thick, and there was no effect noticed as far as prevention of rockburst damage is concerned. The steel liner used, however, had a relatively long thickness (length) of about 140 mm, and considering that both clay and steel liner are "reflective" materials, it is probably safe to assume that varying liner thickness of reflective material in an attempt to prevent rock damage is worthless, compared with concrete, and concrete/clay liner combination, characterized by "perfect" impedance.

From the above, it has been observed that having "perfect" impedance mismatch alone is not sufficient to guarantee prevention of dynamic rock failure. For instance, when a minimal thickness of concrete liner is used for instance, it only traps the momentum transferred from the excited rock without necessar-

ily altering the strength of stress wave at the contact. In contrast, relatively long specimens permit the passage of the stress wave through the liner, and the liner is damaged upon reflection of the stress wave from its free end.

In the case of the concrete/clay liner combination, test specimens of all rock types were prevented from damage when a certain threshold of composite liner thickness was reached. The behaviour of the rock was primarily influenced by mechanical impedance of concrete as described above, and by the clay liner as a secondary effect.

In closing this discussion, it is evident that varying liner thickness and mechanical impedance between rock and support liner play a significant role in limiting rockburst damage. However, it is not possible at present to provide definitive answers regarding the relationship between a liner's thickness and the mechanical impedance. What is evident, however, is that the use of "soft" and very stiff liner materials relative to rock is not ideal in attempting to help combat rockburst damage.

4.4 Chapter summary

From experimental observations described in this chapter, some of the support liner materials investigated behaved in a sacrificial manner. A concrete liner and a concrete/clay liner combination proved to be effective in preventing dynamic rock failure (*i.e.* rockburst). Analysis of results revealed that varying liner thickness and mechanical impedance between rock and support liner play a significant role in limiting rockburst damage. The following chapter investigates the behaviour of sacrificial support using numerical modeling.

5 Numerical modelling of the behaviour of sacrificial support using Universal Distinct Element Code (UDEC)

The previous chapter established that varying support liner thickness and mechanical impedance between rock and support affect dynamic rock fracturing. The results are in reasonable agreement with the observations of sacrificial support behaviour made after rockburst events in a mine. From a practical point of view, assuming that a sacrificial liner with "perfect" impedance is used to provide support to tunnel sidewalls or floor, it is unknown whether the seismic wave characteristics generated from mine-induced seismicity will influence the overall behaviour of sacrificial support. As a result, numerical modelling was considered as a means of investigating this unknown. UDEC is a sophisticated numerical tool with a track record of use in studying the response of layered media systems (such as jointed rock masses) in both static and dynamic situations. The dynamic analysis option available in UDEC permitted this study to assess the response of sacrificial layer/liner materials subjected to seismic loading.

This chapter will first provide an overview of UDEC followed by steps nec-

essary when one embarks on numerical modelling, especially when it comes to dynamic analysis. The main aim of this chapter, as highlighted earlier, is to present numerical interpretations pertaining to physical behaviour of sacrificial support, with reference to the effect of varying sacrificial liner thickness, and the wavelength characteristic (*i.e.* wavelength or wave frequency) of the propagating p-wave, on the overall behaviour of sacrificial support. The models built involve the use of weak concrete as support liner material. The contact between rock media and support liner was assigned a high normal fracture stiffness to allow maximum transmission of the wave at the interface. The models generated are simple elastic models not intended to simulate plastic deformations associated with spalling rock as described in the previous chapter, but to demonstrate the tensile wave mechanism of a "perfect sacrificial support liner" by altering support liner thickness and seismic wave characteristics.

5.1 An overview of UDEC in computing rock mass response

The Universal Distinct Element Code (UDEC), a discrete element method, is a two-dimensional numerical program originally developed by Cundall (1971) to simulate the response of jointed rock masses based on discontinuum theory. In UDEC, discontinuities, such as natural joints or cracks representing a jointed rock mass, are treated as boundaries, and the jointed rock medium is represented as an assemblage of discrete blocks. The individual blocks can behave either as rigid or deformable material, and large displacements and rotations along the discontinuities are permitted, unlike in continuum-based numerical methods, where large displacements of fractures and rotation of discrete blocks are restricted. The deformable blocks in UDEC can be subdivided into small internal zones or elements (*i.e.* finite difference elements). The response of

individual zones against each other is governed by a constitutive law (whether linear or nonlinear) defined beforehand for a particular model. Newtonian laws of motion, specifically the second law of motion (F = ma) is applied at the contacts of blocks, which in turn allows the block motions to be computed from both applied and body forces (Itasca, 2004).

5.2 Steps necessary for generation of models in UDEC

Sahayi (2013) summarized general yet fundamental steps necessary for building a model in UDEC, which include the following:

- Building the geometry of the model
- Meshing or zoning of the model
- Assigning the material properties
- Assigning the static boundary conditions
- Assigning the dynamic boundary conditions (if necessary)
- Applying the disturbance to the model (such as excavation of a tunnel) and running the model until the model reaches equilibrium (if necessary)
- Imposing the dynamic load (if necessary) and running the model for the stipulated time

Without reducing the effort above, it is of significant importance to add to the list the need for a constitutive law, which dictates the overall behaviour of the model. The following sections present details pertaining to models generated in this study in light of the steps above.

5.2.1 Conceptual model for dynamic analysis in this study

Figure 5.1 is the geometry of a conceptual model designed to study the effect of wave propagation on the behaviour of sacrificial support. The conceptual model simply highlights the geometry of the model, the boundary conditions (*i.e.* viscous, fixed and free boundaries) and history monitoring positions. All the history points within the rock block are located 10 m away from one another. A single vertical joint separates the rock media from the sacrificial layer.

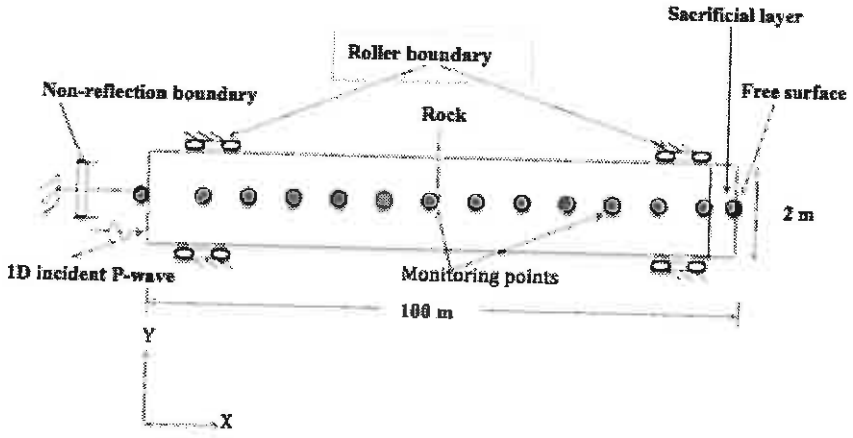

Figure 5.1: Configuration of UDEC model to study the behaviour of a sacrificial layer

5.2.2 Model geometry and meshing

The dimensions chosen for the model were carefully considered in order to simplify the problem as much as possible. The choice of slenderness ratio for the model described above allows prevention of wave reflections from top and bottom boundaries, which might introduce wave propagation interference on reflection back to the model, and therefore compromise the accuracy of the results. Alternatively, non-reflecting boundaries can be imposed in the model to address such problems. Chen and Zhao (1998) used similar model geometry

to investigate seismic waves propagation in jointed rock masses.

The choice of mesh size has a great deal of influence in solving dynamic analysis problems, since the density of the mesh could affect wave transmission accuracy and hence the results. It is recommended that the size of the zone must be smaller than one-tenth to one-eighth of the wavelength associated with highest frequency component of the input wave in the model, and the following equation is used to determine the size of the zone.

$$\triangle L \leq \frac{\lambda}{10} \tag{5.1}$$

In the equation above, $\triangle L$ is the zone size and λ is the wavelength, here considered to be a representation of the highest component of the wave. Wavelength can easily be obtained if the wave speed (C) and frequency (f) are known.

$$\lambda = \frac{C}{f} \tag{5.2}$$

From equation 5.1, the denominator value can be increased if more accuracy is desired. However, this can increase computational time and introduce errors in the model (Chen and Zhao, 1998). In this study, a zone size ratio of 1/28 was used to achieve the balance between computation efficiency and accuracy (Zhang *et al.*, 2015).

5.2.3 Material properties and constitutive model

The current model configuration requires material properties for both rock and sacrificial layer. Mechanical properties for both rock component and sacrificial liner material (*e.g.* weak concrete) in the model are given in the following table.

Table 5.1: Mechanical properties of rock and liner materials

Mechanical properties of rock material								
Rock Type	UCS (MPa)	BTS (MPa)	Young's modulus (GPa)	Poisson ratio	Density (g/cm^3)	P-wave velocity (m/s)	Friction angle ϕ^o	Cohesion (MPa)
Anorthosite	239	11	93	0.30	2.78	4463	59	51
Mechanical properties of liner material								
Liner type	UCS (MPa)	BTS (MPa)	Young's Modulus (GPa)	Poisson ratio	Density (g/cm^3)	P-wave velocity (m/s)	Friction angle ϕ^0	Cohesion (MPa)
Weak concrete	6.5		1.62	0.31	2500	3440	35.50	3.50

The above are properties of rock and liner materials which were obtained in the laboratory. The Elastic materials model was chosen in this study, which only requires density and deformation properties such as Young's modulus and Poisson's ratio as input parameters from the above data. The contact between rock media and sacrificial layer in the model was represented by area contact coulomb-slip criteria. The joint (*i.e.* an interface between rock media and sacrificial layer) is treated as a displacement discontinuity.

5.2.4 Model boundary conditions

As highlighted in figure 5.1, three boundary conditions, *viz* viscous, fixed and free boundaries, were assigned to the model. The model was restricted to move in the y-direction, with the degree of freedom only allowed in x-axis direction, which is the direction of wave propagation. The right boundary was specified to be free to permit reflection of waves at the free surface.

5.2.5 Dynamic input in the model

Dynamic input in UDEC models is mainly applied as velocity or stress history. In this case, seismic loading was applied as normal stress at the left boundary of the model given by the following:

$$\sigma_n = 2(\rho C_p)\, v_n \tag{5.3}$$

where,

σ_n = applied normal stress (MPa)

ρ = mass density $\left(kg/m^3\right)$

C_p = wave velocity through medium (m/s)

v_n = input normal particle velocity (m/s)

A half sinusoidal p-wave with *ppv* amplitude of 2 m/s was applied at the left boundary of the model for all the models reported in this chapter. Figure 5.2 is an example of a one-dimensional P-wave signal recorded at the left and right boundaries of the model, expressed in terms of peak particle velocity. The first peak is the original dynamic pulse applied at the left boundary of the model with amplitude of 2 m/s. The middle peak is characterized by twice the *ppv* value of the first peak, and this was recorded at the right free surface boundary of the model. Amplification of the wave by a factor of 2 affirms the theoretical value suggested by Kolsky (1963). High amplification values greater than 2 are, however, common in actual rock masses subjected to seismic loading in underground excavations. The last peak is a signal of the reflected wave recorded at the boundary of the model. There is no attenuation, in terms of wave amplitude, with distance travelled by the wave, since damping was set to zero in the model.

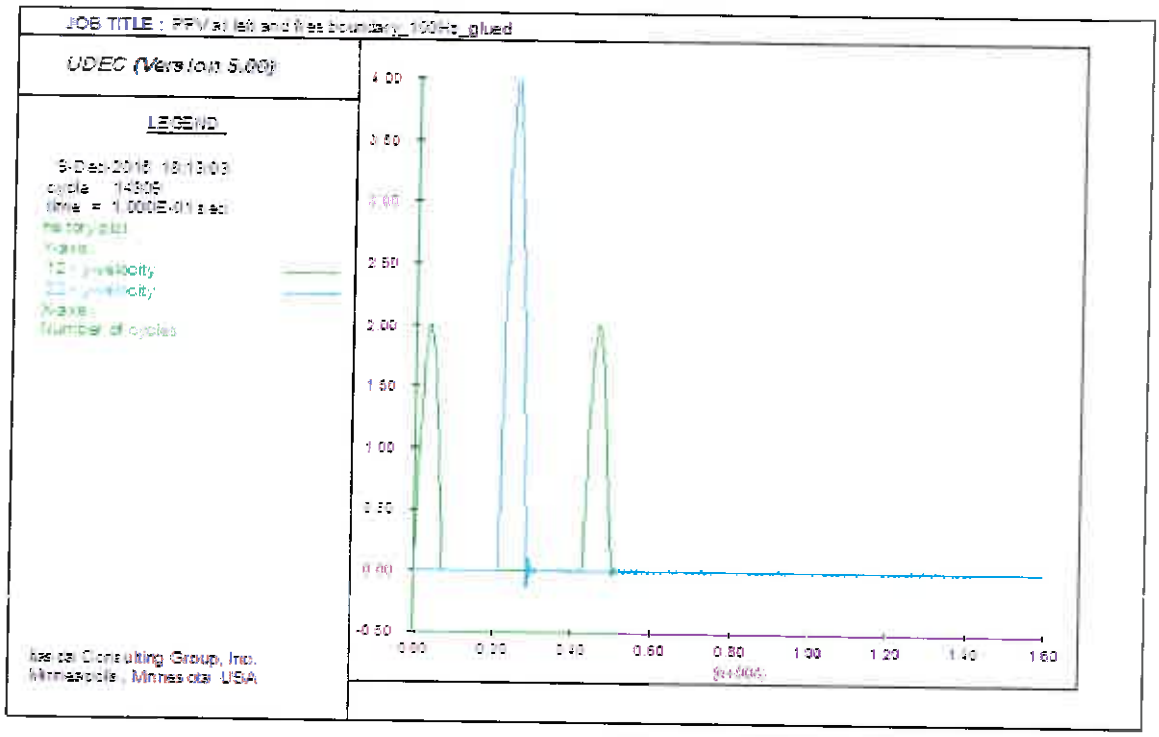

Figure 5.2: 1D p-wave signal expressed as peak particle velocity

In the following section, details of numerical interpretations regarding the behaviour of a sacrificial layer are presented.

5.3 Behaviour of a sacrificial layer under dynamic loading – a numerical study

Two types of models are considered in this section. The first model type is characterized by a welded joint as the interface between the rock and the sacrificial layer. The second type of model is characterized by an "unwelded" joint separating the rock from the sacrificial layer. In addition, the liner thickness and wavelength of the input P-wave are varied in this second category. Both the rock and sacrificial layer in both categories are assumed to be elastic, isotropic and homogeneous.

5.3.1 Effect of elastic wave propagation on the behaviour of a sacrificial layer characterized by welded and unwelded interfaces

From the conceptual models presented by Stacey (1991) and Stacey and Rojas (2013) on the behaviour of sacrificial support, detachment of a sacrificial layer providing support to the rock will manifest after reflection of the tensile wave from the free surface due to low or no tensile strength at rock/liner interface. To probe this behaviour numerically, welded and unwelded contacts between the rock and the support liner were considered. In the first case, the contact between the rock and sacrificial liner treated as a joint was assigned infinite cohesion and tensile strength to produce a welded interface between two media. In the other case, the joint was assigned zero cohesion and tensile strength to represent an unwelded interface characteristic. In both cases, high normal joint stiffness of 100 GPa was assigned, using area contact Coulomb slip criteria. Such a high value of fracture normal stiffness allowed 100 % of the p-wave into the sacrificial layer, as can be seen in figures 5.5 and 5.8, thereby neglecting wave attenuation and effect of impedance mismatch between rock/support liner medium. Figure 5.3 shows displacement of the model after propagating the wave from the bottom of the model. Of particular interest is to monitor displacement of the sacrificial layer due to reflection of the p-wave from the free surface. Figure 5.4 displays the concrete liner in place without any form of movement. This behaviour is apparent since the interface is welded. The *ppv* value monitored on the free surface of the concrete liner is twice that of the original applied stress pulse (figure 5.5).

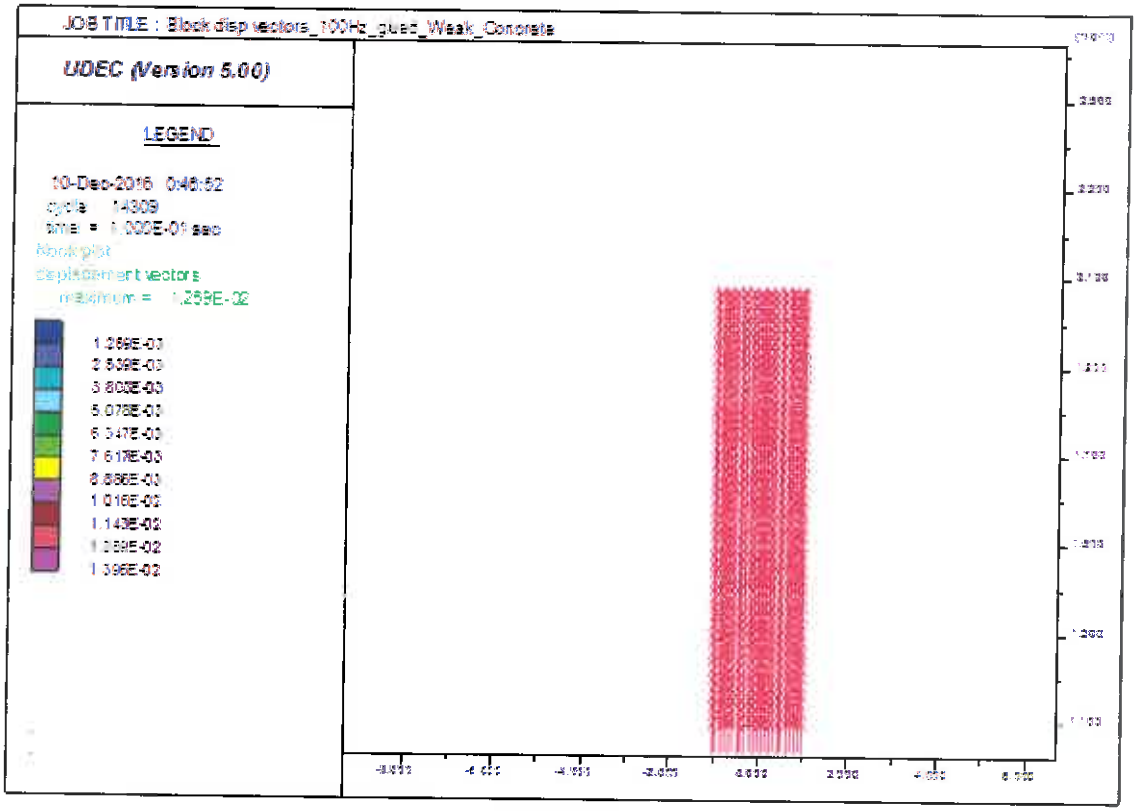

Figure 5.3: Displacement velocity for welded joint model

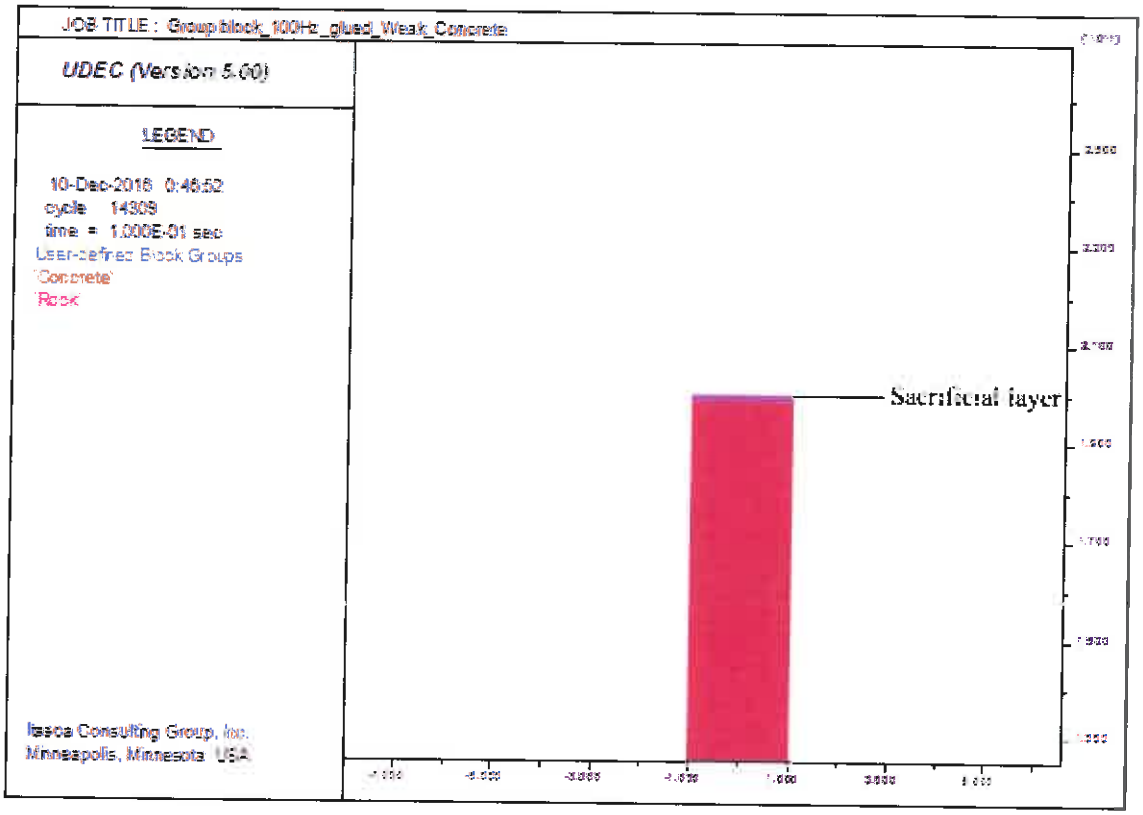

Figure 5.4: Stable sacrificial liner in welded interface model

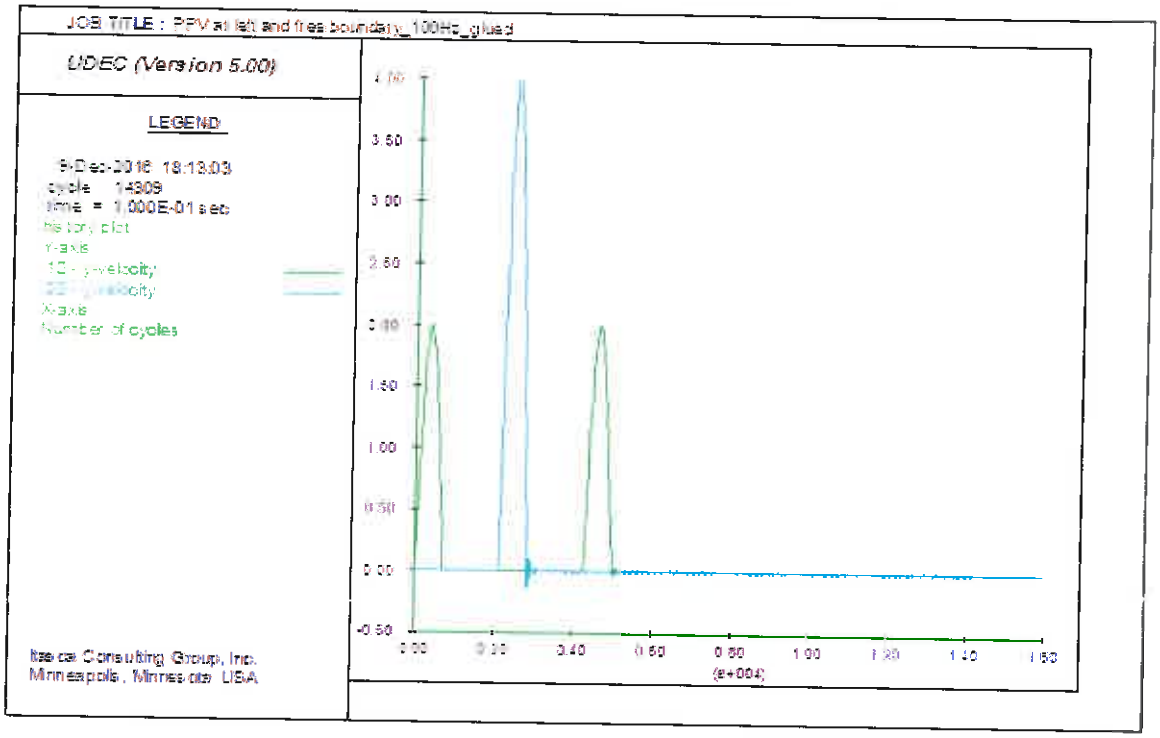

Figure 5.5: Peak particle velocities recorded in welded model

For the unwelded interface, the sacrificial support is ejected from the rock surface due to the tensile wave trap mechanism experienced by the liner (figures 5.6 and 5.7). The liner was ejected at a velocity of about 4 m/s (figure 5.8).

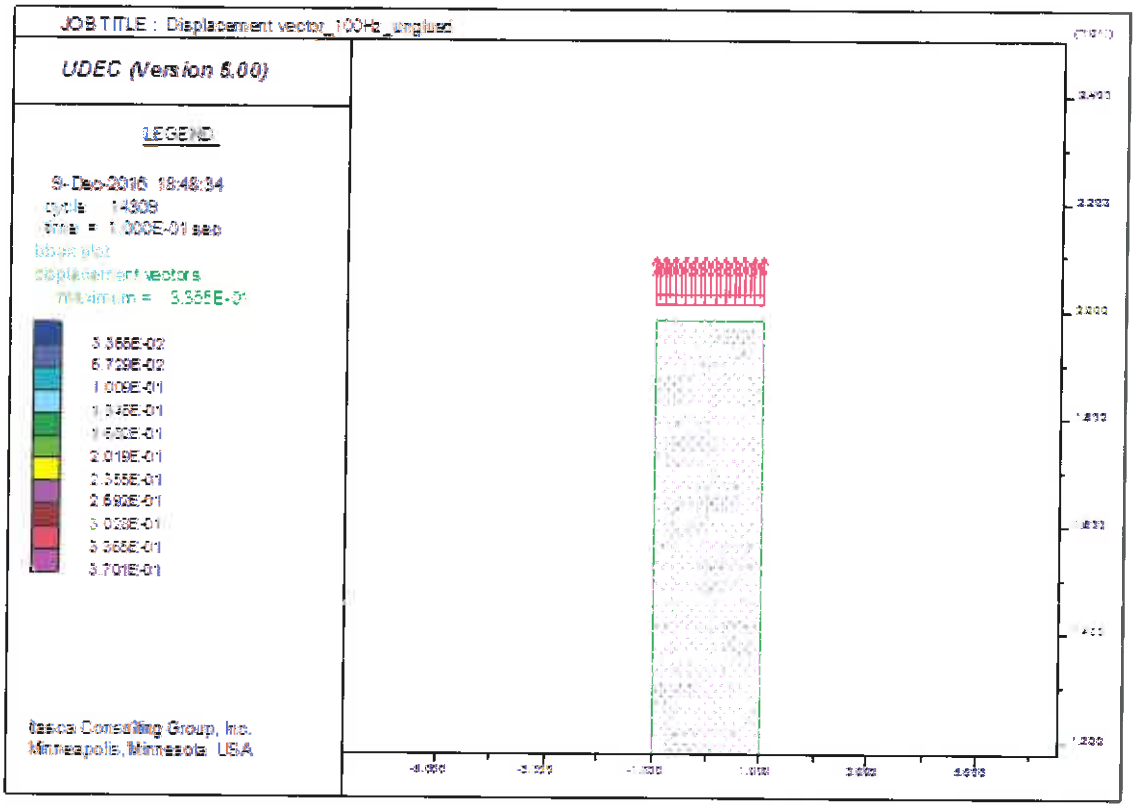

Figure 5.6: Displacement of sacrificial liner due to reflection of seismic wave from free surface

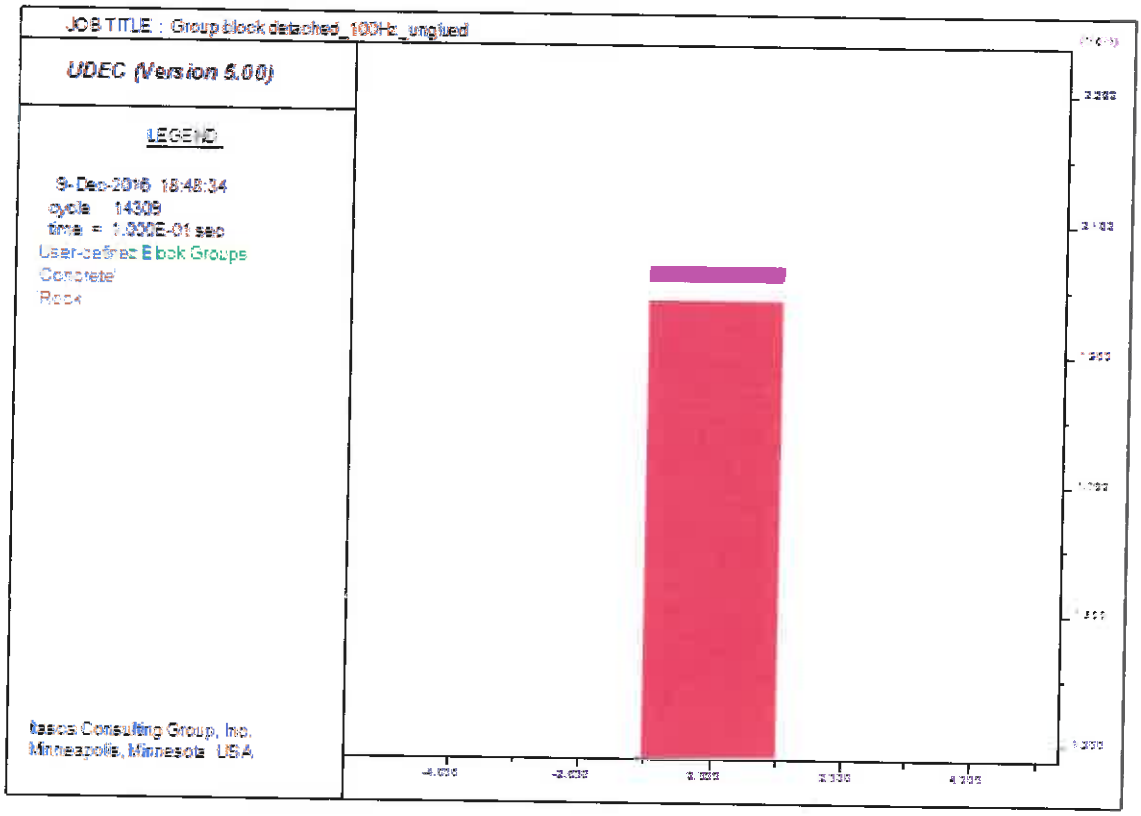

Figure 5.7: Ejection of the sacrificial liner resulting from the tensile wave trap mechanism

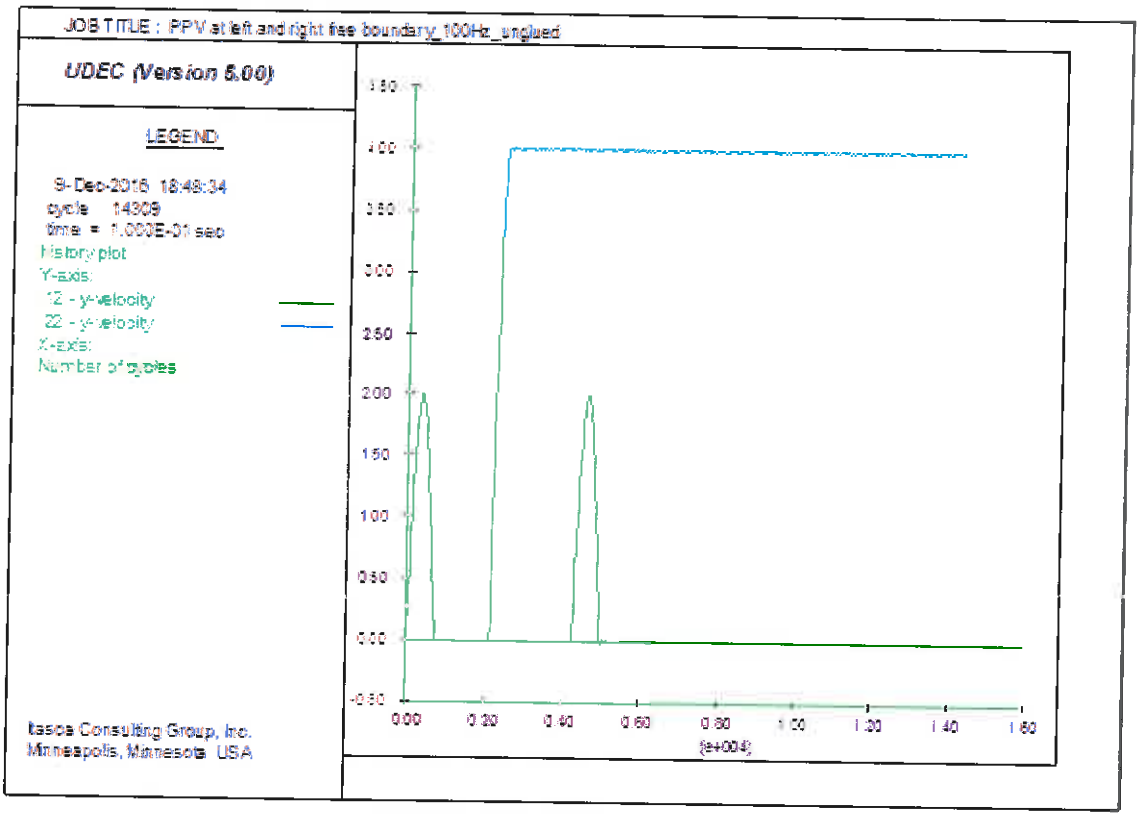

Figure 5.8: Ejection velocity of the sacrificial liner

In the following section, the effect of varying the wavelength characteristic on the behaviour of the sacrificial layer is investigated.

5.3.2 Effect of seismic wavelength on the behaviour of a sacrificial layer

Waves generated by seismic events are generally characterized by long wavelengths (especially s-waves). A long wavelength has a low frequency as shown by the following relationship.

$$\lambda = \frac{1}{f} \tag{5.4}$$

where λ =wavelength and f = frequency.

The dynamic stress wave generated in Hopkinson pressure bar tests is, how-

ever, characterized by short wavelengths. From practical point of view, it is not known how wavelength contributes to the behaviour of sacrificial liner. For this reason, the effect of wavelength is investigated in this section. The unwelded joint model presented above, with all parameters kept constant, is used in this case. The frequency of the wave was varied from 10 Hz to 1000 Hz. At the lowest frequency values, the sacrificial liner behaviour is characterized by low displacement and velocity vectors at ejection (see figure 5.9 below). The ejected sacrificial liner is well pronounced in figure 5.10.

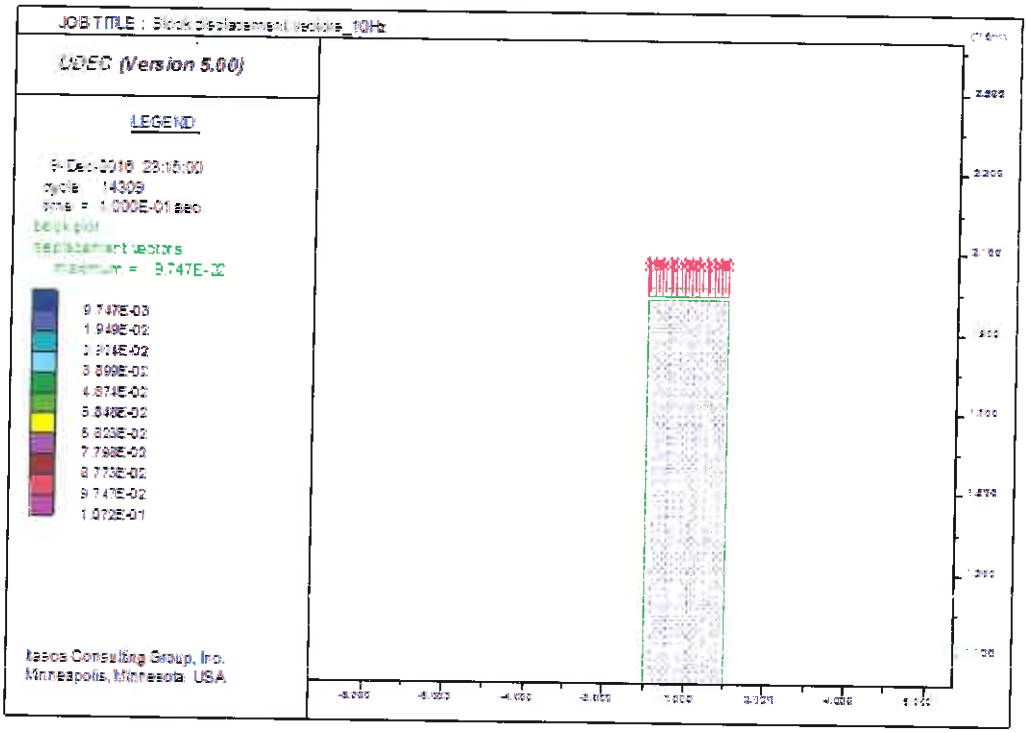

(a)

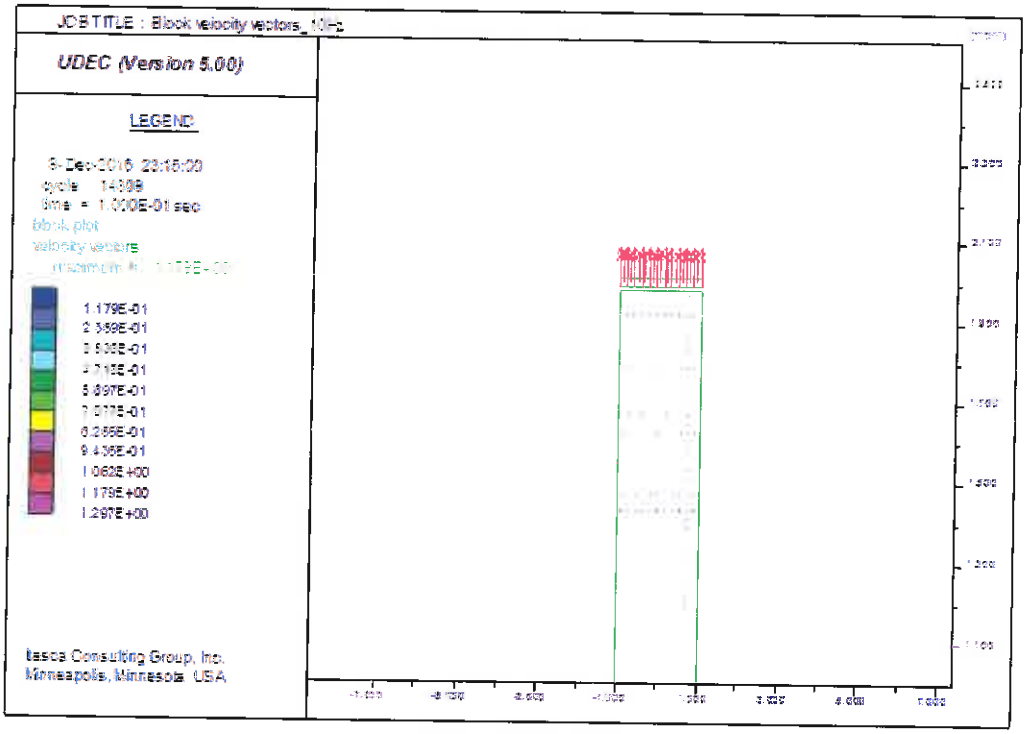

(b)

Figure 5.9: (a) Displacement and (b) velocity vectors of sacrificial support caused by low frequency P-wave propagation

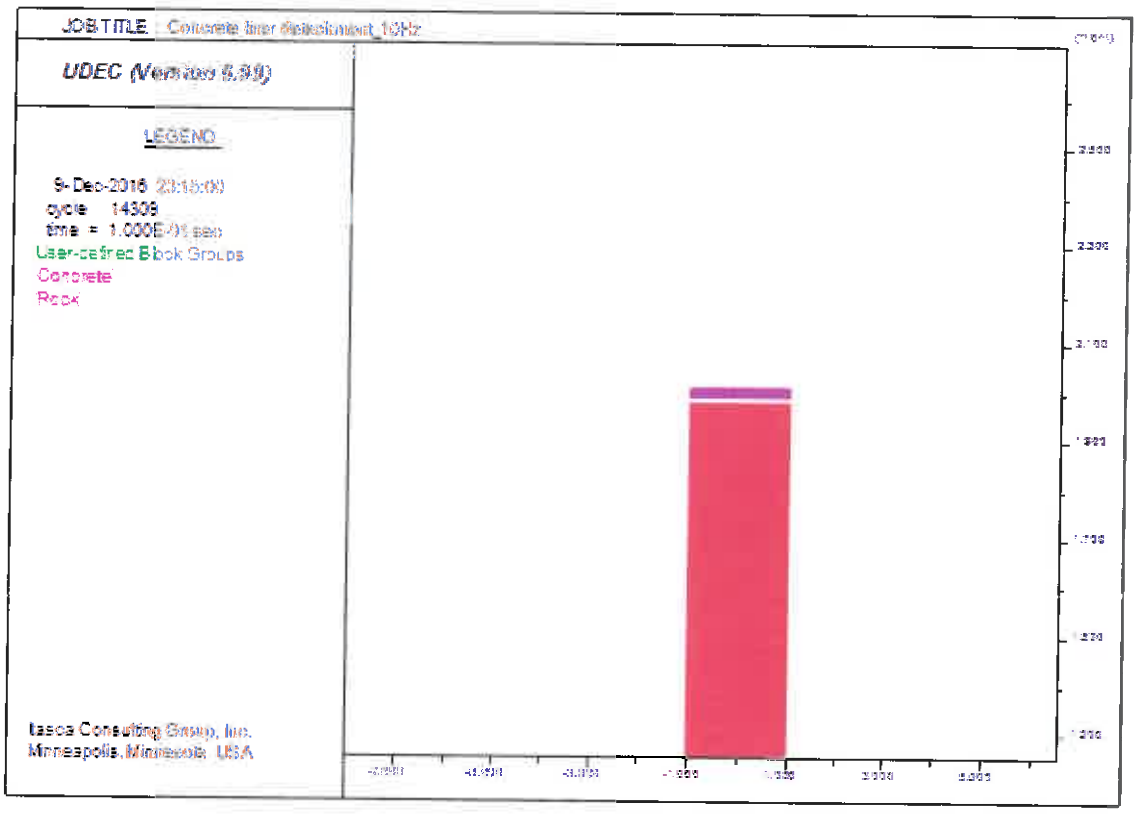

Figure 5.10: Ejected sacrificial support caused by low frequency P-wave propagation

In contrast with the low frequency wave type, results for high frequency (*e.g* 1000 Hz) waves, reported in figure 5.11, show large displacement and velocity vectors exhibited by the sacrificial layer. From the wavelength spectrum studied, the highest ejection velocity of sacrificial liner corresponds with the shortest wavelength, while the lowest ejection velocity was recorded for the lower limit value in the frequency spectrum.

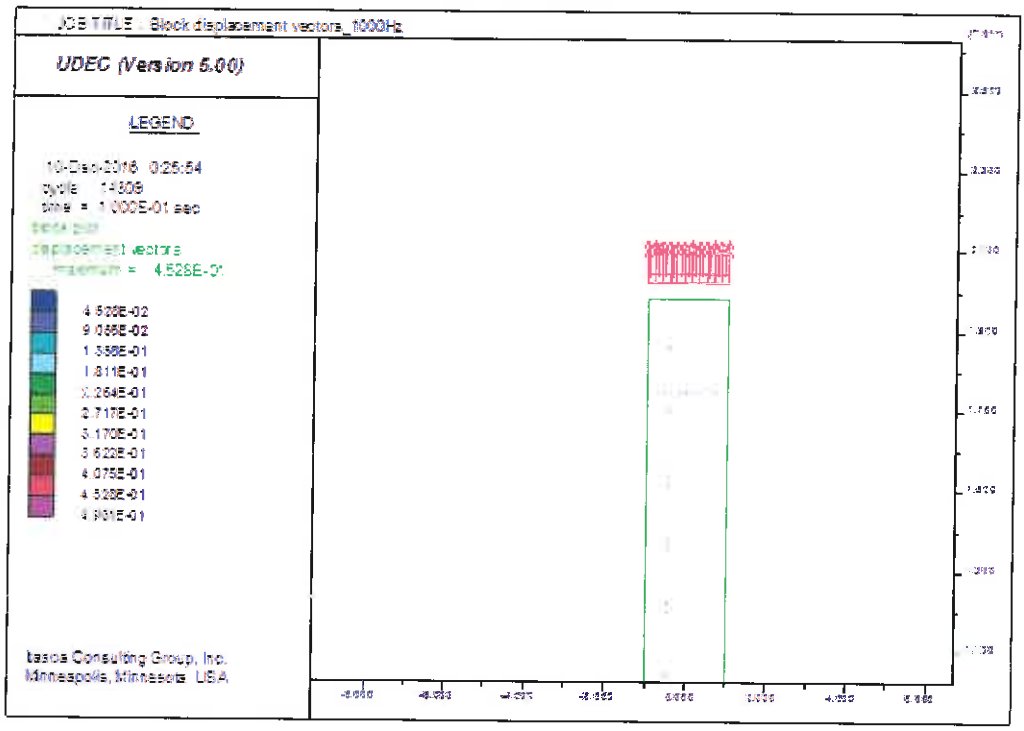

(a)

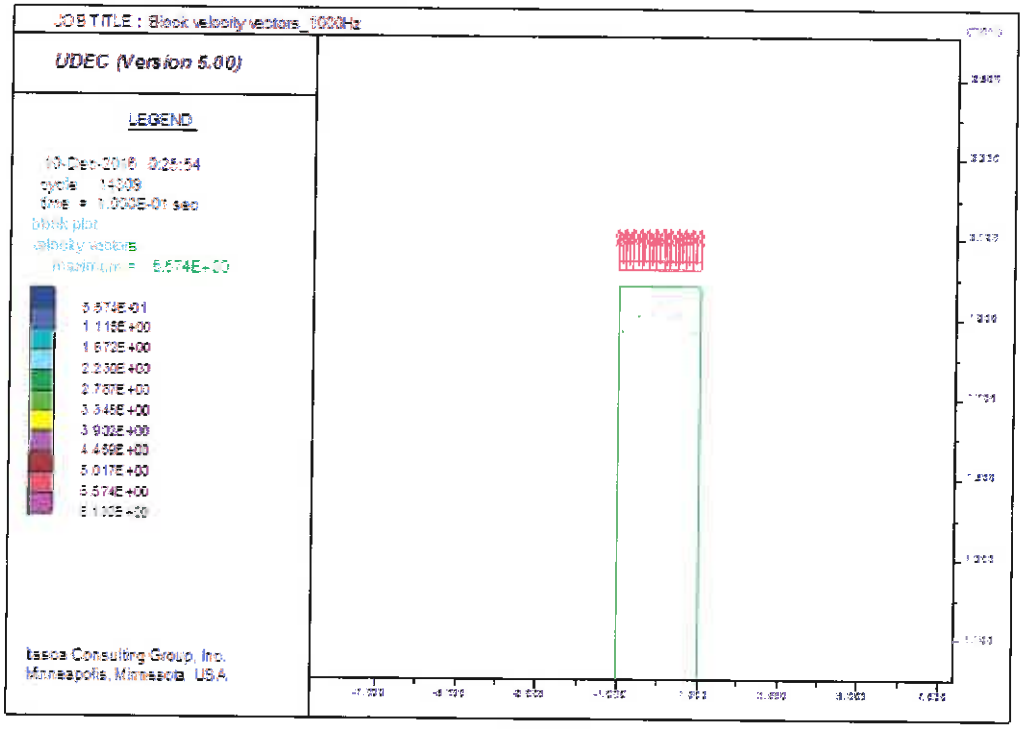

(b)

Figure 5.11: (a) Displacement and (b) velocity vectors of sacrificial support caused by high frequency P-wave propagation

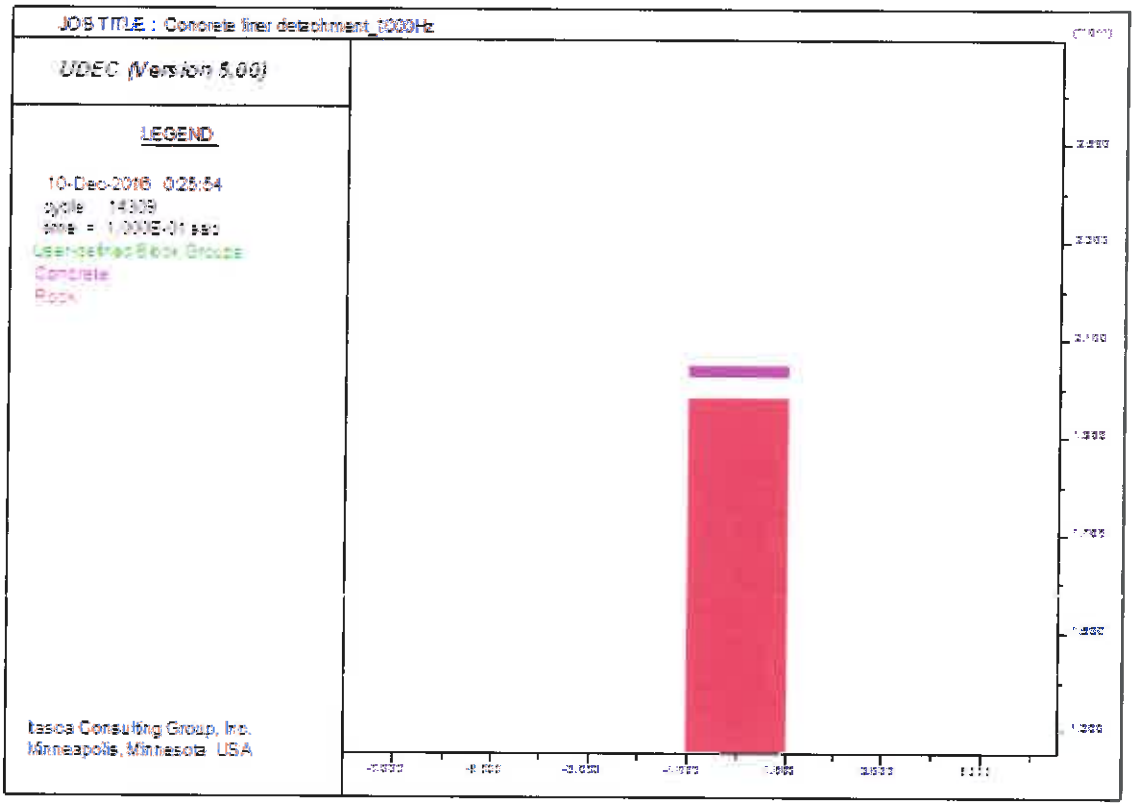

Figure 5.12: Ejected sacrificial support caused by high frequency P-wave propagation

5.3.3 Effect of varying liner thickness

Results for different liner thicknesses are reported in this section. Different liner thicknesses (δ = 0.05, 0.1, 0.15, 0.2 in metres) of weak concrete material (reported in previous sections) were investigated. Two indicators, namely displacement vectors and ejection velocity, are used to assess the behaviour of the support liner in this regard. In this parametric study, wave frequency was kept constant at 100 Hz. Figures 5.13 and 5.14 compare displacement vectors of 0.05 m and 0.2 m thick concrete liners. The sacrificial liner in both cases is characterized by similar maximum displacement vectors.

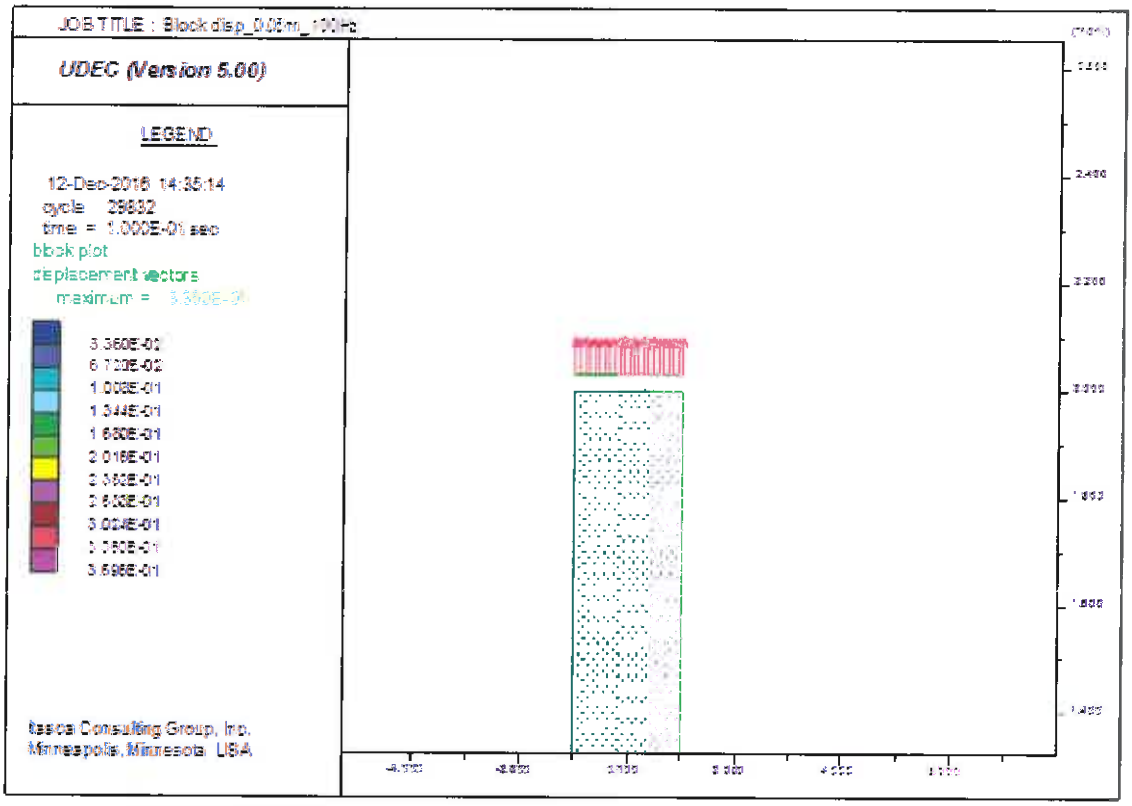

Figure 5.13: Displacement vectors for 0.05 m thick concrete support liner in ejection

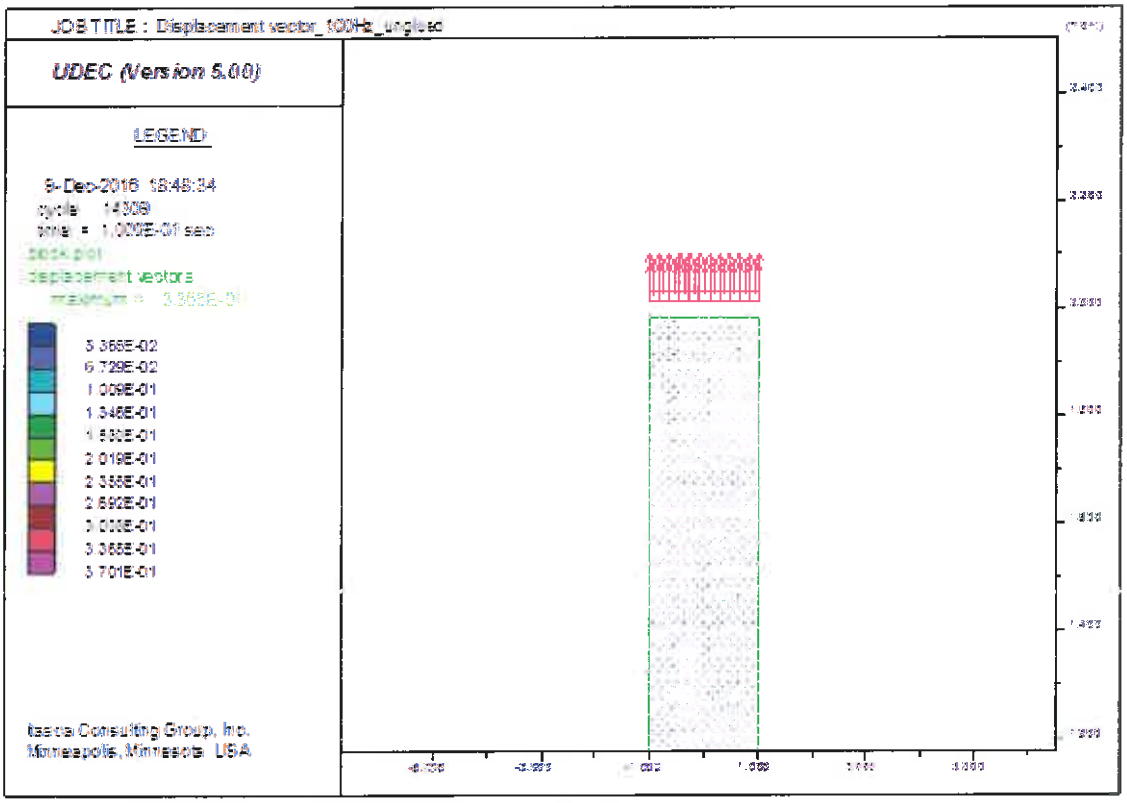

Figure 5.14: Displacement vectors for 0.2 m thick concrete support liner in ejection

Figures 5.15 and 5.16 show that both liners are ejected at an equal velocity of about 4 m/s independent of their thickness variation. Similar behaviour for 0.1 m and 0.15 m thick concrete liners, described by displacement vectors and ejection velocities, was also observed.

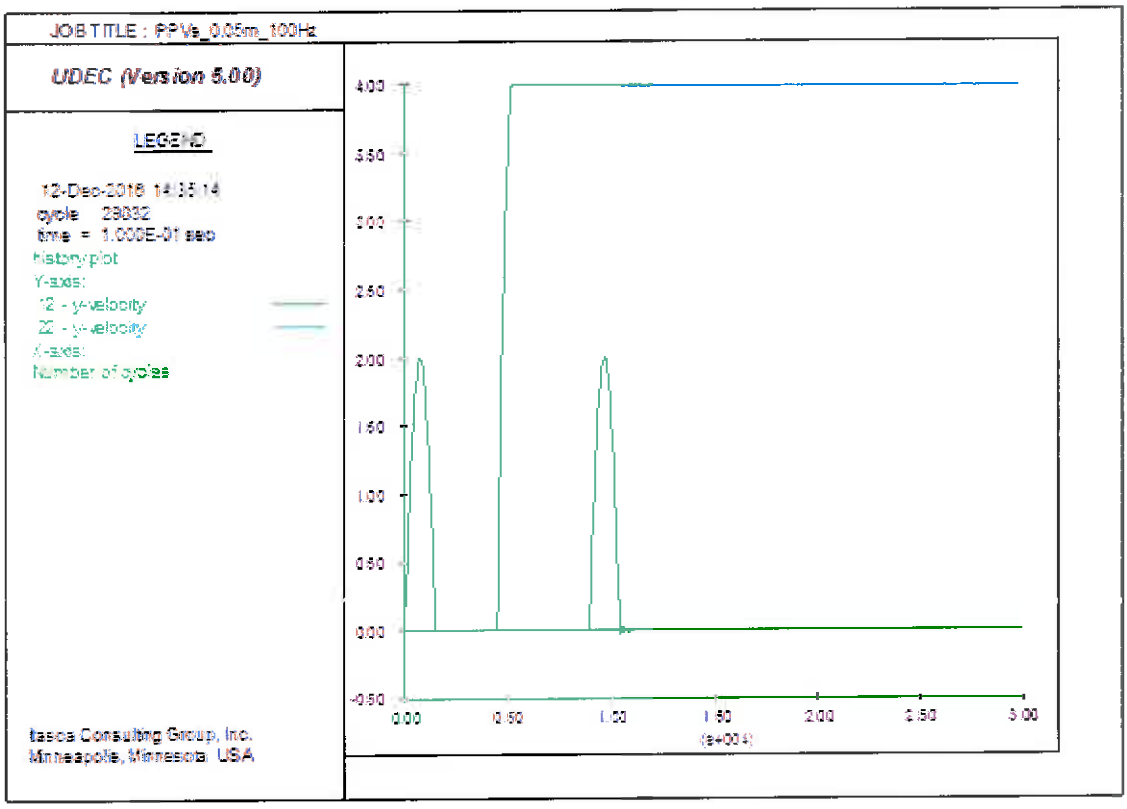

Figure 5.15: Ejection velocity for 0.05 m thick concrete liner

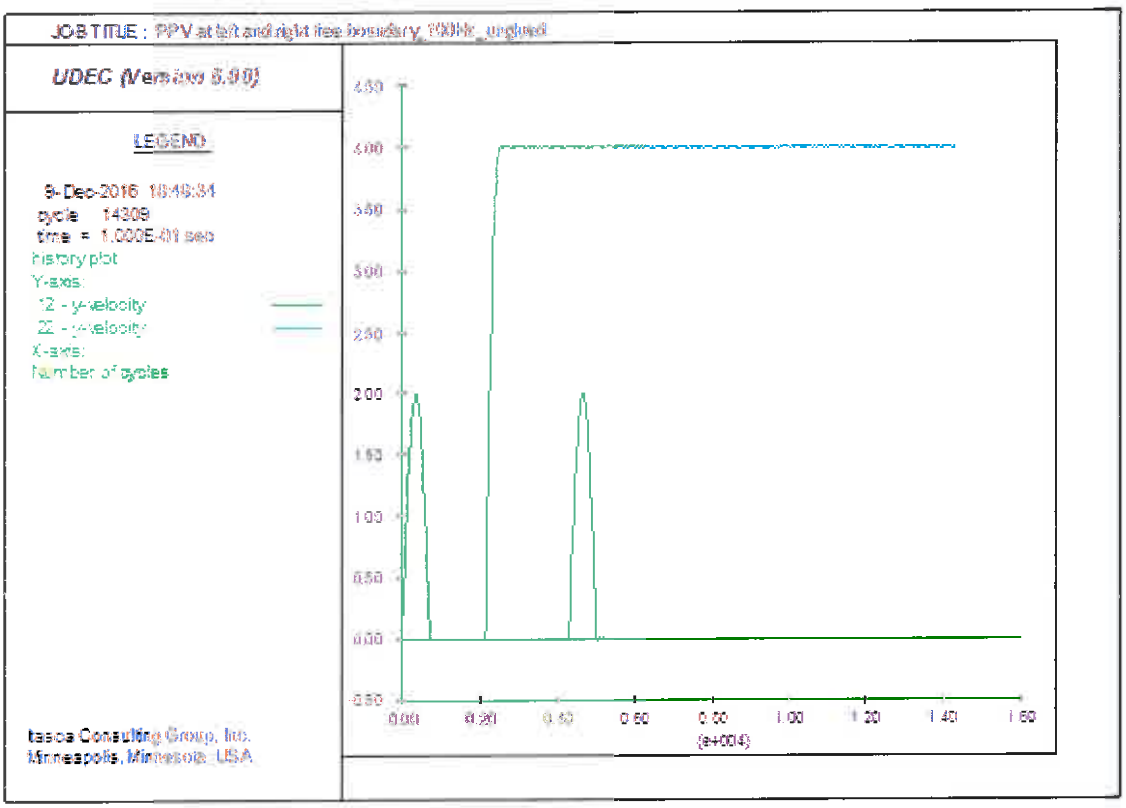

Figure 5.16: Ejection velocity for 0.2 m thick concrete liner

5.4 Discussion of numerical modelling findings

In this chapter, parametric studies have been conducted to explore the effects of seismic wave parameters such as wave frequency, and liner thickness variation on the overall behaviour of sacrificial support. It was noted that the higher wave frequencies are associated with increased support liner ejection velocities. Results revealed that despite liner thickness variation for thicknesses studied, ejection of liner will take place as a result of tensile wave trap mechanism. This contrasts with the results from the SHPB tests, and therefore represents a limitation of the numerical analyses. In addition, the velocity with which the liners of different thickness were ejected remains the same, provided that the wave frequency is kept constant. Most recently, Raffaldi and Locken (2016)

modelled rock ejection for homogenous rock mass containing a single joint near a free surface. Their findings showed that ejection of a block of rock of particular thickness is affected by wave frequency, *i.e.* the higher the frequency of wave the higher is the ejection velocity. This confirms the findings obtained in the present research. These results are, however, constrained by the simplicity of the model and the theory built into the analysis *i.e.* no amplification due to "erratic" wave behaviour which does occur in rock masses. The analyses have been useful in confirming the influence of the wave frequency. This is important since it implies that, in practice, greater rockburst damage is likely to be observed for "close" sources, even if their magnitudes are not large. This situation has often been observed in mines – large magnitude, but distant seismic events may result in much less damage than with smaller events located much closer to the excavations.

5.5 Chapter summary

This chapter reported numerical modelling results on the behaviour of sacrificial layer. Numerical analysis shows that wavelength plays a role in the behaviour of sacrificial liners. High frequency waves are associated with high ejection velocities and this is an issue of concern from safety point of view (Raffaldi and Locken, 2016). Numerical results also revealed that varying liner thickness, and using liner material with different mechanical properties has no effect to the overall behaviour of sacrificial behaviour. The following chapter provides a synthesis of experimental and numerical modelling results.

6 Synthesis of experimental and numerical modelling results

Chapter 5 presented numerical interpretations regarding the concept of the tensile wave trap mechanism related to sacrificial layer behaviour, with specific interest in the effects of varying liner thickness and wave characteristics, on the overall behaviour of a sacrificial liner. The current chapter synthesizes results of the performance and behaviour of sacrificial support in combating rockburst damage based on the experimental and numerical modelling investigations undertaken in this study.

The main aim of the research in this thesis was to identify and investigate a rock support method designed to reduce the drastic impacts induced by shock waves, which cause damage both to the underground excavations and conventional support systems themselves. The specific objectives relevant to the identified support method (*i.e.* sacrificial support) were investigated experimentally and are as follows:

- To evaluate the performance of support liners consisting of materials with differing mechanical properties in resisting rockburst damage;
- To investigate the benefits of varying the thicknesses of different support liners with regard to preventing dynamic rock failure.

In summary, the following are the outcomes from the SHPB experimental

testing and the numerical modelling:

1. Experiments based on the split Hopkinson pressure bar configured for spalling were conducted. Tests specimens of different rock types were allowed to fail dynamically in tension at high strain rates without a support liner (Figure 4.1).

2. Different liners and liner combinations were then introduced at the free end of the rock specimen to investigate their effectiveness in preventing rock damage.

3. Different rock test specimens, supported with a minimum liner thickness of each liner types, failed to prevent rock failure under dynamic loading (Figures 4.2, 4.3 and 4.4).

4. The effect of increasing support liner thickness demonstrated the protective action of thicker liners in limiting dynamic rock failure (Figures 4.6 and 4.7). This observation is, however, not supported by either steel or clay liners in preventing rock damage (Figure 4.5 and 4.8). This is because less dense and stiff materials relative to rock exhibit high coefficients of reflection at rock/liner interface, resulting in significant rock damage due to the effect of the reflected tensile wave. The concrete type used as support in this study had a high transmission ratio, thereby preventing rock damage. A clay liner in a concrete/clay liner combination, was advantageous in helping to prevent spalling of the rocks tested. This experimental finding supports the observation in real rockburst damage cases that the presence of mud, blast muck and water, appeared to have been beneficial in limiting damage (Figures 2.41 and 2.42).

5. The question that arises is: how do wave characteristics and variation in sacrificial liner thickness affect the overall behaviour of sacrificial support? Numerical interpretations revealed that varying wavelength may

significantly affect ejection velocities of a sacrificial liner, which is important from a safety point of view. The higher the frequency, the higher the displacement of the liner, and the ejection velocity. Based on numerical analysis results, the effect of varying liner thickness for a wave characterized by a certain frequency is inert as far as displacement and ejection velocity of the liner is concerned (Figures 5.9–5.16).

In closing, Chapters 4 and 5 reported experimental observations results and numerical interpretations regarding the effectiveness of sacrificial liner in combating dynamic rock failure caused by seismically-induced stress waves, respectively and the summary is presented above. From experimental observations, it became apparent that mechanical impedance between rock and support liner, and varying liner thickness play a significant role in reducing susceptibility of rock damage by altering the strength of reflected stress waves. The liner material/s which performed better had high transmission ratios and the liner failed following tensile wave trap mechanism. It follows that liner materials characterized by high coefficient of reflection, despite their thickness, are more susceptible to cause significant dynamic rock failure. Interaction of high frequency waves with sacrificial layer affect the overall behaviour of sacrificial layer as compared to low frequency waves, *i.e.* the higher the frequency the higher is the displacement of the liner so also the ejection velocity. The effect of varying liner thickness is negligible in the overall behaviour of support liner provided that the wave frequency is constant.

The following chapter presents concluding remarks and recommendations for future work.

7 Conclusions

In the previous chapter, experimental and numerical modelling results were synthesized, and certain conclusions regarding the mechanisms of behaviour of sacrificial support concept were drawn. Such concluding remarks are emphasized in this chapter. In addition, practical applications of sacrificial support in various environments are also outlined.

7.1 Concluding remarks

More than two decades ago, Stacey (1991) proposed a wave trap mechanism concept for rock support, aimed at preventing rockburst damage. The mechanism of behaviour of the suggested support concept to prevent rock damage was proven years later in real rockburst events in a mine (Stacey and Rojas, 2013). Such cases helped to validate the mechanism of sacrificial support in rockburst events.

The research described in this thesis demonstrated, through controlled laboratory experiments, the potential benefits of using a sacrificial layer to help combat the effects of rockbursts caused by seismically induced shock/seismic waves. The comparison of case studies reported earlier in the thesis (chapter 2) and observations from laboratory experiments (chapter 4) showed significant agreement in terms of the behaviour and performance of sacrificial support. For instance, the use of relatively weak concrete and a concrete/clay combina-

tion as liners performed significantly better in preventing dynamic rock failure, as indicated in the schematics presented in the tensile wave trap mechanism section for both cases of sacrificial support behaviour reported by Stacey and Rojas (2013).

The following are the two main conclusions arrived at in this research regarding the mechanism of behaviour of sacrificial support in combating rock failure under dynamic loading conditions, based on both experimental and numerical modelling findings.

- Experimental observations revealed that variation in mechanical impedance between rock and support liner, and liner thickness, play significant roles in preventing rock damage by altering the strength of the reflected stress waves. Support liner materials which exhibit high wave transmission ratios, for example, the relatively weak concrete used in this study, have the potential to prevent dynamic rock failure, when a certain threshold of liner thickness, say 200 mm, is reached. In contrast with these, support liner materials characterized by high transmission ratios of wave passage at the rock/liner interface, soft and very stiff liner materials are unsuitable to combat the effects of shock/seismic waves because of their high wave "reflective" nature at rock/liner boundary.

- Numerical simulations provided some useful insights concerning the behaviour of a sacrificial layer under simulated seismic loading conditions. It was observed that high frequency waves are characterized by high ejection velocities of the support liner. The effect of varying liner thickness on the overall behaviour of sacrificial layers was found to be negligible. This contradicts the experimental results and is perhaps a limitation of the numerical analysis approach.

7.2 Practical application of sacrificial support

The sacrificial support method reported in this study can find a wide range of applications in different areas such as tunnels (including the floor), shafts subjected to seismic loading, and to underground buried structures subjected to external blast loads. This research is the first of its nature carried out to specifically investigate the feasibility of using sacrificial support liners, and to gain some preliminary design information regarding such liners. The SHPB experiments are also the first such tests to practically demonstrate the potential use of sacrificial support in helping to limit rockburst damage and to enhance safety in mines. Other support elements such as cable anchors, yielding rock bolts, wire mesh and straps will be required in addition to the sacrificial liner to retain and contain the detached sacrificial layer (Stacey, 2016b; Rizwan and Stacey, 2015; Stacey and Rojas, 2013). The important result is that the rock is protected from damage.

8 Recommendations for future work

Future work should be aimed at development of design guidelines for sacrificial support. A quantitative relationship between liner thickness, mechanical impedance of both rock and liner and loading parameters must be established analytically. Verification of this relationship would entail a broader experimental programme involving different liner materials, supported by numerical simulations. Once design guidelines are established, field observations can then follow in real, seismically-active mining environments.

From an experimental point view, blasting experiments (an extension of those presented in chapter three) should provide value in evaluating the performance of various liner materials aimed at providing sacrificial protection in dynamic loading environments.

Numerical models presented in this study were simple elastic models of limited scope, used to demonstrate the behavior of sacrificial support under the influence of p-wave seismic loading. An investigation into the behaviour of sacrificial layers subjected to s-waves would be beneficial since these waves are known to induce more damage than p-waves. At present, it is also not known how effective would the sacrificial support be if used to provide support in a highly fractured rock mass, and more sophisticated numerical modelling may be useful in researching this more complex situation.

References

Adams, D.J. 1995. *Develop criteria for designing mining layouts at depth so as to reduce seismicity and enhance worker safety.* Safety in Mines Research Advisory Committee, SIMRAC GAP Project 034.

Ahmed, L. 2012. *Models for analysis of shotcrete on rock exposed to blasting.* Licentiate Thesis, KTH Royal Institute of Technology, Stockholm, Sweden.

Ahmed, L. & Ansell, A. 2014. Vibration vulnerability of shotcrete on tunnel walls during construction blasting. Tunnel. Undergr Space Technol. 42: 105–111.

Aki, K. & Richards, P.G. 1980. *Quantitative Seismology Theory and Methods.* W. H. Freeman, San Francisco, California. 932 pp.

Akinbinu, V.A. 2015. *Investigation of the relationship between fragmentation and brittleness of rocks, in particular Class II rock type.* PhD Thesis, University of the Witwatersrand.

Akinbinu, V.A. 2016. Class I and Class II rocks: Implication of self-sustaining fracturing in brittle compression. *Geotech. Geol Eng.* 34 (3): 877–887.

Ansell, A. 2005. Laboratory testing of a new type of energy absorbing rock bolt. *Tunnel. Undergr Space Technol.* 20 (4): 291–300.

Ansell, A. 2006. Dynamic testing of steel for a new type of energy absorbing rockbolt. *J. Constr Steel Research.* 62 (5): 501–512.

Araneda, O. & Sougarret, A. 2007. Lessons learned in cave mining: El Teniente 1997–2007. *Proc. 1st Int. Symp. on Block and Sublevel Caving*: Cape Town, October, S. Afr. Inst. Min. Metall., pp 1–13.

Bacco, M. 2010. Analisis de estallidos de roca. Powerpoint presentation, El Teniente Mine.

Bienaiwski, Z.T. 1989. *Engineering Rock Mass Classifications*, Wiley, New York.

Blake, W. 1972. Destressing test at the Galena Mine, Wallace, Idaho. *Soc. Min. Engng. AIME Trans.* 252: 294–299.

Brara, A. & Klepaczko, J.R. 2006. Experimental characterization of concrete in tension. Mech Mater. 25: 253–267.

Brara, A. & Klepaczko, J.R. 2007. Fracture energy of concrete at high loading rates in tension. *Int. J. Impact Engng.* 34: 424–435.

Broch, E. & Sorheim, S. 1884. Experiences from the planning, construction and supporting of a road tunnel subjected to heavy rockbursting. *Rock Mech. Rock Engng.* 17: 15–35.

Cai, M., Kaiser, P.K., Suorineni, F. & Su, K. 2006. A study on the dynamic behaviour of the Meuse/Haute-Marne argillite. *Phys. Chemstr. Earth.* 32: 907–916.

Cai, M. & Champaigne, D. 2009. The art of rock support in burst-prone ground. Keynote Lecture. In: RaSiM 7: Controlling Seismic Hazard and

Sustainable Development of Deep Mines, Tang. C.A. (editors), 33-46.

Cai, M. Principles of rock support in burst-prone ground. *Tunnel. Undergr. Space Tec.* 36 (6): 46–56.

Charette, F. & Plouffe, M. 2008. A new rock bolt concepts for underground excavations under high stress conditions. *Proc. 6th Int. Symp. on Ground Support in Mining and Civil Engineering Construction*: 225–240. Cape Town, South Africa, S. Afr Inst. Min. Metall., Symposium Series S51.

Chen, S.G. & Zhao, J. 1998. A study of UDEC modelling for blast wave propagation in jointed rock masses. *Int. J. Rock Mech. Min. Sci.* 35 (1): 93–99.

Chen, W.W. & Song, B. 2011. *Split Hopkinson (Kolsky) bar: design, testing and applications.* New York: Springer-Verlag.

Cundall, P.A. 1971. A computer model for simulating progressive, large-scale movements in blocky rock systems. *Proc. Int. Symp. on Rock Fracture*: Paper II, 1–12, Nancy, France.

Daehnke, A. 1997. *Stress wave and fracture propagation in rock.* PhD Thesis, Technical University of Vienna.

de Frey, F.S.A., Handley, M.F. & Webber, R.C.W. 2002. *Examine the criteria for establishing the small span pillars concept as a safe mining method in deep mines.* Safety in Mines Research Advisory Committee, SIMRAC GAP Project 828.

Diamaruya, M., Kobayashi, H. & Nonaka, T. 1997. Impact tensile and fracture of concrete. *J de Phys.* IV. 7: 253–258.

Diaz-Rubio, F.G., Perez, J.R. and Galvez, V.S. 2002. Spalling of long bars as reliable method of measuring the dynamic tensile strength of ceramics. *Int. J. Impact Engng.* 27 (2):161 – 177.

Diederichs, M.S. 2000. *Instability of hard rock masses: the role of tensile damage and relaxation.* PhD Thesis, University of Waterloo.

Diederichs, M.S. 2007. Mechanistic interpretation and practical application of damage and spalling prediction criteria for deep tunneling. *Can. Geotech. J.* 44: 1082–1116.

Durrheim, R.J. 2012. Functional specifications for in-stope support based on seismic and rockburst observations in South African mines. In Y. Potvin (ed), *Seminar on Deep and High Stress Mining, Deep Mining 2012*: 41–56, Perth, Australia Centre for Geomechanics.

Dyskin, A.Y. & Germanovich, L N. 1993. Model of rockburst caused by cracks growing near free surface. In R.P. Young (ed.), *Proc. 3rd Int. Symp. on Rockbursts and Seismicity in Mines*: 169–174, Kingston, Canada, A.A. Balkema, Rotterdam.

Espley, S.J., Heilig, J. & Moreau, L.H. (2002) Assessment of the dynamic capacity of liners for application in highly-stressed mining environments at INCO Limited. In Y. Potvin, T.R. Stacey & J. Hadjigeorgiou (eds.), *Surface Support in Mining*: 187–192, Australian Centre for Geomechanics.

Ewy, R.T. & Cook, N.G.W. 1990. Deformation and fracture around cylindrical openings in rock. *Int. J. Rock Mech. Min. Sci. & Geomech. Abstr.* 27(5): 387–407.

Fairhurst, C. & Cook, N.G.W. 1966. The phenomenon of rock splitting parallel

to the direction of maximum compression in the neighbourhood of a surface. *Proc. 1st Int. Cong. Int. Soc. Rock Mech*: 687–692, Lisbon, Portugal.

Field, J.E., Walley, S.M., Proud, W.G., Goldrein, H.T. & Siviour, C.R. 2004. Review of experimental techniques of high rate deformation and shock studies. *Int. J. Impact. Eng.* 30 (7): 725–775. Galvez, F., Rodrıguez, J. & Sanchez,

V. 1997. Tensile Strength Measurements of Ceramic Materials at High Rates of Strain. *J. de Physique IV Colloque.* 7 (C3): 151–156.

Gama, B.A., Lopatnikov, S.L. & Gillepsie, J.W. 2004. Hopkinson bar experimental technique: a critical review. *Appl Mech Rev.* 57 (4): 223–250.

Gaudreau, D.M., Aubertin, S. & Simon, R. 2004. Performance assessment of tendon support systems submitted to dynamic loading. In E. Villaescusa & Y. Potvin (eds.). *Ground support in mining and underground construction*: 299–312, Balkema, London.

Gay, N.C. 1973. Fracture growth around openings in thick-walled cylinders of rock subjected to hydrostatic compression. *Int. J. Rock Mech. Min. Sci. & Geomech. Abstr.* 10: 209–233.

Gibowicz, S.J. & Kijko, 1994. *An Introduction to Mining Seismology.* New York: Academic Press.

Govender, R.A., Louca, L.A., Pullen, A. & Nurick, G.N. 2009. High strain rate delamination of glass fiber reinforced polymers using a Hopkinson bar configured for spalling. *Proc Int. Conf. on the Mechanical and Physical Behaviour of Materials*: 449–455, Brussels, Belgium.

Govender, R.A., Louca, L.A., Pullen, A., Fallah, A.S. & Nurick, G.N. 2011.

Determining the thorough-thickness properties of thick glass fiber reinforced polymers at high strain rates. *J. Compos. Mater.* 46: 1219–1228.

Govender, R.A., Langdon, G.S., Cloete, T.J. & Nurick, G.N. 2012. High strain rate compression testing of glass fibre reinforced polypropylene. EPJ Web of Conferences. 26 (01039): 1–6.

Guler, G., Kuipers, J.S., Wojno, L., Milev, A.M. & Hailer, A. 2001. *Determine the effect of repeated dynamic loading on the performance of tunnel support systems.* Safety in Mines Research Advisory Committee, SIMRAC GAP Project 616.

Gray III, G.T. 2000. Classic Hopkinson bar testing. In ASM handbook, vol. 8, H. Kuhn and D. Medlin (eds.). Materials Park, OH: ASM International. pp. 462–476.

Hadjigeorgiou, J. & Potvin, Y. 2011. A critical assessment of dynamic rock reinforcement and support testing facilities. *Rock Mech. Rock Engng.* 44: 565–578.

Hagan, T.O., Milev, A.M., Spottiswoode, S.M., Hildyard, M.W., Grodner, M., Rorke, A.J., Finnie, G.J., Reddy, N., Haile, A.T., Le Bron, K.B. & Grave, D.M. 2001. Simulated rockburst experiment – an overview. *J. S. Afri. Inst. Min. Metall.* 101 (5): 217–222.

Haile, A.T. and Le Bron, K. 2001. Simulated rockburst experiment – evaluation of rock bolt reinforcement performance. *S. Afr. Inst. Min. Metall.* 101 (5): 247–251.

Handley, M.F., de Lange, J.A.J., Essrich, F. & Banning, J.A. 2000. A review of sequential grid mining method employed at Elandsrand Gold Mine. *J. S.*

Afri. Inst. Min. Metall. 91: 157–168.

Hasegawa, H.S., Wetmiller, R.J. & Gendzwill, D.J. 1989. Induced seismicity in mines in Canada–an overview. *PAGEOPH.* 129: 423–452.

He, M.C., Miao, J.L. & Feng, J.L. 2010. Rock burst process of limestone and its acoustic emission characteristics under true-triaxial unloading conditions. *Int. J.Rock Mech. Min. Sci.* 47 (2): 286–298.

He, M.C., Gong, W.L., Wang, J., Qi, P., Tao, Z., Du, S. & Peng, S.D. 2014. Development of a novel energy-absorbing bolt with extraordinary large elongation and constant resistance. *Int. J. Rock Mech. Min Sci.* 67: 29–42.

He, M.C., Li, C., Gong, W.L. & Liu, D.Q. 2016. Dynamic behaviour of NPR bolt and its application to rockburst control, Rock Dynamics: From Research to Engineering, *Proc. Int. Conf. RocDyn* 2: 25–35, Suzhou, China, CRC Press/Balkema, Taylor & Francis Group.

Heal, D., Potvin, Y. & Hudyma, M. 2006. Evaluating rockburst damage potential in underground mining, *Proc 41st U.S. Symp. on Rock Mechanics (USRMS): 50 Years of Rock Mechanics—Landmarks and Future Challenges*, Golden, Colorado.

Heal, D.P. 2010. *Observations and analysis of incidences of rockburst damage in underground mines.* PhD Thesis, University of Western Australia.

Hedley, D. G. F. 1992. *Rockburst handbook for Ontario hardrock mines.* (No. SP92-1E). Ottawa, ON: CANMET.

Hildyard, M.W., Young, R.P., Collins, D.S. & Prettitt, W. 2005. Seismic wave propagation to diagnose the state of fracturing. *J. S. Afri. Inst. Min. Metall.*

105: 437–446.

Hino, K. 1959. Theory and Practice of Blasting. Nippon Kayaku, Tokyo. 169 pp.

Hoek, E. & Brown, E.T. 1980. *Underground Excavations in Rock.* The Institution of Mining and Metallurgy, London.

Hoek, E., Kaiser, P.K. & Bawden, W.F. 1995. *Support of Underground Excavations in Hard Rock.* A.A. Balkema, Rotterdam, 71 p.

Hopkinson, B. 1914. A method of measuring the pressure produced in the detonation of high explosives or by the impact of bullets. *Trans. R. Soc. Lond.* 213A: 437–456.

Hudyma, M.R. 2008. *Analysis and interpretation of clusters of seismic events.* PhD Thesis, University of Western Australia.

ISRM 1999. Draft ISRM suggested method for the complete stress-strain curve for intact rock in uniaxial compresssion. *Int. J. Rock Mech. Min Sci.* 36: 281–289.

Itasca Consulting Group, Inc. 2004. UDEC Version 4.0 User's Guide. Minneapolis.

Jager, A.J. 1992. Two new support units for the control of rockburst damage. In P.K. Kaiser & D.R. McCreath (eds.). Rock Support in Mining and Underground Construction: 621–633. Balkema, Rotterdam.

Johnstone, C. and Ruiz, C. 1995. Dynamic tensile strength of ceramics. *Int. J. Solid. Struct.* 32: 2647–2651.

Kaiser, P.K. 1993. Support of tunnels in burst-prone ground – Toward a rational design methodology. In R.P. Young (ed), *Proc. 3rd Int. Symp. on Rockbursts and Seismicity in Mines*: 13–27, Kingston, Canada.

Kaiser, P.K., McCreath, D.R. & Tannant, D.D. 1996. *Canadian Rockburst Support Handbook: Volume 2: Rockburst*, Canadian Rockburst Research Program 1990–1995, CAMIRO.

Kaiser, P.K. & Cai, M. 2012. Design of rock support system under rockburst condition. *Rock Mech. Geotech Engng.* 4 (3): 215–227.

Kaiser, P.K. & Cai, M. 2013. Critical review of design principles for rock support in burst-prone ground – time to rethink! Keynote Paper. In Y. Potvin & B. Brady (eds.), *Proc. 7th Int. Symp. on Ground Support in Mining and Underground Construction, Ground Support 2013*: 3–38, Australian Centre for Geomechanics.

Kasuka, A., Garvey, R. & Ozbay, U. 2013. A study of the influence of tunnel shape on rockburst proneness using numerical modelling. *Proc 41st U.S. Symp. on Rock Mechanics/Geomechanics*, San Francisco, California.

Klepaczko, J.R. & Brara, A. 2001. An experimental method for dynamic tensile testing of concrete by spalling. *Int. J. Impact Engng.* 25: 387–409

Kolsky, H. 1949. An investigation of the mechanical properties of materials at very high rates of loading. *Proc. R. Soc. Lond.* 62B: 676–700.

Kolsky, H. 1963. Stress Waves in Solids, Dover, New York.

Kuijpers, J.S., Milev, A.M., Jager, A.J. & Acheampong, E. 2002. *Performance of various types of containment support under quasi-static and dynamic loading*

conditions, Part I. Safety in Mines Research Advisory Committee, SIMRAC GAP Project 810.

Li, T., Cai, M.F. & Cai, M. 2007. A review of mine-induced seismicity in China. *Int. J. Rock Mech. Min Sci.* 44: 1149–1171.

Li, C.C. 2010. A new energy-absorbing bolt for support in high stress rock masses. *Int. J. Rock Mech. Min Sci.* 47 (3): 396–404.

Li, C.C. & Doucet, C. 2012. Performance of D-bolts under dynamic loading. *Rock Mech. Rock Eng.* 45: 193–204.

Lifshitz J.M. & Leber H. 1994. Data processing in the Split Hopkinson Pressure Bar tests. *Int. J. Impact Engng.* 15: 723–733.

Lockner, D.A., Byerlee, J.D., Kuksenko, V., Ponomarev, A. & Sidorin, A. 1991. Quasi-static fault growth and shear fracture energy in granite. *Nature.* 350: 39–42.

Manzi, M.S.D., Durrheim, R.J., Hein, K.A.A. & King, N. 2012. 3D edge detection seismic attributes used to map potential conduits for water and methane in deep gold mines in the Witwatersrand basin, South Africa. *Geophysics.* 77: WC133–WC147.

Martin, C.D. 1994. *The strength of massive Lac du Bonnet granite around underground openings.* PhD Thesis, University of Manitoba.

Martin, C.D., Kaiser, P.K. & McCreath, D.R. 1999. Hoek–Brown parameters for predicting the depth of brittle failure around tunnels. *Can. Geotech. J.* 36: 136–151.

McGarr, A., Green, R., & Spottiswoode, S. M. 1981. Strong ground motion of

mine tremors: Some implications for near-source ground motion parameters. *Bull. Seismol. Soc. America.* 71(1): 295-319.

Mendecki, A.J., van Aswegen, G. & Mountfort, P. 1999. A guide to routine seismic monitoring in mines. *A handbook on rock engineering practice for tabular hard rock mines*, In A.J. Jager & J.A Ryder (eds), Creda Communications, Cape Town, South Africa.

Mendecki, A.J., Napier, J.A.L., IIchev, A. & Sellers, E. 2001. *Fundamental aspects of the integration of seismic monitoring with numerical modelling.* Safety in Mines Research Advisory Committee, SIMRAC GAP Project 603.

Mikula, P.A. 2012. Progress with empirical performance charting for confident selection of ground support in seismic conditions. *J. Min. Technol.* 121 (4): 192–203.

Milev, A.M., Spottiswoode, S.M., Rorke, A.J. & Finnie, G.J. 2001. Seismic monitoring of a simulated rockburst on a wall of an underground tunnel. *S. Afri. Inst. Min. Metall.* 101 (5): 253–260.

Mitri, H.S. 2000. *Practitioner's guide to destress blasting in hard rock mines.* McGill University.

Mogi, K. 1962. Study of elastic shocks caused by the fracture of heteregeneous materials and its relations to earthquake phenomena, *Bul. Earthqua. Res. Inst.* 40: 125–173.

Morissette, P.N.R. 2015. *A ground support design strategy for deep underground mines subjected to dynamic-loading conditions.* PhD Thesis, University of Toronto.

Mudau, A., Govender, R.A. & Stacey, T.R. 2016. A step towards combating rockburst damage using sacrificial support. *J. S. Afr. Inst. Min. Metall.* 116: 1065–1074.

Myer, L.R., Pyrak-Nolte, L.J. & Cook, N.G.W. 1990. Effects of single fracture on seismic wave propagation. *Proc. of ISRM Symp. on Rock Fractures*: 47–56, Leon, Spain.

Najar, J. 1994. Dynamic tensile fracture phenomena at wave propagation in ceramic bars. *J. De Physique.* 4: 647–652.

Nemat-Nasser, S. & Horii, H. 1982. Compression induced nonplanar crack extension with application to splitting, exfoliation, and rockburst. *J. Geophys. Res.* 87 (B8): 6805–6821.

Nyungu, D. & Stacey, T.R. 2014. Time-depenent tensile sterngths of Bushveld Complex rocks and implications for rock failure around mining excavations. *J. S. Afr. Inst. Min. Metall.* 114: 765–772.

Ortlepp, W.D. 1969. An empirical determination of the effectiveness of rock-bolt support under impulse loading. In T.L. Brekke & F.A. Jorstad (eds.). *Proc. Int. Symp. on Large Permanent Underground Openings*: 197–205. Oslo, Universitats-forlaget.

Ortlepp,W.D., More-O'Ferrall, R.C. & Wilson, J.W. 1972. Support methods in tunnels. *Association of Mine Managers of South Africa, Papers and Discussion*, 167–195 pp.

Ortlepp, W.D. 1983. Considerations in the design of support for deep hard-rock tunnels. *Proc. 5th Int. Congr. Int. Soc. Rock. Mech.*: D179–D187, Melbourne, Australia.

Ortlepp, W.D. 1992a. The design of support for containment of rockburst damage in tunnels. *Proc. Int. on Rock Support in Mining and Underground Construction*: 593–609, Sudbury, Canada, Laurentian University.

Ortlepp, W.D. 1992b. Implosive-load testing of tunnel support. In P.K. Kaiser & D.R. McCreath. (eds.). Rock Support in Mining and Underground Construction: 675–682. Balkema, Rotterdam.

Ortlepp, W.D. 1994. Grouted rock-studs as rockburst support: A simple design approach and an effective test procedure. *J. S. Afr. Inst. Min. Metall.* 94: 47–63.

Ortlepp, W.D. & Stacey, T.R. 1994. Rockburst mechanisms in tunnels and shafts. *Tunnel. Undergr. Space Tech*nol. 9 (1): 59–65.

Ortlepp, W.D. 1997. *Rock Fracture and Rockbursts – An Illustrative Study.* Southern African Institute of Mining and Metallurgy, Johannesburg, 255 pp.

Ortlepp, W.D. & Stacey, T.R. 1997. *Testing of tunnel support: dynamic load testing of support containment systems.* Safety in Mines Research Advisory Committee, SIMRAC GAP Project 221.

Ortlepp, W.D. 2005. RasiM comes of age – A review of the contribution to the understanding and control of mine rockbursts. In Y. Potvin & M. Hudyma (eds.), *Proc. 6th Int. Symp. on Rockbursts and Seismicity in Mines*: 3–20, Australian Centre for Geomechanics, Perth, Australia.

Piper, P.S. 1983. *Chamber of Mines Research Organization* (COMRO), Internal Report.

Player, J.R., Thompson, A.G. & Villaescusa, E. 2004. Dynamic testing of

rock reinforcement using the momentum transfer concept. In E. Villaescusa & Y. Potvin (eds.). *Ground support in mining and underground construction*: 327–340, Balkema London.

Player, J.R., Thompson, A.G. & Villaescusa, 2008a. Dynamic testing of reinforcement systems. In T.R. Stacey & D.F. Malan (eds.). *Proc. 6th Int. Symp. on Ground Support in Mining and Civil Engineering Construction*: 597–622. Cape Town, South Africa, S. Afr Inst. Min. Metall., Symposium Series S51.

Player, J.R., Morton, E.C., Thompson, J.R. & Villaescusa, E. 2008b. Static and dynamic testing of steel wire mesh for mining applications of rock surface support. In T.R. Stacey & D.F. Malan (eds.). *Proc. 6th Int. Symp. on Ground Support in Mining and Civil Engineering Construction*: 693–706. Cape Town, South Africa, S. Afr Inst. Min. Metall., Symposium Series S51.

Player, J.R., Villaescusa, E. & Thompson, A.G. 2009. An examination of dynamic test facilities. *Australian Mining Technology Conference*: 1–32.

Plouffe, M., Anderson, T. & Judge, K. 2008. Rock bolt testing under dynamic conditions at CANMET-MMSL. In T.R. Stacey & D.F. Malan (eds.). *Proc. 6th Int. Symp. on Ground Support in Mining and Civil Engineering Construction*: 581–595. Cape Town, South Africa, S. Afr Inst. Min. Metall., Symposium Series S51.

Potvin, Y. 2009. Strategies and tactics to control seismic risks in mines. *J. S. Afr. Inst. Min. Metall.* 109: 177–186.

Potvin, Y., Jarufe, J. & Wesseloo, J. 2010a. Interpretation of seismic data and numerical modelling of fault reactivation at El Teniete, Reservas Norte Sector. *J. Min. Technol.* 119 (3): 175–181.

Potvin, Y., Wesseloo, J., & Heal, D. 2010b. An interpretation of ground support capacity submitted to dynamic loading. *J. Min. Technol.* 119 (4): 233–245.

Potvin, Y. & Wesseloo, J. 2013a. Improving seismic risk management in hardrock mines. Keynote Lecture. In A. Malovichko & D. Malovichko (eds.), *Proc. 8th Int. Symp. on Rockbursts and Seismicity in Mines*: 371–386, Saint–Petersburg, Moscow, Russia.

Potvin, Y. & Wesseloo, J. 2013b. Towards an understanding of dynamic demand on ground support. *J. S. Afri. Inst. Min. Metall.* 113: 913–922.

Qiu, S., Feng, X. & Zhang, C. 2014. Estimation of rockburst wall-rock velocity invoked by slab flexure sources in deep tunnels. *Can. Geotech. J.* 51: 520–539.

Raffaldi, M.J. & Loken, M.C. 2016. Rock mass modeling approach for simulating wave propagation, rock fracture, and rock ejection. *ARMA/USRMS 16 Conference*, Houston, Texas.

Read, R.S., J.B. Martino, E.J. Dzik, S. Oliver, S. Falls & R.P. Young. 1998. *Analysis and interpretation of AECL's heated failure tests.* Ontario Hydro, Nuclear Waste Management Division, Report 06819-REP-01200- 0070 R00.

Reddy, N. & Spottiswoode, S.M. 2001. The influence of geology on a simulated rockburst experiment. *J. S. Afr. Inst. Min. Metall.* 101 (5): 267–272.

Rizwan, M. & Stacey, T.R. 2015. Conceptual support systems to limit damage to tunnel floors in rockbursting environments. *Proc. 13th Int. Congr. Int. Soc. Rock Mech.*, Montreal, Canada. Paper no. 264.

Roberts, M.K.C & Brummer, R.K. 1988. Support requirements in rockburst

conditions. *J. S. Afr. Inst. Min. Metall.* 88 (3): 97–104.

Roux, A.J.A., Leerman, E.R. & Denkhaus, H.G. 1957. De-stressing means of ameliorating rockburst conditions. Part 1 – The concept of de-stressing and the results obtained from its application. *J. S. Afr Inst. Min. Metall.* October: 101 – 119.

Sahayi, F. 2013. *Numerical simulation of the response of an underground opening at different locations under fault-slip induced seismic wave.* Masters Thesis, Luleå University of Technology.

Scholz, C. W. 1968. Microfracturing and the inelastic deformation of rock in compression, *J. Geophys. Res.* 73 (4): 1417–1432.

Schuler, H., Mayrhofer, C. & Thoma, K. 2006. Spall experiments for the measurement of tensile strength and fracture energy of concrete at high strain rates. *Int. J. Impact. Engng.* 32: 1635–1650.

Shan, Z. & Yan, P. 2010. Management of rockbursts during excavation of the deep tunnels in Jinping II Hydropower Station. *Bul. Engng Geol Environ.* 69: 353–363.

Sheory, P.R. 1994. A theory for in situ stresses in isotropic and transversely isotropic rock. *Int. J. Rock Mech. Min. Sci. & Geomech. Abstr.* 31(1), 23–34.

Shirzadegan, S., Nordlund, E. & Zhang, P. 2016. Large scale dynamic testing of rock support system at Kiirunavaara mine. *Rock Mech. Rock Eng.* 49 (7): 2773–2794.

Simser, B., Andrieux, P., Langevin, F., Parrott, T. & Turcotte, P. 2007. Field

behaviour and failure modes of Modified Conebolts at the Craig, LaRonde and Brunswick Mines in Canada. In Y. Potvin, J. Hadjigeorgiou & T. R. Stacey (eds.), Challenges in deep and high stress mining: 347–354, Perth, Australia, Australian Centre for Geomechanics.

Stacey, T.R. & de Jongh, C.L. 1977. Stress fracturing around a deep-level bored tunnel. *J. S. Afr. Inst. Min. Metall.* 78 (5): 124–133.

Stacey, T.R. 1981. A simple extension strain criterion for fracture of brittle rock. *Int. J. Rock Mech. Min. Sci. & Geomech. Abstr.* 18: 469–474.

Stacey, T.R. 1989. Boring in massive rocks–rock fracture problems. *Proc. Seminar on Mechanized Underground Excavation*, S. Afr. Nat. Council on Tunneling. 87–90.

Stacey, T.R. 1991. *Method of and means for inhibiting rockbursts.* Patent Application, Provisional Specification, registered through Adams and Adams, Patent Attorneys, Pretoria.

Stacey, T.R. & Thompson, P.W. 1991. A large borehole breakout? *Proc. Int. Cong. Int. Soc. Rock Mech*: 1019–1021, Aachen, Germany, A.A. Balkema, Rotterdam.

Stacey, T.R. 2001. Tunnel surface support - capacities of various types of wire mesh and shotcrete under dynamic loading. *S. Afri. Inst. Min. Metall.* 101 (7): 337–342.

Stacey, T.R. & Ortlepp, W.D. 2002. The contribution of wire rope lacing in surface support. *Proc. 2nd Int. Seminar on Surface Support Liners: Thin Spray-On Liners, Shotcrete, Mesh*: 1–8. Johannesburg, South Africa, S. Afr Inst. Min. Metall.

Stacey, T.R. & Yathavan, K. 2003. Examples of fracturing of rock at very low stress levels. *ISRM 2003 – Technology Roadmap for Rock Mechanics*: 1155–1159. S. Afr. Inst. Min. Metall.

Stacey, T. R. & Ortlepp, W. D. 2007. Yielding rock support – the capacities of different types of support, and matching of support type to seismic demand. In Y. Potvin, J. Hadjigeorgiou & T. R. Stacey (eds.), Challenges in deep and high stress mining: 407–411, Perth, Australia, Australian Centre for Geomechanics.

Stacey, T.R., Ortlepp, W.D. & Ndlovu, X. 2007. Dynamic rock failures due to "high" stress at shallow depth, *Proc. 4th Int. Seminar on Deep and High Stress Mining*: 193–204, Perth, Australian Centre for Geomechanics.

Stacey, T.R. 2009. Design – a Strategic Issue. *J. S. Afr. Inst. Min. Metall.* 109 (3): 157–162.

Stacey, T.R. 2011. Support of excavations subjected to dynamic (rockburst) loading. Keynote Paper. *Proc. 12th Int. Cong. Int. Soc. Rock Mech*: 137–145, Beijing, China, CRC Press/Balkema.

Stacey, T.R. 2011. (https://www.youtube.com/watch?v=GuOkOHnsAc)

Stacey, T.R. 2012. A philosophical view on the testing of rock support for rockburst conditions. *J. S. Afr. Inst. Min. Metall.* 113 (7): 227–245.

Stacey, T.R. 2013. Dynamic rock failure and its containment – a Gordian Knot design problem, Rock Dynamics and Applications State of the Art, *Proc. Int. Conf. RocDyn 1*: 57–70, Lausanne, Switzerland, CRC Press/Balkema, Taylor & Francis Group.

Stacey, T.R. & Rojas, E. 2013. A potential method of containing rockburst

damage and enhancing safety using a sacrificial layer. *J. S. Afr. Inst. Min. Metall.* 113: 565–573.

Stacey, T.R. 2016a. Addressing the consequences of dynamic rock failure in underground excavations. *Rock Mech. Rock Eng.* 49: 4091–4101.

Stacey, T.R. 2016b. Innovative and controversial support systems for rockbursting conditions. In E. Nordlund, T.H. Jones & A. Eitzenberger (eds.), *Proc. 8th Int. Symp. on Ground Support in Mining and Underground Construction*, Lulea University of Technology, Lulea, Sweden, ISBN: 978–91–7583–804–5 (electronics), 15p.

Stacey, T.R. 2017. Dynamic rock failure and its containment, in Rock Mechanics and Engineering, ed X.T. Feng, CRC Press, to be published.

Tannant, D.D., McDowell, G.M. & McCreath, D.R. 1994a. Shotcrete performance during simulated rockbursts. In *4th South American Congress on Rock Mechanics*, Workshop on Applied Rockburst Research, (SOCHIGE): 241–248, Santiago, Chile.

Tannant, D.D., Brummer, R.K. & Kaiser P.K. 1994b. Response of rockbolts to nearby blasts. In *4th South American Congress on Rock Mechanics*, Workshop on Applied Rockburst Research, (SOCHIGE): 257–264, Santiago, Chile.

Tannant, D.D., Brummer, R.K. & Yi, X. 1995. Rockbolt behaviour under dynamic loading: Field tests and modelling. *Int. J. Rock Mech. Min. Sci. & Geomech. Abstr.* 32 (6): 537–550.

Tarasov, B.G. & Potvin, Y. 2013. Universal criteria for rock brittleness estimation under triaxial compression. *Int. J. Rock Mech. Min Sci.* 59: 57–69.

Tarasov, B.G. 2014. Fan-structure shear rupture mechanism as a source of shear rupture rockbursts. *J. S. Afr. Inst. Min. Metall.* 114: 773–784.

Tedesco, J.W. & Landis, D.W. 1989. Wave propagation through layered systems. *Comput. Struct.* 48; 625–638.

Thompson, A.G., Player, J.R. & Villaescusa, E. 2004. Simulation and analysis of dynamically loaded reinforcement systems. In E. Villaescusa & Y. Potvin (eds.). *Ground support in mining and underground construction*: 341–358. Balkema, London.

Toper, A.Z. 2003. *The effect of blasting on the rockmass for designing the most effective preconditioning blasts in deep-level gold mines.* PhD Thesis, University of the Witwatersrand, 359p.

Varden, R., Lachenicht R., Player J.R., Thompson, A.G. & Villaescusa, E. 2008. Development and implementation of the Garford Dynamic Bolt at the Kanowna Belle mine. *10th underground operators conference*: 95–104, Launceston, AusIMM, Melbourne.

Vieira, F.M.C.C. & Durrheim, R.J. 2002. Probabilistic mine design methods to reduce rockburst risk. *J. S. Afri. Inst. Min. Metall.* May/June: 231–242.

Vogler, U.W.O.L. & Stacey, T.R. 2016. The influence of test specimen geometry on the laboratory-determined Class II characteristics of rocks. *J. S. Afr. Inst. Min. Metall.* 116 (11): 987–1000.

Wagner, H. 1982. Support requirements for rockburst conditions. In Gay & Wainwright (eds), *Proc. 1st Int Symp. Rockbursts and Seismicity in Mines*, S. Afr. Min. Metall. Symp. Series No 6 (1984): 209–218.

Wawersik, W.R. & Fairhurst, C. 1970. A study of brittle rock fracture in laboratory compression experiments. *Int. J. Rock Mech. Min. Sci.* 7: 561–575.

Wesseloo, J. & Stacey, T.R. 2000. Face and sidewall fracturing in circular excavations and effects on excavation and support. *AITES-ITA 2000 World Congress*: 553–557, Durban, South Africa, S. Afr Inst. Min. Metall.

Wesseloo, J. & Stacey, T.R. 2006. Updated in situ stress database for Southern Africa. In M. Lu, C.C. Li, H. Kjorholt & H. Dahle (eds.), *Proc. Int. Symp. on In-Situ Rock Stress*: 473–482, Trondheim, Norway, CRC Press, Taylor & Francis Group, ISBN: 978–0–415–40163–0 (electronics).

Wu, Y.K. & Oldsen, J. 2010. Development of a new yielding bolt – Yield-Lok bolt. *The 44th US Rock Mechanics Symposium*: 102–107, Salt Lake City, USA, ARMA.

Yi, X. & Kaiser, K.P. 1994. Impact testing for rockbolt design in rockburst conditions. *Int. J. Rock Mech. Min. Sci. and Geomech. Abstr.* 31 (6): 67–68.

Zhang, C., Xia-Ting., F., Zhou., H., Qui, S. & Wu, W. 2012. Case histories of four extremely intense rockbursts in deep tunnels. *Int. J. Rock Mech. Rock Engng.* 45 (3): 275–288.

Zhang, P., Swan G. & Nordlund, E. 2015. 1D numerical simulation of velocity amplification of P-wave travelling through fractured rock near a free surface. *J. S. Afr. Inst. Min. Metall.* 115:1121–1126.

Zhang, Q.B. & Zhao, J. 2014. A review of dynamic experimental techniques and mechanical behaviour of rock materials. *Int. J. Rock Mech. Rock Engng.* 47: 1411–1478.

Zheng, Z., Kemeny, J. & Cook, N.G.W. 1989. Analysis of borehole breakouts. *J. Geophys. Res.* 94 (B6): 7171–7182.

Zhou Z.L., Ma G.W. & Li X.B. 2007. Dynamic Brazilian splitting and spalling tests for granite. *Proc. 11th Int. Congr. Int. Soc. Rock Mech*: 1127–1130, Lisbon, Portugal. Taylor & Francis, London.

Zhou, Y.X., Xia, K., Li, X.B., Li, H.B., Ma, G.W., Zhao, J., Zhou, F., & Dai, F. 2012. Suggested methods for determining the dynamic strength parameters and mode-I fracture toughness of rock materials. *Int. J. Rock Mech. Min. Sci.* 49: 105–112.